Fetal and placental oxygenation estimated by BOLD MRI

PhD thesis

Sørensen, Anne Nødgaard

Publication date:
2014

Document Version
Early version, also known as pre-print

Fetal and placental oxygenation estimated by BOLD MRI

Anne Sørensen

PhD thesis

Department of Obstetrics and Gynecology

Department of Clinical Medicine

Aalborg University Hospital

Faculty of Medicine

Aalborg University

Supervisors

Niels Uldbjerg, Professor, MD, DMSc
Department of Obstetrics and Gynecology
Aarhus University Hospital, Skejby, Denmark

David Peters, MSc, PhD
Department of Clinical Engineering
Arhus University Hospital, Skejby, Denmark

Ole Bjarne Christensen, Professor, MD, DMSc
Department of Obstetrics and Gynecology
Aalborg University Hospital, Denmark

Göran Lingman, Professor, MD, DMSc
Department of Obstetrics and Gynecology
Lund University Hospital, Sweden

Evaluation committee

Magnus Westgren, Professor, MD, DMSc
Division of Obstetrics and Gynecology, Department of Clinical Science
Intervention and Technology Center for Fetal Medicine
Karolinska University Hospital, Stockholm, Sweden

Penny Gowland, Professor, MSc, PhD
Sir Peter Mansfield Magnetic Resonance Center
University of Nottingham, Nottingham, UK

Finn Ebbesen, Professor, MD, DMSc (chairman)
Department of Neonatology
Aalborg University Hospital, Aalborg, Denmark

Acknowledgement

This PhD thesis was carried out during my time as a part-time PhD student at the Department of Obstetrics and Gynecology, Aalborg University Hospital from 2010 to 2013. The BOLD MRI method was introduced to us in 2006 by Michael Pedersen at the MRI Research Center, Aarhus University Hospital in Skejby. And the BOLD MRI studies were conducted over the years 2006 – 2013. The sheep study and the human fetal study were performed at the MRI Research Center at Aarhus University Hospital. In 2010 the human placental study was initiated in the Department of Radiology at Aalborg University Hospital. Over the years a number of people made this work possible.

First of all, I wish to thank my principal supervisor Professor Niels Uldbjerg for being a mentor to me. By sharing his knowledge in research and fetal medicine and by always relevant criticism he provided me a perfect base for this work. Thanks to David Peters for patiently sharing his knowledge in MRI physics and software development. Without whom, we never would have continued past the software problems. Thanks to Professor Göran Lingman for fruitful discussions, educational visits to the Department of fetal medicine in Lund and for good company at the yearly ISUOG world congress. Moreover I wish to thank Professor Ole Bjarne Christiansen for important support and scientific contribution to the studies. Also a very special thanks to Hans Madsen, for believing in me and for always finding a way.

I wish to thank Carsten Simonsen, Torben Fründ and Jens Brøndum Frøkjær at the Department of Radiology at Aalborg University Hospital for good collaboration, high standards and good service. Thanks to Peter Skovbo, Eva Hoseth, Ingelise Quist and other colleges for working even harder when I was off for research. Thanks for moral support and lots of laughs.

Finally, most heartfelt thanks to my friends, to my entire family, and to Kim, Rasmus and Laurids for always being there and for putting life into the right perspective.

Anne Sørensen

Aalborg, September 2013

Papers

This PhD thesis is based on the following papers:

Paper 1
Sørensen A, Pedersen M, Tietze A, Ottosen L, Duus L, Uldbjerg N.
BOLD MRI in sheep fetuses: a non-invasive method for measuring changes in tissue oxygenation.
Ultrasound Obstet Gynecol. 2009 Dec;34(6):687-92.

Paper 2
Sørensen A, Holm D, Pedersen M, Tietze A, Stausbøl-Grøn B, Duus L, Uldbjerg N.
Left-right difference in fetal liver oxygenation during hypoxia estimated by BOLD MRI in a fetal sheep model.
Ultrasound Obstet Gynecol. 2011 Dec;38(6):665-72

Paper 3
Sørensen A, Peters D, Simonsen C, Pedersen M, Stausbøl-Grøn B, Christiansen OB, Lingman G, Uldbjerg N.
Changes in human fetal oxygenation during maternal hyperoxia as estimated by BOLD MRI..
Prenat Diagn. 2013 Feb;33(2):141-5

Paper 4
Sørensen A, Peters D, Fründ E, Lingman G, Christiansen O, Uldbjerg N.
Changes in human placental oxygenation during maternal hyperoxia as estimated by BOLD MRI.
Ultrasound Obstet Gynecol. 2013 Sep;42(3):310-4

Paper 5
Peters D, Sørensen A, Simonsen C, M. Sinding, Uldbjerg N.
The reproducibility of human placental T2* measurements and the hyperoxic response.
Radiology 2013 (Submitted)

Funding

This Phd study was supported by Aarhus University, Alborg University, Aalborg University Hospital and Forsknings Initiativet at Aarhus University.

Fetal and placental oxygenation estimated by BOLD MRI

PhD thesis

Anne Sørensen

Content

Corresponding author

Anne Sørensen, MD

Department of Obstetrics and Gynecology

Aalborg University Hospital

Reberbansgade, 9100, Aalborg, DK

E-mail: anns@rn.dk

List of abbreviations

BOLD	Blood Oxygen Level Dependent
MRI	Magnetic resonance imaging
CTG	Cardio tocography
FGR	Fetal growth restriction
PI	Pulsatility Index
TR	Repetition Time
TE	Echo Time
ROI	Region of Interest
NMV	Net Magnetization Vector
RF	Radio Frequency
Hgb	Hemoglobin
DeoxyHgb	Deoxyhemoglobin
FHR	Fetal heart rate

Aim of the thesis

The overall aim of this PhD thesis is to evaluate the feasibility of Blood Oxygen Level Dependent (BOLD) magnetic resonance imaging (MRI) as a non-invasive method for estimating changes in fetal and placental oxygenation.

The specific aims of this PhD thesis were:

- In ewes
    1. To estimate the association between changes in the BOLD signal and changes in fetal liver oxygenation during maternal hyperoxia and hypoxia. (Paper 1)
    2. To investigate fetal and placenta oxygenation changes during maternal hyperoxia and hypoxia by BOLD MRI. (Paper 1+2)

- In healthy human pregnancy
    1. To investigate fetal oxygenation changes during maternal hyperoxia by BOLD MRI. (Paper 3)
    2. To investigate placenta oxygenation changes during maternal hyperoxia by BOLD MRI. (Paper 4)
    3. To investigate the reproducibility of placental T2* and the hyperoxic response (Paper 5)

Introduction

A normal placental function ensures adequate supply of oxygen and nutrients for the developing fetus. Impaired placental function leads to fetal growth restriction (FGR) and increased risk of neonatal morbidity and mortality because of hypoxia and acidosis. One of the main purposes of fetal monitoring is to identify the growth restricted fetus in order to plan adequate monitoring intervals and ensure timely delivery. In each case of FGR the time of delivery will be determined by a balance between excessive intrauterine fetal stress and neonatal complications due to prematurity. In modern obstetrics fetal monitoring is based on various methods, such as cardiotocography (CTG), biophysical profile and ultrasound Doppler measurements of fetal and umbilical blood flow. These techniques are integrated in a focused strategy as a timeline of changes is associated with the progression of fetal hypoxia into acidosis and stillbirth. Current methods focus on fetal wellbeing and thus only indirectly estimate placental function. The only method available for direct estimation of placental oxygen transport is cordocentesis. However, this invasive procedure is not used because of an associated risk of fetal loss. In neuroscience Blood oxygen level dependent (BOLD) magnetic resonance imaging (MRI) provides non-invasive information about oxygenation changes of the brain, as changes the BOLD signal is closely related to changes in the saturation of hemoglobin. Over the last decade, BOLD MRI has become the main method for mapping brain function in cognitive studies. However, in fetal medicine the method is only briefly described. In this thesis the feasibility of BOLD MRI as a non-invasive method for estimating fetal and placental oxygenation is investigated in healthy pregnancies.

Background

This section contains three parts. The first part describes basic information about the BOLD MRI technique followed by a brief review of the literature previously published on fetal BOLD MRI. The second part summarizes the current methods in fetal monitoring. Finally, the third part is dedicated to the physiology of the fetus and the placenta.

Magnetic resonance imaging (MRI)

Basic MRI physics

In atoms the positively charged nucleus is surrounded by negatively charged electrons. Most atom nuclei contain an equal number of protons and neutrons. These pairs of subatomic particles spin in opposite directions, and therefore the nucleus itself has no net spin. However, MR active nuclei have an uneven number of protons and neutrons, and these nuclei therefore exhibit net spin. Because of the spin and the positive charge the MR active nuclei acquire a magnetic moment. The body contains several MR active nuclei; however, the hydrogen nucleus is the one used in clinical MR because of its high natural abundance in human tissue. Furthermore, the solitary proton of the nucleus produces a relatively large magnetic moment. In the absence of a magnetic field the hydrogen nuclei are randomly orientated in the body; however, when placed in an external magnetic field (B_0) the magnetic moments of the hydrogen nuclei will align with the magnetic field. Some nuclei align parallel (low energy) with the field while others align anti-parallel (high energy). The longitudinal magnetization reflects the relative balance between the numbers of nuclei in each alignment group as slightly more protons align parallel to B_0. At higher magnetic fields greater proportions align in parallel therefore, the longitudinal magnetization is increased.

The hydrogen nucleus is spinning on its axis. Furthermore, the influence of an external magnetic field B_0 produces an additional spin around B_0, which is called precession (Figure 1).

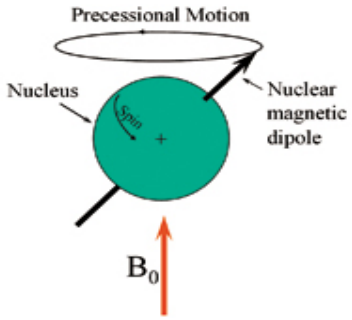

Figure 1 A hydrogen nucleus spinning around its axis and around B_0

In this secondary spin each MR active nucleus has a specific speed called the precessional frequency. When the hydrogen nucleus is exposed to a radio frequency (RF) pulse of energy at exactly its precessional frequency, the nucleus gains energy, it is excitated. This phenomenon is known as resonance. The results of resonance are as follows:

- An increasing number of nuclei join the high energy population orientated antiparallel to B_0, which decreases longitudinal magnetization.
- The magnetic moments of the nuclei move into phase, as they move to the same position on the precessional path. This is known as coherence, which generates transversal magnetization.

When the RF-pulse is stopped the hydrogen nucleus releases its energy. It continues to precess, and the net magnetic vector (the sum of the longitudinal and the transversal magnetic vectors) follows a spiraling path.

According to Faraday's law of induction, voltage is induced in a receiver coil when placed close to a moving magnetic field. The precessing NMV induces an electric oscillating current in the receiver coil of the MR scanner, also known as the free induction decay (FID) signal. This process is the basis of the MRI signal. The MRI signal intensity is related to the magnitude of the NMV, which depends on the tissue relaxation properties, magnetic field strength, proton density etc.

The release of energy following the RF-pulse is also known as relaxation and it is characterized by two parallel but independent processes T1 and T2 relaxation (Figure 2).

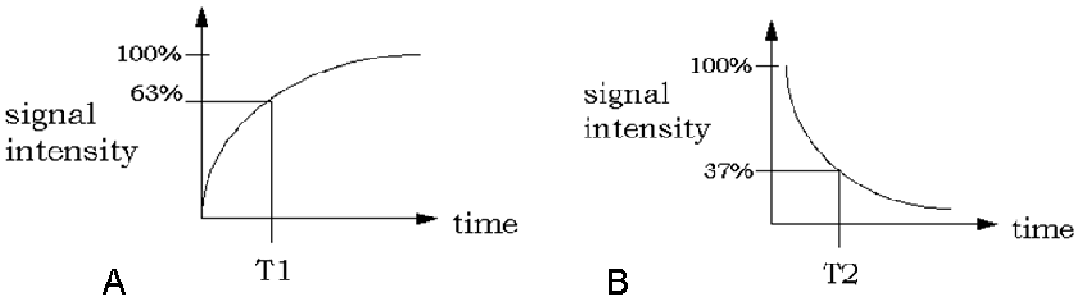

Figure 2 A) T1 recovery curve. B) T2 decay curve

- **T1 recovery**: Recovery of the longitudinal or spin-lattice magnetization. The T1 relaxation time is defined as the time when 63% of the original longitudinal magnetization is reached.

- **T2 decay**: Decay of the transversal or spin-spin magnetization (spin coherence). The T2 relaxation time is defined as the time when the transversal magnetization is reduced to 37%. T2 relaxation time is faster than T1 (Figure 3).

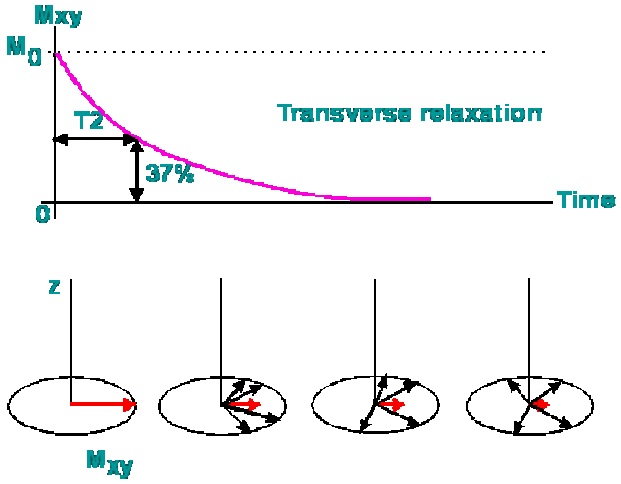

Figure 3 T2 decay curve with demonstration of the transversal vectors loosing coherence.

- **T2* decay:** T2* decay is the sum of the T2 decay as described above and the effect of local magnetic field inhomogeneities, which can be caused by machine imperfections, the

presence of iron (e.g. implants) or contrast agents such as deoxyHgb. T2* relaxation time is faster than T2 (Figure 4).

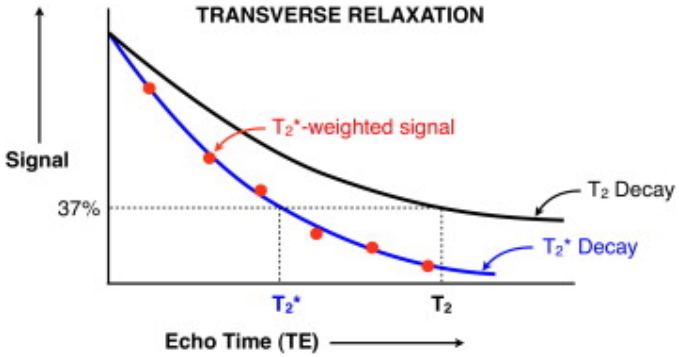

Figure 4 A comparison of T2 and T2* decay curves. T2* decay is faster than T2 decay.

Each tissue has a specific and characteristic T1, T2 and T2* relaxation time depending on the interaction between the protons and their surrounding environment. Tissue specific relaxation times are very important for image contrast. Image contrast is determined by differences in signal intensity, which depends on tissue relaxation times. Weighting of an MRI image allows one mechanism of relaxation to dominate the other (1). For instance, in the T2* weighted image, the difference in signal intensity between tissues (tissue contrast) is dominated by differences in the T2* relaxation time. However other mechanisms such as tissue proton density will also contribute to tissue contrast at least to some extent. The weighting of image contrast is determined by selecting specific timing parameters of the RF pulse sequence. The sequence parameters and their effect on the contrast weighting are outlined below:

Time of repetition (TR): The time from the application of one RF-pulse to the next RF-pulse. The TR determines the amount of T1 weighting. When the TR is short (<50 ms) T1 weighting is increased.

The echo time (TE): The time from the application of the RF-pulse to the peak FID in the receiver coil. The TE is dependent on the timing of the re-phasing pulse. The TE determines the amount of T2 weighting. When the TE is long (>15-20 ms) T2 weighting is increased.

Flip angle: The RF excitation pulse tips the NMV and transverse magnetization occurs. The flip angle determines the amount of longitudinal magnetization that is moved to the transversal plane. If the TR is short and the flip angle is large, the image is T1 weighted because of NMV saturation.

Spin echo pulse sequence: Following the RF-pulse an additional 180° pulse at time=TE/2 is used to refocus the dephasing protons at time TE. The 180° pulse rotates the protons 180° which makes them process in the opposite direction. The slower protons catch up with the faster ones and come into phase. Therefore, the spin echo compensates for the T2* dephasing due to local or intrinsic magnetic field inhomogeneities. The spin echo contains predominantly T1 and T2 information as the effect of T2* dephasing has been neutralized.

Gradient echo pulse sequence: In a gradient echo two gradients are applied – a dephasing and an opposite rephasing gradient (Figure 5). The magnetic field inhomogeneities persist in a gradient echo, as the gradient refocuses only the protons that have been de-phased by the gradient itself. The gradient echo is predominantly T1 and T2* weighted. When compared to the spin echo the gradient echo is faster, however the signal loss is greater because of the magnetic field inhomogeneities.

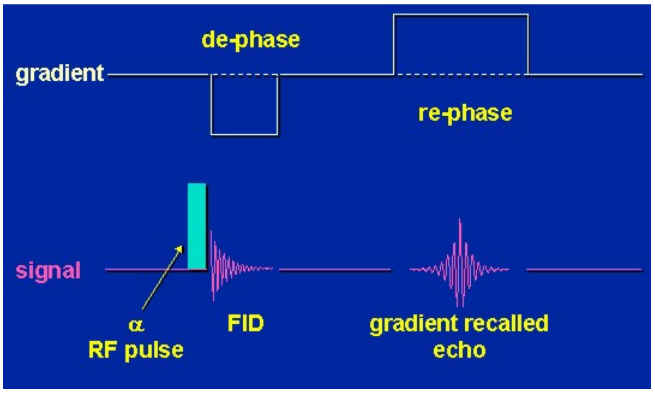

Figure 5 A gradient echo pulse sequence

BOLD MRI

Different MR applications have been developed for assessing tissue function and physiology as opposed to conventional structural imaging. BOLD MRI represents one of these functional MRI techniques. The BOLD effect was discovered in 1990 when Ogawa et al. demonstrated that the oxygenation of the blood had a measurable effect on the MRI signal of blood in vitro (2) and in the rodent brain (3). These publications were followed by BOLD MRI studies of the human brain during visual stimulation, and a close relationship between brain activation and changes in BOLD signal was demonstrated (4). During the last decades BOLD MRI has become the most important tool in cognitive studies of the human brain (5), and the number of publications has increased exponentially (4,6). However, in fetal medicine the method is only briefly described.

The BOLD signal should be obtained in a T2* weighted MRI scan as the BOLD contrast depends on differences in T2* relaxation. T2* weighting is obtained by a gradient echo pulse, a long TE and a long TR. The basis of the BOLD signal relies on the magnetic properties of hgb, which depend on the oxygenation state of the heme group. The paramagnetic effect of deoxyHgb is caused by the unpaired electrons of the heme groups which produces currents and thereby generates internal magnetism that affects the surounding protons (1). The binding of O_2 alters the structure of the hgb dramatically. The iron bindings are changed from ionic to covalent, and this is believed to explain why the paramagnetic effect is lost in oxyhemeglobin (7). Because of its paramagnetic effect deoxyHgb can be regarded as an intrinsic T2* contrast agent. It increases the local magnetic field surrounding it and reduces the T2* relaxation time of the neighboring protons. During hypoxia the amount of deoxyHgb is increased, so is the T2* decay, and following the BOLD signal intensity is reduced giving a darker appearance of the BOLD image. Likewise, during hyperoxia the amount of deoxyHgb is decreased, which decreases T2* decay and so the BOLD signal intensity is increased. When referring to BOLD MRI in this thesis, it includes the relative BOLD response obtained by an BOLD scan as well as the absolute T2* relaxation time obtained by a single measurement. Each of these estimates will be described separately in the following section.

A BOLD scan usually consists of an initial basal state followed by an activated state due to some kind of stimulation for instance visual stimulation. The BOLD response indicates the change in BOLD signal during activation (Figure 6).

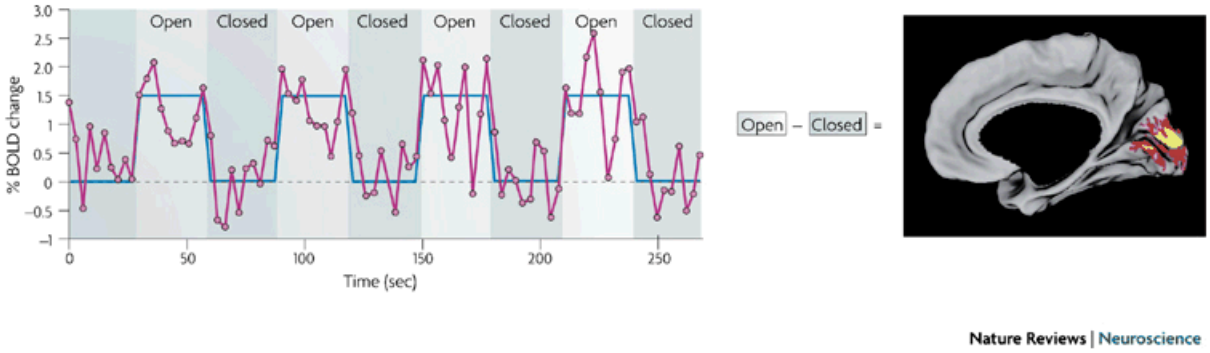

Figure 6 A functional MRI study of the human brain. Brain activation in the visual cortex is demonstrated during visual stimulation (open eyes) by an increase in the normalized BOLD signal (left) An anatomic map of the BOLD response demonstrates the location of the activation (right) (5)**.**

The absolute BOLD signal (S) depends on the following parameters

$$S = S_0 e^{-TE/T2^*} \quad (1)$$

The baseline BOLD signal (S_0) depends on 1) technical factors, such as the magnetic field strength, the pulse sequence, the distance to the receiver coil, and the shimming effects and 2) baseline tissue physiology such as heamatocrite and oxygen (Figure 7) (8-10).

Because of baseline signal variation the absolute BOLD signal tends to vary between individuals even when the oxygenation level of the blood is the same. For this reason only relative changes in BOLD signal can be directly compared between individuals, and a normalization of the BOLD signal is usually performed.

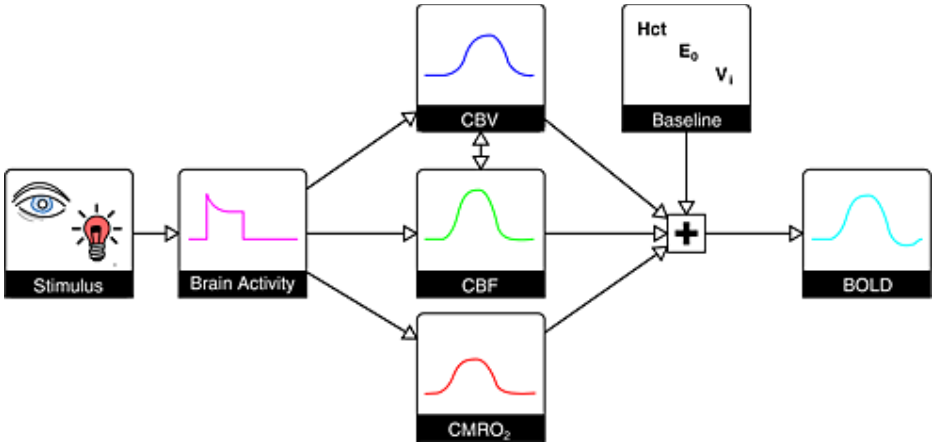

Figure 7 The complexity of the cerebral BOLD response during visual stimulation. The BOLD response depends on blood volume (CBV) and blood flow (CBF) and metabolism ($CMRO_2$). The maximum BOLD response is determined by baseline physiology, such as haematocrit (Hct), resting O_2 extraction (E_0) and blood volume (10)**.**

As indicated by Formula (2) the initial basal state absolute BOLD signal is used as a reference and at any given time x, the normalized BOLD signal will be expressed as a percentage of the reference level.

(2) $$\text{Normalized BOLD signal (x)} = (S_X - S_{Basal})S_{Basal} \times 100\%$$

S_X and S_{Basal} indicate the absolute BOLD signals at time x and at basal state.

The relative change in BOLD signal during activation, also known as the BOLD response (ΔBOLD), can be expressed by the following formula

(3) $$\Delta BOLD = (S_{Activated} - S_{Basal})/S_{Basal} \times 100\%$$

$S_{Activated}$ and S_{Basal} indicate absolute BOLD signal of the steady state level in the activated and the basal state.

As indicated in Figure 7 the BOLD response is closely related to physiological factors such as blood flow, blood volume and oxygen metabolism. These factors will influence the BOLD signal and therby the BOLD response in different ways. Any increase in blood flow would decrease the amount of deoxyHgb and thereby increase the BOLD signal. An increase in blood volume would

increase the amount of deoxyHgb, and thereby decrease the BOLD signal. An increase in tissue metabolism would increase the amount of deoxyhemglobin and thereby decrease the BOLD signal. All of these factors need to be taken into consideration when interpreting the BOLD response (10,11). In its traditional use BOLD MRI provides information about brain activation in cognitive studies (4). These studies have demonstrated a rather surprising increase in BOLD signal during brain activation. This finding was rather unexpected as the amount of deoxyHgb is supposed to increase during activation and as a result of this increase, the BOLD signal was expected to decrease. However, the increase in cerebral BOLD response can be explained when taking the changes in cerebral blood flow into consideration. During brain activation a compensatory increase in the cerebral perfusion exceeds the metabolic demand and thus, the cerebral oxygenation is actually increased (12-14).

In a BOLD experiment curves of tissue T2* decay can be drawn at basal and activated states by performing a gradient echo sequences with multiple readouts. For each echo-time the mean MRI signal of the region of interest (ROI) is plotted and an exponential decay curve is formed for the basal as well as the activated state.

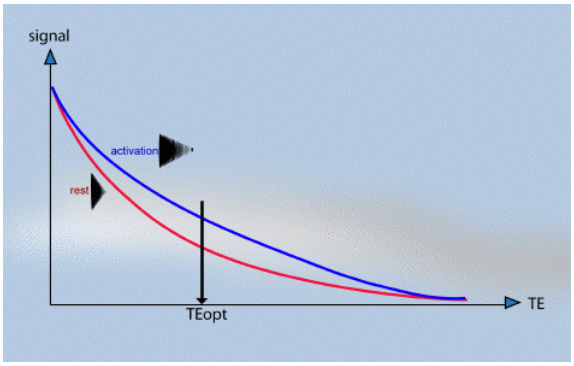

Figure 8 T2* decay curves demonstrating the resting and activated state of a specific tissue. The optimal echo-time (TEopt) where the curves are the most distant is indicated in the figure.

At any given echo-time the BOLD response will be determined by the difference between the two curves. As shown in Figure 8, the optimal TE would be the time where the curves of the basal and activated state are the furthest apart and where the BOLD signal intensity is still above the background noise level.

The tissue specific T2* relaxation time can be calculated from the mono exponential T2* decay curve by fitting the formula 1 using a non-linear least squares fitting algorithm.

The hgb molecule has an intravascular localization, with deoxyHgb present predominantly in the veins and to some degree in the capillaries. DeoxyHgb creates magnetic field gradients around the red blood cells and these gradients extend into the surrounding tissue, also known as blooming. Therefore the BOLD response has an intravascular as well as extravascular component. In the brain only 4% of the tissue volume consists of vessels; however, at 1.5 Tesla the intravascular component contributes with 50% of the total BOLD response (15).

In summary, the presence of the paramagnetic deoxyHgb reduces tissue T2* relaxation time and thereby the T2*-weighted BOLD signal. The BOLD response is determined by the amount of deoxyHgb present in the basal and the activated state. In BOLD MRI either the relative BOLD response (ΔBOLD) or the absolute tissue T2* relaxation time can be estimated.

Fetal BOLD MRI

To date 19 studies have been published on fetal and placental BOLD MRI. The studies are listed in the Review Table of the Appendix. The studies differ in several ways. The studies have been conducted either in the human fetus or in an animal model such as the sheep or the rat fetus. The kind of stimulation varies from in utero acoustic and visual stimulation to changing the oxygen content of the maternal breathing air. The studies estimate the BOLD response by relative changes in the BOLD signal or absolute changes in the T2* value of the fetal organs and the placenta.

The very first fetal BOLD MRI study was published in 1999. In this study human fetal brain activity was demonstrated during acoustic stimulation in utero (16). This study was followed by three other studies demonstrating fetal brain activation during vibroacustic and visual stimulation in utero (17-19). In 2001 a pilot study demonstrated increasing liver oxygenation during maternal hyperoxia in the human fetus (20); but unfortunately, this finding could not be reproduced in a larger group (21). The human studies were followed by studies investigating the oxygenation changes of the sheep fetus. Oxygenation changes were induced by changing the oxygen content of the maternal ventilation gas. The fetal oxygenation was estimated invasively by fetal arterial blood

samples (22-24) and fetal oxygen sensors (25), and a strong association between changes in the BOLD signal and changes in fetal oxygenation was demonstrated. Just recently, a few studies have demonstrated increasing oxygenation of the human fetus and the placenta during maternal hyperoxia when using the BOLD MRI method (26-28), and placental T2* relaxation time has been estimated for the healthy human pregnancy (26). By unilateral ligation of the left uterine artery a model of FGR has been created in the rat, and the hyperoxic BOLD response has been investigated in the fetoplacental unit. This model allows direct comparison of the BOLD response in the normal fetus (the non ligated uterine horn) and the FGR fetus (the ligated uterine horn) within one rat, and according to the rat model, the BOLD response of the fetoplacental unit is significantly reduced in the FGR fetus (29,30).

Safety in MRI

Safety is a major issue when scanning fetuses. Since MRI does not involve any form of ionizing radiation, it is considered safer than imaging modalities based on X-Rays and Computerized Tomography (CT). The American College of Radiology (ACR) states that fetal MRI is an established modality for evaluating fetal abnormalities that are not well assessed with ultrasound. The 2010 guidelines from ACR recommend that fetal MRI is performed at 1.5 Tesla only, and preferably in the second and third trimester without the use of intravenous contrast agents (31). There is no evidence that MRI poses a risk to the developing fetus. Fetal MRI is still a new modality, so the lack of evidence is the main reason for the clinical guidelines being rather conservative. The main areas of concern discussed below.

Static magnetic fields

The natural magnetic field of the earth is approximately 50μT, and most clinical MRI procedures are performed in the range of 0.15 – 3T; however, experimental MRI systems of 10T are in use. The static magnetic field interacts with the living tissue in three ways: 1) magnetic induction of electric currents caused by moving electrocytes, 2) magneto-mechanical effects causing reorientation of macromolecules, and 3) electron spin interactions (32). Based on in vitro, animal and human studies there is no evidence of cancer induction or any adverse effects induced by

static magnetic fields. Animal studies of repetitive fetal exposure to magnetic field strength up to 9 Tesla have not demonstrated any adverse morphological, cognitive or behavioral effects (33).

Tissue heat

RF-pulse excitation generates tissue heat. This effect is related to different factors such as the magnetic field strength, the type of RF-coil used and the duration of the MRI scan. The fetal effects of tissue heating have been extensively investigated in relation to fetal ultrasound examination (34,35). The fetus lives in a well insulated environment in which heat dissipation is restricted to two pathways conduction through the amniotic fluid and most importantly convection through the placental blood flow (36). In normal pregnancy fetal core temperature typically exceeds maternal temperature by 0.5°C because of accumulated heat generated by fetal metabolism. The compromised fetal heat loss mechanism needs to be taken into consideration when estimating induced heat during MRI examination (37). Experimental animal studies have demonstrated an exponential relation between temperature and tissue damage. Proliferating cells are particularly sensitive to elevated temperature, and the teratogenic effect is mediated by reduced mitotic activity and cell death (38). It is generally accepted that a threshold value of temperature elevation of 1.5°C should be considered safe for the fetus (34). For every MRI scan a specific absorption rate (SAR) value can be calculated, which correlates to the tissue heat deposited. It has been estimated that at 1.5T the peak SAR value of the fetus is approximately 50% of that generated in the mother (39). According to the recommendations by the International Commission on Non-Ionizing Radiation Protection (ICNIRP) the whole body SAR value should be kept below 2 W/kg during a one hour scan equivalent to a rise in adult and fetal tissue temperature of 0.5C and 0.3C, respectively (40).

Acoustic noise

During acquisition of images the MRI machine generates noise in the range of 80 to 120 dB (41). It is recommended that adults wear ear protection to reduce sound levels. The fetus is protected by the maternal abdomen and by the amniotic fluid, which reduces fetal noise by at least 30 dB (42). It has been demonstrated that daily fetal exposure to noise > 99 dB increases the risk of specific hearing loss, prematurity and FGR (43). However, the noise generated during an MRI examination

is of short duration and the intensity should be well below 99 dB. A marked increase in fetal movements during MRI examination has been demonstrated (44). It is generally accepted that the transient increase in fetal movements is a response to the sudden noise arising from the MRI machine.

Current methods in human fetal monitoring

The purpose of antenatal care is identification of the growth restricted fetus in order to ensure rational monitoring intervals and timely delivery. In modern obstetrics assessment of fetal well being is based on various methods; CTG, biophysical profile, and the ultrasound Doppler measurements of fetal and umbilical blood flow. For optimal fetal surveillance these methods should be integrated into a focused strategy. As demonstrated by Figure 9 a certain timeline of changes is associated with the progression of fetal hypoxia into acidosis and stillbirth (45). In each case of FGR the time of intervention will be a balance between the risk of intrauterine stress due to hypoxia and acidosis and the risk of neonatal complications due to prematurity.

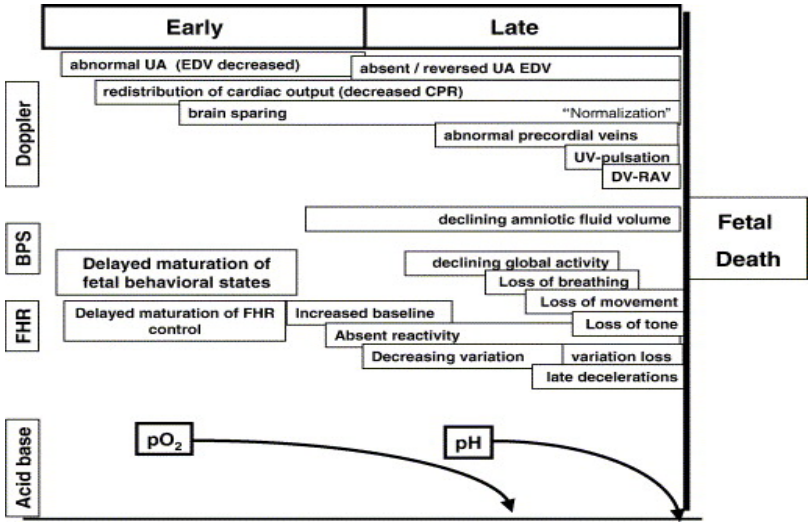

Figure 9 Fetal cardiovascular and behavioral response to placental insufficiency. A timeline of changes is associated with the progression of fetal hypoxia into acidosis and stillbirth. Umbilical artery (UA), middle cerebral artery, umbilical vein (UV), and ductus venosus (DV). End-diastolic velocity (EDV). Cerebroplacental ratio (CPR). Reversed or abscent atrial forward velocity (RAV). Biophysical profile score (BPS) and fetal heart rate (FHR) (45)**.**

CTG

Antepartum CTG includes registration of the fetal heart rate (FHR) by an external ultrasound transducer placed on the mother's abdomen and simultaneous registration of uterine contractions. The following components of the FHR pattern can be assessed: baseline rate, baseline variability, accelerations and decelerations. The latter should be categorized according to the relationship with the uterine contractions. FHR pattern is a product of the central nervous system's sympathic and parasympathic outflow, and it could be considered a measurement of central nervous system performance. During initial hypoxia the fetal chemoreceptor is stimulated, and bradycardia occurs as a result of increased parasympathic activity. These decelerations are rapid and their depth is directly related to the degree of hypoxia (46). These variable decelerations are easy to detect, but unfortunately their diagnostic value is unclear. This is in contrast to decreasing variability and late prolonged decelerations, which are considered pathological. This abnormal FHR is related to chronic hypoxia, acidosis and placental insufficiency (47). The latter indicates an increased risk of antenatal neural injury because of reduced cerebral oxygenation (48). Despite the widespread use of CTG in obstetric clinics, the benefit of CTG as a predictor of fetal hypoxia and neurological injury still needs to be proven (49). The reassuring CTG almost always predicts a well oxygenated fetus. In contrast, the nonreassuring CTG is complicated by a high false positive rate as it is very often associated with a well oxygenated fetus (50). An additional tool for the interpretation of the non-reassuring CTG is analysis of the ST-segment of the fetal electrocardiogram (ECG) and the combined analysis is known as STAN. Fetal hypoxia affects the fetal cardiac metabolism, which leads to significant changes in the ST-segment and in the ratio of the T-wave and the QRS amplitude of the fetal ECG (51). The fetal ECG is obtained from a scalp electrode; therefore, this method is available for intrapartum surveillance only.

Biophysical profile

The biophysical profile combines CTG (20 minutes) with ultrasound assessments of fetal movements, tone, breathing and amniotic fluid volume. It is well known that the fetus adapts to hypoxia by decreasing fetal activity, probably to reduce oxygen consumption (52). Furthermore, fetal hypoxia causes redistribution of fetal renal blood flow towards the central organs, which leads to oligouria and oligohydramnious (53). The biophysical profile as a test of fetal hypoxia is

also complicated by a high false positive rate as fetal movements are often transiently reduced in well oxygenated fetuses and the amount of amniotic fluid has broad limits even in healthy fetuses. It has been documented that including the biophysical profile does not reduce perinatal mortality and morbidity when compared to CTG only, and unfortunately the biophysical profile has been shown to increase the rate of caesarean section and induction of labour (54).

Umbilical and fetal Doppler ultrasound

By Doppler ultrasonography fetal and umbilical blood flow velocity can be measured. Arterial Doppler waveform reflects downstream vascular resistance (Figure 10). However, venous Doppler waveform reflects cardiac forward function; thus, the forward flow in the venous system is determined by cardiac function (compliance, contractility and afterload). The complicated calculation of absolute blood flow volume requires accurate measurements of both the vessel diameter and blood flow velocity. Given these difficulties, reproducible angle independent indices of blood flow velocity such as pulsatility index (PI) have been developed for clinical use. The PI is calculated as the difference between the peak systolic velocity and the minimum diastolic velocity divided by the mean velocity through the cardiac cycle (55).

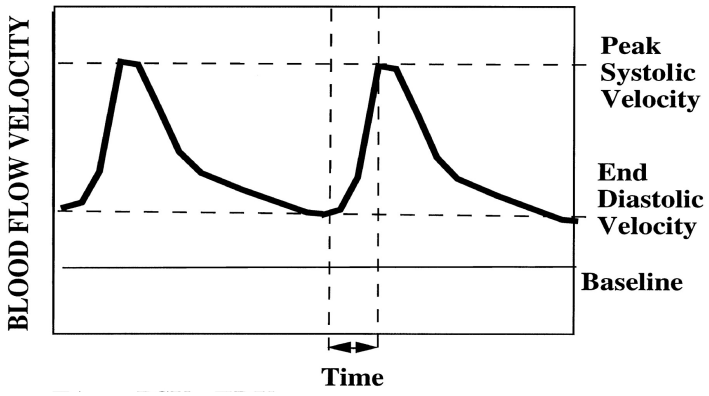

Figure 10 Arterial Doppler waveform demonstrating the blood flow velocities of the cardiac cycle.

Specific changes in fetal, umbilical and placental circulation are important indicators of impaired placentation and fetal redistribution of blood flow due to hypoxia and acidosis (45). The effect of the implementation of ultrasound Doppler flow in fetal surveillance on fetal outcome is difficult to estimate. In 2010 reviews by Cochrane have addressed this question in normal (56) and high risk

pregnancy (57). Both reviews are limited by poor methodological quality of the included trials because of insufficient data included and possible publication bias. In normal pregnancy, it is suggested that the use of fetal and umbilical Doppler does not improve fetal outcome or increase obstetrical interventions (56). However, in high risk pregnancies fetal mortality is reduced without any increase in obstetrical interventions when Doppler examination is compared to no Doppler examination or CTG only (57). The GRIT study (58), a randomized controlled trial, evaluated the effect of immediate versus delayed delivery in FGR fetuses, when the obstetrician was uncertain about when to deliver the fetus. The GRIT study demonstrated a trend towards a better short-term (2 year) outcome in the delayed group of fetuses in regard to neonatal morbidity (59). However, with long-term (6-9 years) outcome no differences were demonstrated between the two groups in regard to motor and intellectual disabilities (60). The GRIT study did not evaluate specific monitoring strategies, but the study highlights the importance of gestational age in regards to neonatal outcome in cases of very early onset FGR. A large multicenter randomized controlled trail, the TRUFFLE trial (61), is designed to evaluate specific monitoring strategies (CTG versus ductus venosus Doppler) in regards to fetal outcome, and the results of this trial still needs to be published. In general neonatal outcome will be determined by 1) neonatal complications due to prematurity and 2) intrauterine hypoxia and acidosis due to impaired placental function. The decision of when to deliver the growth restricted fetus will be a balance between the two. At early gestational age, the major determinant of neonatal outcome is gestational age as demonstrated by the GRIT study. At later gestation, when the prematurity-related morbidity decreases, intrauterine hypoxia and acidosis become the major determinants of neonatal outcome. Abnormal ductus venosus Doppler flow is the only Doppler finding that is directly related to fetal acidosis and stillbirth independent of gestational age (62,63). The association between brain sparing and fetal hypoxia is well known (64); however, studies indicate that fetal outcome in late onset FGR is compromised even before brain sparing can be observed by Doppler ultrasound examination (65). This finding suggests that even with optimal fetal Doppler ultrasound surveillance fetal morbidity cannot be prevented.

In the following sections the physiology of the placenta and the fetus is described, and Doppler examination of placental, fetal and umbilical blood flow is mentioned when relevant.

Placental physiology

The main function of the placenta is the transport of gases and nutrients between the mother and the fetus. Moreover, the placenta serves as an important endocrine organ as placental hormones are released to the maternal as well as the fetal circulation (66).

Placental structure and development

Placentation begins in the early first trimester, and this process is a major determinant of pregnancy outcome. The placenta consists of a maternal region (the basal plate) and a fetal region (the chorionic plate) and the space in between these two regions (the intervillous space). The latter contains the extensively branched fetal villous tree. On the maternal side of the placenta blood of the uterine arteries enter the intervillous space via the low resistance spiral endometrial arteries. The transformation of the spiral arteries into low resistance vessels should be complete within 24 weeks of gestation, and it is mandatory for adequate maternal perfusion and development of the placenta. The waveform of the uterine artery reflects the resistance in the spiral arteries, and placentation abnormalities can be detected by uterine artery Doppler ultrasound examination (67). The maternal blood bathes the villous tree in the intervillous space and drains back through the endometrial veins.

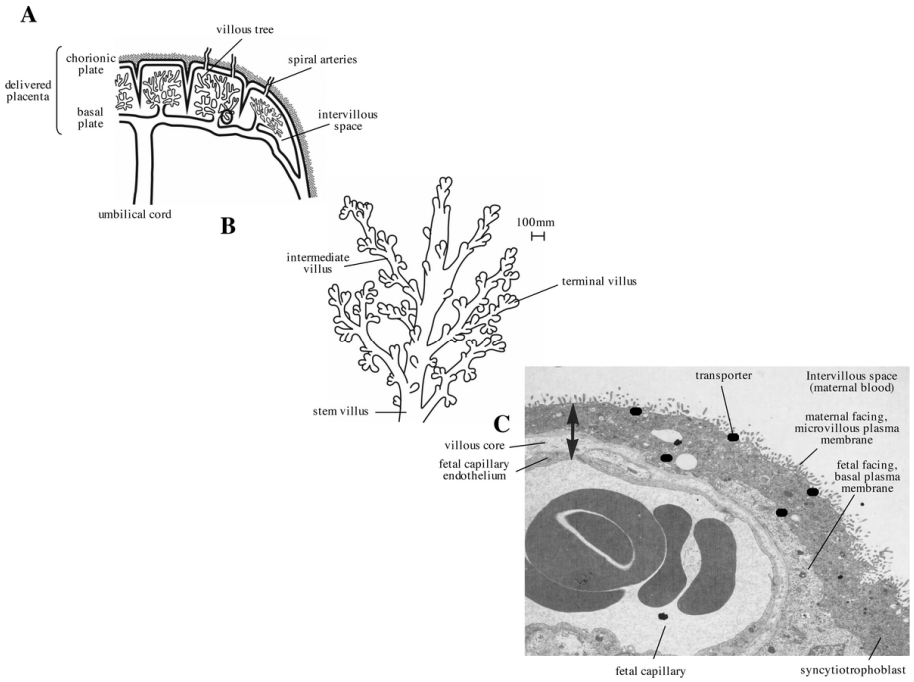

Figure 11 Morphology of the normal human placenta. A) Cross section of the placenta demonstrating the chorionic and basal plate. B) A villous tree, the functional unit of the placenta. C) An electron micrograph of the placental exchange barrier consisting of the syncytiotrophoblast, the villous matrix and the fetal capillary endothelium (68)**.**

Anatomically the human placenta is classified as a hemochorial placenta in which maternal blood is in direct contact with the fetal trophoblast (69). This is in contrast to the sheep placenta, an epitheliochorial placenta, in which the distance between maternal and fetal blood is increased by the epithelium of the maternal vessels. The functional unit of the placenta is the villous tree, and it is in the terminal villi are the major sites of maternal-fetal exchange (Figure 11). Fetal capillaries within the terminal villi are separated from the maternal blood in the intervillous space by only a small layer of syncytiotrofoblast.

The development of placental villi from trophoblasts starts around gestational week 4 followed by hypoxia stimulated angiogenesis of fetoplacental capillaries in gestational week 5-6 (70). At gestational week 12 maternal arterial blood enters the intervillous space, and the increase in oxygen stimulates further growth and maturation of the villus tree (71). By the end of the second trimester the formation of terminal villi occurs exponentially to meet the increasing metabolic

demand of the growing fetus. The thickness of the placental membrane is decreased and the surface area of the villous three increased, at term reaching 13m^2 (70). This placental maturation of normal the pregancy increases placental oxygen transport capacity by approximately 40% (72). The directions of maternal and fetal vessels are of major importance for the efficiency of exchange functions. There are two main types of arrangements (73); the counter current system, in which the pO_2 of the umbilical vein equilibrates with the uterine artery, and the concurrent system, in which the pO_2 of the umbilical vein equilibrates with the uterine vein. The human placenta is considered a multivillous system, which is a combination of the two. This arrangement should ensure the pO_2 of the umbilical vein to equilibrate at least with the uterine vein (74,75).

The vascular resistance on the fetal side of the placenta is determined by the architecture of the villous tree, and in normal pregnancy the resistance decreases gradually throughout pregnancy (76-78). Abnormalities of the placental villous tree can be detected by Doppler ultrasound examination of the umbilical artery (79). The vascular resistance of the maternal side of the placenta is determined by the resistance of the uterine arteries (80,81). Abnormal placentation can be detected by Doppler ultrasound examination of the uterine arteries, and increased resistance of the uterine arteries is a predictor of FGR and preeclampsia (82,83).

Placental function

The placenta is responsible for any feto-maternal exchange of nutrients and respiratory gases. Furthermore, the placenta serves as an important endocrine organ, and placental hormones are released into maternal as well as fetal circulation (66). The placenta is not innervated by the autonomic nervous system, and so any communication between the fetus, the mother and the placenta is regulated by blood borne substances. Examples of well known endocrine factors produced by the placenta are progesterone, human chorionic gonadotrophin (hCG), pregnancy-associated plasma protein A (PAPP-A), human placental lactogen and placental growth hormone (66,84). Through very complicated interactions placental hormones regulate placental function, fetal growth and maternal adaption to pregnancy.

The placenta is a highly active metabolic organ. In the third trimester the uterine arteries receive 30% of maternal cardiac output, and about 40% of the uterine oxygen supply is consumed by the placenta itself (85). This rather high oxygen consumption of the placenta is mainly a consequence of protein synthesis (30%) and active transport mechanisms via the Na^+-K^+-pump (30%) (86).

Placental exchange function is determined by feto-maternal concentration differences, uterine and umbilical blood flow and the permeability of the placental membrane (87). In general placental transport is mediated by two different mechanisms: diffusion and transporter proteins. Lipophilic molecules such as respiratory gasses diffuse easily across the placental membrane, and therefore such diffusion is limited by concentration and blood flow (85,88). Hydrophilic molecules as amino acids and carbohydrates do not diffuse easily through the placental membrane, and therefore this diffusion is less dependent on concentration gradients. Instead surface area, membrane thickness and molecular size play import roles (89,90). Transporter protein mediated transport of hydrophilic molecules is energy consuming and require ATP from the Na^+-K^+-pump. This transport is dependent on the number and characteristics of transporter proteins in the plasma membrane, which is carefully regulated by endocrine control throughout pregnancy (88,91).

In healthy human pregnancy the normal oxygen partial pressure (pO_2) of the uterine and umbilical blood is as follows; uterine artery pO_2=80-100mmHg (sat:98-100%); uterine vein pO_2=40-45mmHg (sat:75-80%); umbilical vein pO_2=25-35mmHg (sat:80-85%); and umbilical artery pO_2=20mmHg (sat:40-50%) (92,93). These values demonstrate a rather inefficient placental oxygen transfer, and a relative hypoxic intrauterine environment of the developing fetus. This can partly be explained by the maternal and fetal blood flow arranged in a multivillous system (73). However, this arrangement should ensure the umbilical vein to equilibrate at least with the uterine vein (74,75). Another contributor of the inefficient placental transfer might be mismatch of maternal and fetal placental perfusion and arterio-venous anastomoses (92,94,94). In spite of the relative hypoxic intrauterine environment fetal adaptations ensure that fetal oxygen supply can be similar to that of extra-uterine life. One of the mechanisms is the high blood perfusion of fetal organs. Because of

the high FHR and the parallel working ventricles the fetal cardiac output is v(94)ery high (300ml/kg/min) when compared to adults (75ml/kg/min) (95). Furthermore the high fetal hgb concentration and the high oxygen affinity of fetal hgb increase the oxygen transport capacity of fetal blood (96).

Placental insufficiency

A normal placentation followed by an adequate placental growth and maturation is the basis of normal fetal growth and development. Abnormal placentation is associated with miscarriage, placental abruption, pre-eclampsia, FGR and intrauterine fetal death (97,98). Cordocentesis performed in FGR fetuses have demonstrated hypoxia, acidosis (75,99), hypoglycemia and reduced levels of essential amino acids (89,91,100) indicating severely impaired placental transport function. The FGR placenta has been extensively investigated for better understanding of this serious condition. The characteristics of the FGR placenta are summarized in the following section.

In cases of FGR placental bed biopsies have demonstrated impaired trophoblast migration into the myometrium and failure of the normal physiological transformation of spiral arteries into low resistance vessels (80), which leads to increased thrombosis and placental infarction. Ultrasound Doppler flow measurement of uterine blood flow has demonstrated increased resistance and a reduction in blood flow of 50% (97). It is generally believed that this maternal hypo-perfusion of the placenta leads to intervillous hypoxia which affects the development of the fetal villous tree and changes the general placental metabolism (71). Hypoxia stimulates fetal angiogenesis and branching of the villus. Biopsies of the FGR placenta demonstrate accelerated maturation and a 40% increase in capillary volume fraction (72). This adaptive response increases placental oxygen transfer, as the surface area of the villous tree is increased and the thickness of the placental membrane is decreased. To a certain limiting these changes prevent fetal hypoxia. If, however, the metabolic demands of the fetus and the placenta cannot be met fetal hypoxia and acidosis might develop.

In the placenta specific hypoxic changes can be demonstrated (70). Biopsies of FGR placentas have demonstrated malformation of the villus tree, especially the gas-exchanging terminal villi. These villus trees consist of fewer branches, and the terminal villi demonstrate a reduced number of capillaries, increased fibrosis and accelerated trophoblast apoptosis (97,101). Furthermore the placental stem vessels show wall hypertrophy consistent with chronic vasoconstriction and loss of local paracrine vascular control of maternal and fetal placental perfusion (70,102). The altered architecture of the villous tree and increased vasoconstriction of the stem vessels increase the total vascular resistance on the fetal side of the placenta, which is reflected by the resistance of the umbilical artery. When examined by Doppler ultrasound the diastolic blood flow of the umbilical artery is decreased and in severe cases it is even reversed (76).

Macroscopic examination of the FGR placenta also demonstrates certain characteristics. When compared to the normal placenta the FGR placenta is smaller and very often it has an abnormal shape with increased thickness, which is directly correlated to poor neonatal outcome (103,104).

Fetal physiology

Our knowledge about fetal physiology is based on invasive experimental animal studies mainly on sheep. In these studies invasive methods such as injection of radioactive microspheres (105-107) and insertion of vascular catheters (108) can be used for investigating fetal circulation and oxygenation in different experimental settings. Non-invasive investigation of fetal circulation can be provided by the ultrasound Doppler flow measurement. And over the last three decades the human fetal circulation has been extensively investigated by the ultrasound Doppler technique (109,110). Normal blood flow has been described for a great number of fetal vessels, and abnormal blood flow has been correlated with fetal hypoxia and acidosis (111-113). Currently ultrasound Doppler examination of fetal and placental blood flow is one of the major tools in fetal monitoring, as demonstrated by Figure 9 (65,114).

Fetal circulation

The umbilical blood flow is determined mainly by the resistance of the umbilical vessels in the fetal side of the placenta. The fetal circulation is characterized a hyperkinetic system with a low

resistance (115), and so it is very different from the adult circulation. The ventricles of the fetal heart pump in parallel circuits, and the intraventricular pressure is similar in the two ventricles (116). The well oxygenated left ventricular blood is directed to the upper part of the fetus including the brain. The less oxygenated right ventricular blood is directed to the placenta as well as the lower part of the fetus including the lungs and the viscera. In contrast to the adult heart, the fetal heart exhibits right-sided dominance with approximately 60% of the total cardiac output going through the right ventricle (117).

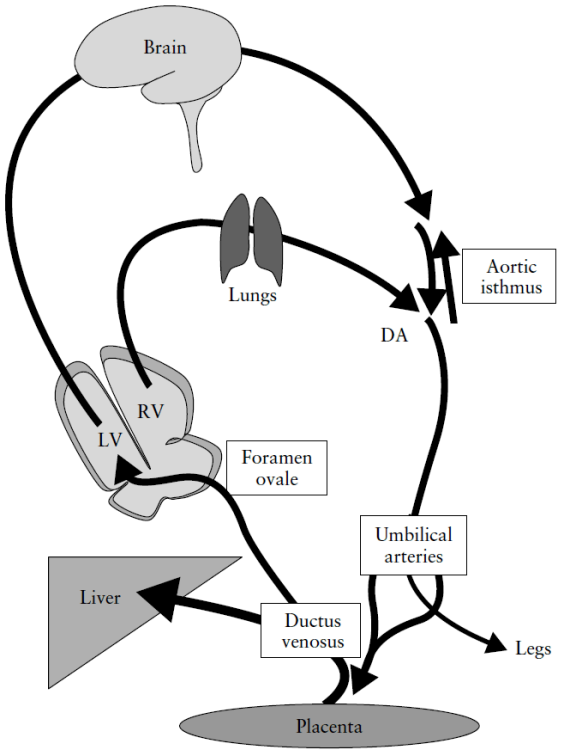

Figure 12 The route of oxygen rich blood reaching the fetus via the umbilical vein. Three important shunts; 1)Ductus venosus, 2)Foramen ovale, and 3)Ductus arteriosus (DA) form dynamic connections between the two parallel circuits of the fetal circulation. (118)**.**

Three shunts, as demonstrated in Figure 12, divert blood between the two circuits, thereby determining the distribution of nutrients and oxygen between the cardinal fetal organs such as the liver, heart and brain (109,110,118). The first fetal organ to receive blood directly from the

placenta is the fetal liver. The circulation of the fetal liver is rather complex as it has two main vascular sources: the oxygen rich umbilical vein and the less oxygenated portal vein (119). The blood supply of the fetal liver is shown in Figure 13 (120).

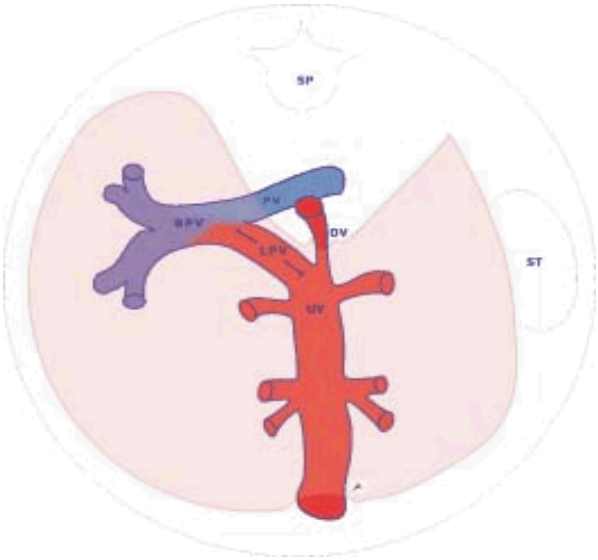

Figure 13 The blood supply of the fetal liver. The well oxygenated (red) umbilical vein (UV) and the poorly oxygenated (blue) portal vein (PV). Left portal vein (LPV). Ductus venosus (DV). Right portal vein (RPV). Spine (SP). Stomach (ST) (120)**.**

These sources are unevenly distributed as the left side of the liver primarily receives umbilical vein blood, and the right side of the liver receives a mixture of the two (121). The contribution of umbilical vein blood to the right side of the liver is directly related to the degree of ductus venosus shunting, as the ductus venosus leads oxygen rich umbilical vein blood away from the fetal liver to the heart and brain (109). The ductus venosus is embedded in the liver parenchyma, and it is considered the first shunt in the fetal circulation. The degree of shunting depends on the oxygen supply of the fetus as shunting is increased during hypoxia (122). Ductus venosus shunting decreases with increasing gestational age from 30% at 20 weeks to 20% at term; this is a consequence of the increasing metabolic demand of the fetal liver during normal pregnancy (123). The next shunt in the fetal circulation is the foramen ovale – the connection between the right and the left atria. Guided by the crista dividens there is a preferential streaming of oxygen rich

umbilical vein blood directly through the foramen ovale to the left side of the fetal heart. This shunt is of critical importance for the oxygenation of the myocardium and the fetal brain. In normal pregnancy the degree of shunting at mid gestation is 33% of the total fetal cardiac output and 75% of the left ventricular output (117). The third shunt is the ductus arteriosus located between the pulmonary arterial trunk and the descending aorta. The ductus arteriosus diverts right ventricular blood directly to the lower fetal body and the placenta without entering the pulmonary circuit. In the second trimester 40% of the total fetal cardiac output and 90% of the right ventricular output is directed through the ductus arteriosus (117). The last vessel to be mentioned is the aortic isthmus, the segment of the fetal aorta between the origin of the left subclavian artery and the entry of the ductus arteriosus to the descending aorta. The aortic isthmus is considered the communication or a watershed area between the two parallel circuits in the fetal circulation. The direction of blood flow through the aortic isthmus is determined by cerebral and placental vascular resistance. In normal pregnancy 10% of the total cardiac output passes through the aortic isthmus and there is a forward flow during both systole and diastole (124).

Fetal response to acute hypoxia

In animal models acute fetal hypoxia can be induced experimentally by reducing maternal oxygen supply. It has been demonstrated that acute changes in maternal oxygenation do not alter the blood flow to the pregnant uterus (102,125) and the oxygen consumption of the placenta remains rather constant during acute changes in uterine oxygen supply (126). During acute hypoxia the fetus initially compensates by increasing the oxygen extraction fraction. It has been demonstrated that fetal oxygen metabolism can be maintained even if the oxygen supply is reduced by 50% (86,92). However, below a certain threshold fetal hypoxia will develop followed by several changes in the fetal circulation. Initially a chemoreceptor response stimulates parasympaticus which reduces FHR. In the absence of acidosis cardiac output and blood pressure are maintained or even increased because of a sympaticus mediated peripheral vasoconstriction (127). Furthermore redistribution of fetal blood tends to maintain oxygenation of vital fetal organs such as the fetal brain and heart (111,118). The first circulatory response to hypoxia is an increase in cerebral blood

flow which is caused by reduced vascular resistance of the cerebral vessels. This change, well known as the brain sparing mechanism, tends to maintain cerebral oxygenation in spite of hypoxia. It can be identified by ultrasound Doppler flow measurements of the middle cerebral artery demonstrating increased diastolic blood flow (113,128,129). As cerebral vascular resistance is reduced there is a gradual change in the direction of the blood flow of the aortic isthmus, which reflects the balance between the two fetal circulatory circuits. Initially the blood flow is reversed only in diastole with the progression towards negative flow throughout the cardiac cycle (124,130). The next step in the redistribution of fetal blood during hypoxia is increasing degree of ductus venosus shunting (122,131-133). The ductus venosus shunts oxygen rich umbilical vein blood away from the fetal liver, through the foramen ovale, directly to the left heart and fetal brain. Experimental studies have demonstrated that the ductus venosus is regulated by hypoxia, which causes the ductus venosus to dilatate (134,135). During hypoxia increasing amounts of oxygen rich blood is diverted away from the fetal liver to increase the oxygenation of the fetal heart and brain. The cerebral oxygenation is maintained at the expense of the liver, especially on the right side of the liver which looses its supply of oxygen rich umbilical vein blood (121). The ductus vensus waveform has been extensively studied by Doppler ultrasound examination. The ductus venosus waveform reflects fetal cardiac function. Abnormalities such as increased PI, reduced velocity or even reverse blood flow during atrial contraction (negative A-wave) are associated with increasing degrees of cardiac failure and fetal acidosis, and it is a gestational age independent predictor of adverse neonatal outcome (132,136,137). During metabolic acidosis the centralization of fetal blood flow cannot be maintained (138). Cardiac failure develops as a consequence of (1) increased afterload caused by progressive peripheral and placental resistance and (2) impaired myocardial contractility which is a direct effect of acidosis (108,139,140). Initially, diastolic failure occurs with elevated central venous pressure. This is followed by systolic failure in which the forward function of the heart is affected, leading to fetal hypotension, vascular collapse and intrauterine fetal death (140-142).

Fetal response to chronic hypoxia

Chronic hypoxia develops if hypoxia is introduced gradually and thereby it can be sustained for a longer period before progression into deteriorating fetal metabolic acidosis. Fetuses suffering

from placental insufficiency are subjected to some degree of chronic hypoxia as well as reduced levels of nutrients such as glucose and amino acids (99). These fetuses exhibit similar redistribution of fetal blood flow as demonstrated during acute hypoxia. Furthermore, they are characterized by increased hematocrits and tachycardia probably mediated by an increased level of chatecolamines (143). Fetal oxygen consumption is gradually reduced by complicated fetal adaptations such as slowing fetal growth and by altering fetal behavioral pattern (138). When fetal oxygen metabolism is decreased the balance between fetal oxygen supply and consumption might be reestablished (138). The fetal consequence of chronic hypoxia is not only intrauterine FGR but also re-programming of fetal metabolism and tissue development, which provides an increased risk of metabolic disease in adult life (144-146). The intrauterine exposure to under-nutrition might alter fetal metabolic set points (147). What seems adequate during intrauterine life turns out to be a disadvantage in nutrient-rich extrauterine life.

Fetal response to maternal hyperoxia

Maternal hyperoxia can be induced by increasing the oxygen content of the breathing air. Several studies have been performed with the purpose of investigating the fetal effects of maternal hyperoxia. In healthy sheep, monkeys and humans it has been demonstrated that maternal hyperoxia does increase fetal oxygenation. Different methods have been used to evaluate fetal oxygenation, including internal fetal electrodes and vascular catheters (148-151), transcutaneous pO_2 measurements (152) and blood-gas analysis of umbilical blood provided by cordocentesis (153). The physiological explanation for this increase in fetal oxygenation is likely due to an increased pO_2 gradient across the placental membrane, which drives the oxygen transfer. Maternal arterial blood is already fully saturated at room air, and that is why hyperoxia does not increase maternal hgb saturation. This is in contrast to the saturation of fetal blood which is only 80% (92), and therefore the increase in fetal pO_2 mediates an increase in fetal hgb saturation (87).

The effect of hyperoxia on fetal circulation has been extensively studied by Doppler ultrasound examination. In FGR fetuses it has been demonstrated that maternal hyperoxia normalizes the resistance of the middle cerebral artery (154-156). In FGR fetuses the circulatory hyperoxic response even has been suggested as a predictor of fetal outcome – with the non-responder fetus

having the poorer outcome (157,158). In normal fetuses, the circulatory effect of maternal hyperoxia is more discrete and the studies have been conflicting. A majority of studies on sheep as well as human fetuses have demonstrated an increase in the cerebral resistance above normal (149,159-161). This finding led to some concern regarding the oxygenation of the fetal brain during hyperoxia. However, studies of fetal sheep using internal tissue pO_2 sensors have demonstrated an increase in cerebral oxygenation during maternal hyperoxia (151,162). Therefore, the observed cerebral vasoconstriction should be considered harmless. Several studies have investigated the effects of hyperoxia on the fetal heart, but no alteration in myocardial function or left/right-ventricular balance could be found (154,159,160). Only one study investigated the effect of hyperoxia on ductus venosus blood flow in normal human fetuses. The study demonstrated that the velocity of ductus venosus blood flow was increased which indicated ductus venosus constriction and a reduced degree of shunting during hyperoxia (163).

The effects of maternal hyperoxia on fetal movements and FHR have also been investigated. In normal fetuses no significant effects were found. In FGR fetuses, however, maternal hyperoxia did increase fetal movements (164), and FHR showed an increasing number of accelerations and increasing heart rate variability (164,165). When returning to normoxia, an increasing number of decellations were described in one study (164). This led to concerns regarding potential adverse fetal effects of maternal hyperoxia, with the major concern being possible oxygen mediated placental vasoconstriction. In-vitro studies of umbilical vessels have demonstrated vasoconstriction in response to hyperoxia (166,167). However, these findings could not be reproduced in several in-vivo studies investigating the hyperoxic response of the uterine and umbilical vessels by ultrasound Doppler flow measurements (125,168,169).

Materials and methods

This section describes how we used the BOLD MRI technique in our studies. Following is a description of the software challenge we faced, and the impact it had on our studies. Furthermore, the method of each study is presented separately.

General aspects

The T2* weighted BOLD MRI scan

The BOLD scans consisted of an initial basal phase of normoxia followed by episodes of altered maternal oxygen supply inducing fetal and placental hypoxia as well as hyperoxia. The BOLD response was assessed by drawing ROIs in selected fetal organs and in the placenta. Large ROIs covering the entire organs were drawn to assess changes in total organ oxygenation, and smaller ROIs were drawn in the fetal liver and the placenta to assess regional oxygenation changes within these organs. A normalization of the BOLD signal was performed using the normoxic BOLD signal as a reference in each ROI.

$$(4) \qquad \text{Normalized BOLD signal (x)} = (S_X - S_{Normox})/S_{Normox} \times 100\%$$

S_X indicates the absolute BOLD signal at time x and S_{Normox} indicates the absolute BOLD signal at steady state level during normoxia. For each organ the BOLD response (ΔBOLD) could be estimated and expressed as a percentage of the normoxic reference level. The hyperoxic BOLD response was estimated by the following formula

$$(5) \qquad \Delta BOLD_{Hyperox} = (S_{Hyperox} - S_{Normox}) / S_{Normox} \times 100\%$$

$S_{Hyperox}$ and S_{Normox} indicate the absolute BOLD signal at steady state level during hyperoxia and the normoxia, respectively. The scan parameters of the three studies are listed in the following Table 2. The BOLD scans are T2* weighted as they use a gradient echo sequence with a long TE and a long TR.

Study	System	TE (ms)	TR(ms)	Flip angle	Sequence	Slice thickness/gab
The sheep study	Philips	40	2500	90°	Gradient echo	6 mm/ 9mm
The human fetal study	Philips	40	1800	30°	Gradient echo	6mm/9mm
The human placental study	GE	50	8000	90	Gradient echo	6mm/9mm

Tabel 1 The scan parameters used in the three studies

Placental T2* measurement

In the human placental study, placental T2* relaxation time was estimated during normoxia and hyperoxia. Multiple gradient echo sequences were performed with 16 echo-times between 3.0 and 67.5 ms, and T2* relaxation curves were drawn by plotting the mean MRI signal of the placental ROI for each echo-time during normoxia and hyperoxia (Figure 14).

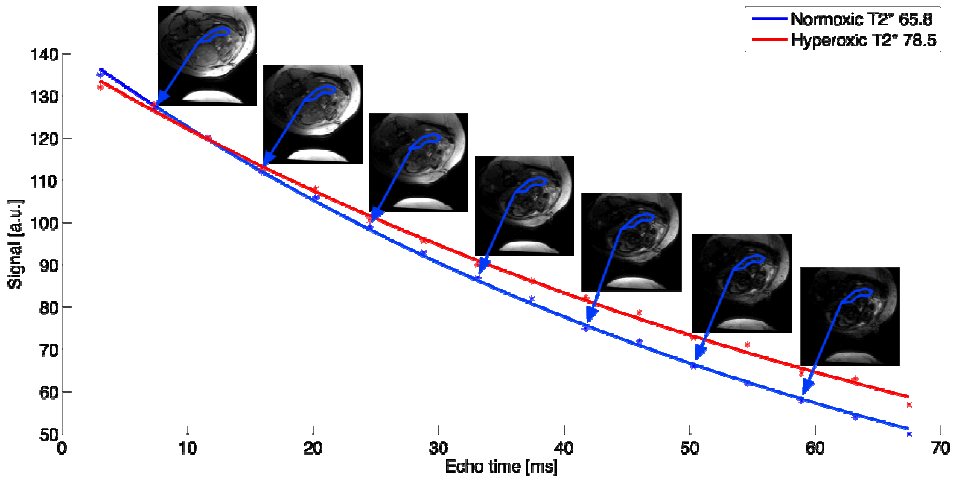

Figure 14 Placental T2* decay curves obtained during normoxia (blue) and hyperoxia (red) by plotting the mean MRI signal of the placental ROI for each echo time (TE). A number of MRI images obtained at different echo times are included in the figure.

The normoxic and hyperoxic placental T2* relaxation time was calculated by fitting the exponential T2* decay curve (Formula 1) using a non-linear least squares fitting algorithm, and the hyperoxic increase in placental T2* value (ΔT2*) was estimated. The optimal echo-time for the T2* weighted BOLD scan was derived from the T2* relaxation curves of normoxic and hyperoxic placental tissue (Figure 14), as the BOLD response reflects the difference between the curves at each echo-time. The T2* curves indicate that by increasing the echo-time the hyperoxic BOLD response could be increased. However, if the TE is too long, the MRI signal intensity is decreased below the background noise level. On the basis of the placental T2* decay curves the scan parameters of the BOLD scan was changed in the placental study. In order to optimize the placental BOLD response, TE was increased from 40 to 50 ms (Figure 14).

The software problem

In the sheep and the human fetal studies the raw data was analyzed using unpatented software developed in California by Fernando Barrio, M.Sc, more than 15 years ago. For several years this software was used for research in the Department of MRI at Aarhus University Hospital; however, a detailed knowledge was lacking about the exact processes of the software. When the MRI system was upgraded I 2009, the raw data was no longer compatible with the old software. We tried to contact the developer of the software, but unfortunately this person was retired and not available for support. It was not possible to change the old software, so MATLAB-based software was developed. The new software deals with DICOM data instead of raw data, and it includes no filtering or transformation of data. The difference between the old and new software is demonstrated in Figure 15, by showing the same data from one patient processed by the two different softwares.

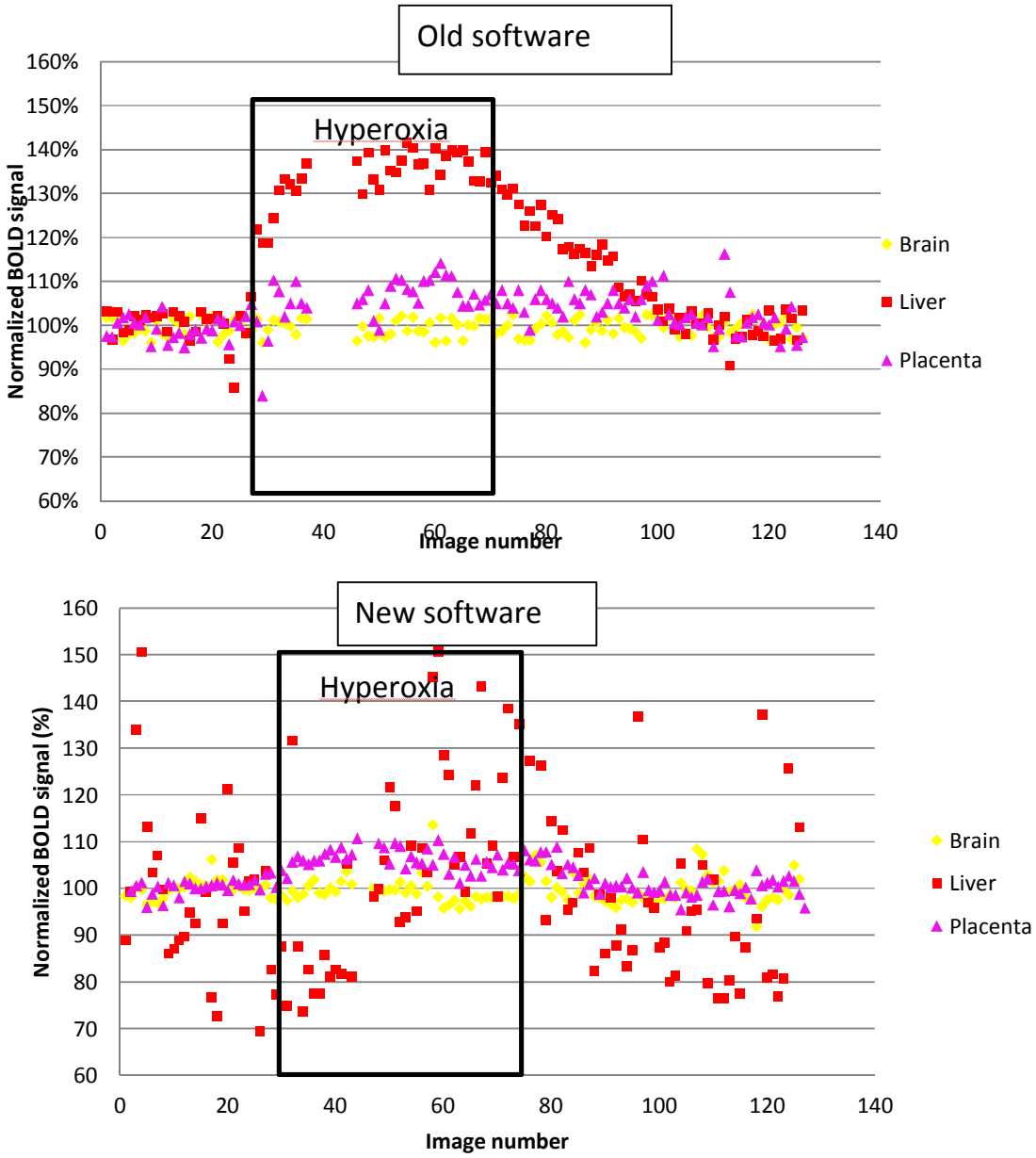

Figure 15 The same set of data processed by either old software (top) or new MATLAB software (bottom).

When using the MATLAB software, the BOLD signal of the fetal liver is interrupted by artifacts; however, the BOLD signal of the fetal brain and the placenta remains intact. This finding can be explained by fetal movements. The fetal head is fixed in the maternal pelvis and the placenta is only moving according to maternal breathing movements; however, the fetal liver is subject to

movement artifacts caused by fetal rotation and kicking movements. During fetal movements the distance between the fetal organs and the coil is altered, which influences the absolute BOLD signal. When using the MATLAB software the changes in the BOLD signal caused by movements outweigh the change in the BOLD signal induced by altered tissue oxygenation.

Because of the limitations of the MATLAB software, the future focus of our study became the placenta rather than the fetal organs. However, biomedical engineers at Aalborg University (Peter Brønnum Nielsen M.Sc, Ph.D and Lasse Riis Østergaard, Associate professor, M.Sc, Ph.D) leads a student project in which an additional motion correction tool for the MATLAB software including a bias field correction will be developed.

The method of each study

The sheep study: Papers 1 + 2

This study was performed at the Department of Clinical Medicine and the MRI Research Center at Aarhus University Hospital in Skejby. Eight ewes carrying singleton fetuses at gestation 125 days (term=145 days) were included in this study. One animal was excluded because of cardiac arrest during induction of anesthesia. Another fetus demonstrated a hepatic hematoma following insertion of the oxygen sensor and this fetus was excluded from the regional examination of fetal liver oxygenation.

Animal preparation: The animals were sedated with Rompune 2.5mg and transported to the hospital unit. Anesthesia was induced by Ketamine 2 mg/kg and Dormicum 0.25mg/kg. Orotracheal intubation was performed followed by artificial ventilation, and anesthesia was maintained by Isoflurane 1.5% in an O_2 /N_2O mixture. Maternal arterial blood gas analysis was provided by catheters in the left common carotid artery. Ruminants develop a considerable amount of gas in the digestive tract; therefore, a gastic probe was installed to reduce the accumulation of intra abdominal gas. To ensure adequate ventilation in spite of the increasing intraabdominal pressure, the expiratory CO_2 was monitored throughout the anesthesia, and pCO_2 was kept below 7.0 kPa. Internal oxygen sensitive optodes were inserted for direct measurement of fetal oxygenation. The optodes were inserted into the fetal organs guided by ultrasound.

Initially, we aimed to insert optodes in several fetal organs for simultaneous oxygenation measurements. However, because of technical difficulties the optodes were only inserted and well functioning in the fetal liver of 4 out of 7 animals. The optode consisted of a 0.9 mm thin fiber-optic cable coated with fluorescent sensor material at the tip. The principle of measurement is dynamic luminescence quenching, which is directly proportional to the local tissue pO_2 (170). When compared to conventional oxygen sensitive electrodes, this optode has the advantage of not consuming oxygen during measurements.

BOLD MRI scan: The ewe was transported to the MRI suite for the BOLD MRI scan. The anesthetized ewe was placed in a left lateral position with a phased array abdominal radio-frequency coil placed over the uterus for optimal fetal imaging. Initially fast axial and coronal T2 weighted scans were performed for anatomic location of the fetus and for planning the BOLD MRI scan to follow. This fetal BOLD MRI scan was performed using varying levels of maternal oxygen content of the ventilated gas (14% O_2 – 100% O_2). The scan parameters are presented in Table 1.

Data handling: The raw MRI data was transferred to an external workstation and filtered using dedicated software. ROIs were drawn corresponding to the fetal liver, spleen, kidney and brain and motion correction was performed manually in each frame in order to keep the ROI inside the selected fetal organ. Due to the experimental setup which included general anesthesia, the fetal movements were greatly reduced. For each ROI the absolute BOLD signal versus time curve was calculated. Mean curves were drawn for each organ based on the data from each of the 7 fetuses. Furthermore, in the fetal liver the regional oxygenation was investigated by several smaller ROIs distributed from the right to the left side of the liver. By comparing the BOLD signal of the very left and the very right ROI of the fetal liver the left-right oxygenation difference was estimated. In the investigation of regional liver oxygenation, a normalization of the BOLD response was performed using the normoxic BOLD signal as a reference in each ROI (Formula 5).

The human fetal study (Paper 3)

The human fetal study was performed at the Department of Obstetrics and Gynecology and the MRI Research Center at Aarhus University Hospital in Skejby. Eight healthy women carrying

singleton fetuses at gestational week 28 to 34 were included in the study. Prior to the BOLD MRI scan a comprehensive fetal ultrasound examination was performed including fetal weight estimation, amniotic fluid index, and Doppler blood flow examination of the following vessels: uterine artery, umbilical artery, middle cerebral artery and ducus venosus. For each fetus all measurements were within the normal range.

BOLD MRI scan: The pregnant women were placed in a left lateral position to avoid vena cava compression during the MRI scan, and a multi-receiver cardiac surface coil was placed over the abdomen. Initially fast coronary and axial T2 weighted scans were performed for the anatomic location of the fetus and for planning the following BOLD MRI scan. The scan parameters are presented in Table 1. Maternal hyperoxia was induced by breathing in a Hudson non-rebreathing facial mask with the oxygen supply of 100%O_2 at 12 liter/minute. Because the facial mask was not perfectly tight, the actual maternal oxygen supply was approximately 70%.

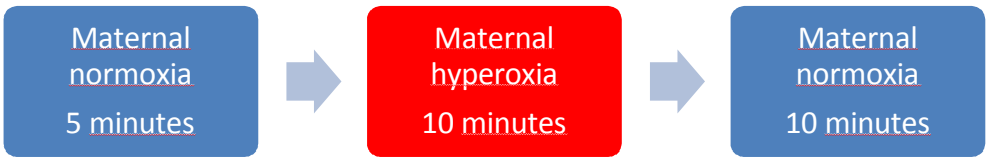

Figure 16 The maternal oxygen supply during the BOLD MRI scan in the human fetal study.

As indicated by Figure 16 each scan lasted a total of 25 minutes, including three consecutive oxygenation episodes: (1) normoxia: 21% O_2 lasting 5 minutes, (2) hyperoxia: 70% O_2 lasting for 10 minutes and finally (3) normoxia: 21% O_2 lasting 10 minutes. The facial mask was applied and removed from the womens' faces without interference with the BOLD scan and maternal position inside the magnet.

Data handling: The MRI raw data were transferred to an external workstation and processed by dedicated software equivalent to the software previously used by our group in the sheep study. ROIs were drawn according to the fetal liver, spleen, kidney brain and the placenta, and motion correction was performed manually in each frame. In this study no anesthesia was included, and

the fetal movements were greatly increased when compared to the sheep study. In each ROI a normalization of the BOLD signal was performed using the normoxic starting BOLD signal as a reference (Formula 4) and normalized BOLD versus time curves were drawn. The calculation of the hyperoxic BOLD response (ΔBOLD) was based on the mean BOLD signal of the last 5 minutes of the hyperoxic episode in each individual (Formula 5). Mean ΔBOLD values were calculated for each organ base based on data from all eight individuals, and ΔBOLD was tested using a paired t-test, in which a p-value < 0.05 was considered statistically significant.

The human placental study (Papers 4+5)

This study was performed in the Department of Obstetrics and Gynecology and the Department of Radiology at Aalborg University Hospital. A total of 24 healthy pregnant women carrying singleton fetuses at gestational weeks 24 to 40 were included in this study. Paper 4 is based on the first 8 women included, and paper 5 is based on all 24 women. At inclusion a comprehensive fetal ultrasound examination (equivalent to the human fetal study), and all measurements were within normal range.

Placental BOLD MRI: The pregnant woman was placed in a left lateral position, and the cardiac surface coil was placed over the abdomen. T2 weighted scan was performed for the anatomic position of the fetus. The scan parameters are presented in Table 1. As shown in figure 17 the BOLD MRI scan lasted a total of 10 minutes including 2 consecutive oxygenation levels: normoxia 21% O_2 (5min.) and hyperoxia 70% O_2 (5min.). Maternal hyperoxia was induced by using a Hudson non-rebreathing facial mask.

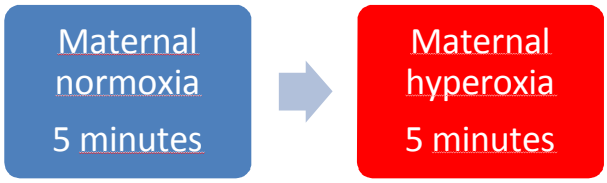

Figure 17 The protocol of the maternal oxygen supply during the BOLD MRI scan in the human placental study.

Placental T2* measurement: The placental T2* relaxation time was estimated during normoxia and hyperoxia by fitting the mono-exponential placental T2* decay curve (Formula 1) of each

oxygenation level. Furthermore, the reproducibility of placental T2* was investigated on three levels: 1) Slice-to-slice reproducibility (n=24), 2) Scan-to-scan reproducibility: repeat scan within a few minutes (n=17) and 3) Session-to-session reproducibility; repeat scan session within 45 minutes (n=8). Bland-Altman plots were performed and 95% limits of agreement were calculated for each level. The relation between placental T2* and gestational age was investigated and tested using a linear regression analysis. Furthermore, the increase in placental T2* value during hyperoxia (ΔT2*) was estimated and tested using a paired t-test. In each test a p-value < 0.05 was considered statistically significant.

Data handling: The DICOM data were transferred to a computer equipped with the new MAT-LAB software. Initially the appearance of placenta in the BOLD image, and the visual hyperoxic changes were described. The total placental oxygenation was estimated by one ROI covering the entire placenta. Furthermore, the regional placental oxygenation was investigated by two smaller ROIs drawn in the bright and dark placental region. Normalization of the BOLD signal was performed using the normoxic BOLD signal as a reference in each ROI (Formula 4). For each ROI the hyperoxic BOLD response (ΔBOLD) was calculated (Formula 5), using the mean BOLD signal of last 2 minutes of the hyperoxic episode in each fetus. ΔBOLD was calculated in each individual and mean ΔBOLD was calculated for the total and regional placenta, respectively.

Summary of results

In the following section the main results of the three studies are summarized. For detailed information references are made to the five publications forming the basis of this thesis.

The sheep study (Papers 1+2)

In four fetuses the changes in fetal liver oxygenation were estimated directly by the oxygen optodes. In these fetuses a close relationship between changes in fetal liver oxygenation and changes in the BOLD signal of the fetal liver was demonstrated (Figure 18); though, it could be concluded, that changes in the BOLD signal reflect changes in fetal tissue oxygenation (25).

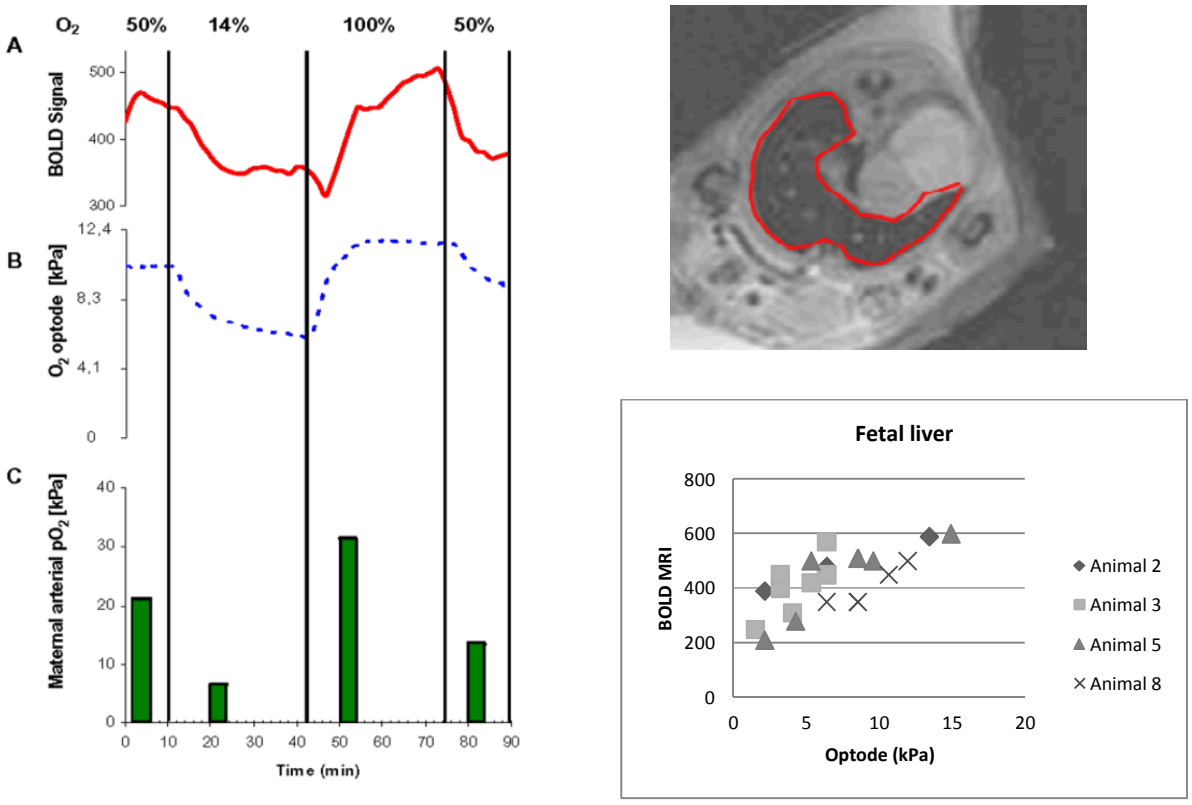

Figure 18 Left: The association between changes in the BOLD signal of the fetal liver (A), the direct measurement of fetal liver oxygenation (B) and maternal arterial pO_2 (C) in one fetus. Top right: BOLD image of the sheep fetus. The fetal liver is selected as the region of interest. Bottom right: The association between the BOLD signal of the fetal liver and direct measurement of fetal liver oxygenation in 4 sheep fetuses (25)**.**

At varying oxygenation levels the corresponding changes in the BOLD signal of the placenta and the fetal spleen, liver, kidney and brain were investigated. The findings in one fetus are shown in Figure 19.

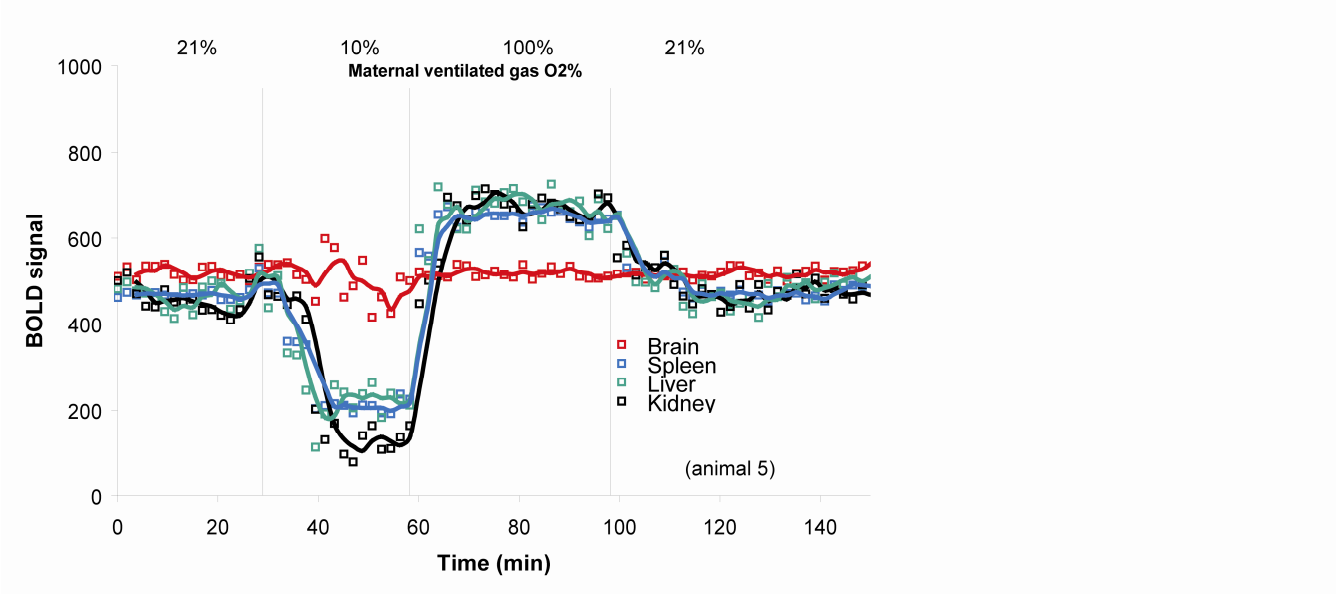

Figure 19 The timeline of changes in the BOLD signal of the fetal brain, spleen, liver and kidney in one fetus during maternal hypoxia (10% O_2) and hyperoxia (70% O_2) (25).

During hypoxia the BOLD signal of the fetal liver, spleen and kidneys was decreased and during hyperoxia it was increased. In contrast, the BOLD signal of the fetal brain did not change during the experiment. This was a consistent finding in all of our seven fetuses (25).

The BOLD signal of 7 smaller regions of the fetal liver was investigated. The distribution of the ROIs in the fetal liver and the changes in BOLD signal of each ROI are demonstrated in Figure 20.

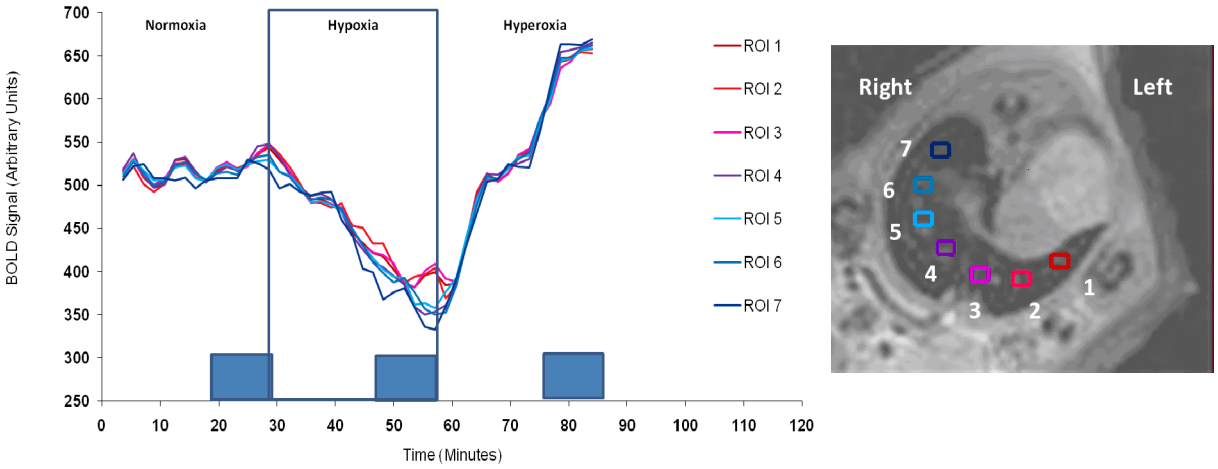

Figure 20 Right: BOLD image of the fetal liver with 7 ROIs placed at regular intervals from the left to the right side of the liver. Left: The changes in BOLD signal of the 7 ROIs during maternal hypoxia and hyperoxia. The blue bars indicate the values included to calculate the BOLD response (ΔBOLD) presented in Figure 21 (171)**.**

During hypoxia the BOLD signal of each region was reduced, and during hyperoxia it was increased. However, during hypoxia a remarkable difference between the regions was demonstrated. The BOLD signal of the right-sided regions was reduced to a lower level than the left-sided regions. Figure 21 demonstrates the BOLD signal of the very left and the very right ROI of each fetus. The left-right difference is calculated during hyperoxia and hypoxia in each fetus, and the mean values are calculated for the total group during each oxygenation level.

Fetus ID-number	Reference (Normoxia)	Hyperoxia			Hypoxia		
	$BOLD_{Reference}$ Entire fetal liver Arbitrary units (100%)	$BOLD_{Left}$ ROI 1 Arbitrary units (%)	$BOLD_{Right}$ ROI 7 Arbitrary units (%)	$\Delta BOLD_{Left-right}$ ROI 7 - ROI 1	$BOLD_{Left}$ ROI 1 Arbitrary units (%)	$BOLD_{Right}$ ROI 7 Arbitrary units (%)	$\Delta BOLD_{Left-right}$ ROI 7 – ROI 1
1	517	627 ± 26 (121,2)	631 ± 27 (122,0)	-0.8 %	407 ± 65 (78,7)	390 ± 70 (75,4)	3.3 %
3	401	439 (109,5)	458 (114,2)	-4.7 %	364 (90,8)	339 (84,5)	6.2 %
5	477	606 (127,0)	598 (125,3)	1.7 %	247 (51,8)	216 (48,3)	6.5 %
6	440	636 (144,5)	641 (145,7)	-1.1 %	382 (86,8)	365 (82,9)	3.9 %
7	443	494 (111,5)	516 (116,5)	-5.0 %	368 (83,1)	355 (80,1)	2.9 %
8	431	478 (110,9)	458 (106,3)	4.6 %	348 (80,7)	312 (72,4)	8.4 %
Mean				-0.9 %			5.2 %
SD				3.7 %			2.2 %
Paired t-test							P=0.002

Figur 21 The BOLD signal (arbitrary units) of the very left ROI ($BOLD_{left}$) and the very right ROI ($BOLD_{right}$) of the fetal liver. The left-right difference is estimated during hyperoxia and hypoxia in each fetus and for the group as a total using the normoxic BOLD signal of the total liver as a reference ($BOLD_{Reference}$) in each ROI (171)**.**

During hyperoxia the mean left-right difference ($\Delta BOLD_{Left-right}$) was -0.9% ± 3.7 (mean ± SD), and during hypoxia it was 5.2% ± 2.2 (mean ±SD). The left-right difference was significantly increased

during hypoxia (p=0.002) (171). Furthermore, a significant linear correlation between the hypoxic left-right oxygenation difference and the degree of hypoxia was found (Figure 22).

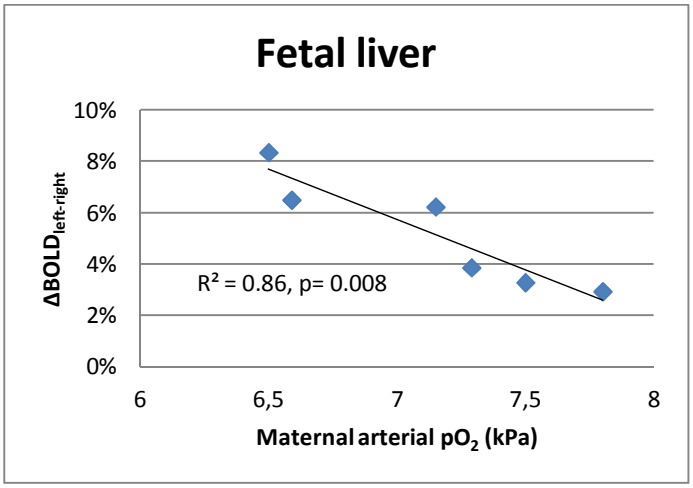

Figure 22 The correlation between the left-right difference in fetal liver oxygenation and the degree of hypoxia indicated by maternal arterial pO_2. Linear regression is performed and Pearson correlation coefficient (R) and the corresponding p-value are presented in the figure (171) **.**

The human fetal study (Paper 3)

In the human fetus the changes in the BOLD signal in a number of fetal organs was investigated during maternal hyperoxia. In the BOLD images the ROI was drawn in different locations according to the fetal organs as demonstrated in Figure 23.

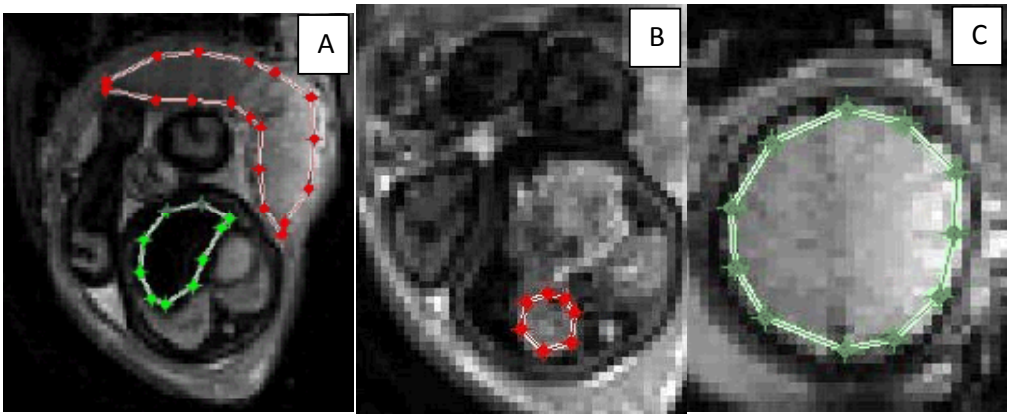

Figure 23 BOLD images of the human fetus and the placenta (axiale planes). The ROIs are drawn according to several fetal organs and the placenta. (A) Placenta (red) and fetal liver (green). (B) Fetal kidney (red). (C) Fetal brain (green) (28)**.**

For each ROI the changes in the normalized BOLD signal can be investigated during maternal hyperoxia as shown in Figure 24. The normalization of the BOLD signal is performed in each ROI using the initial normoxic BOLD signal as a reference.

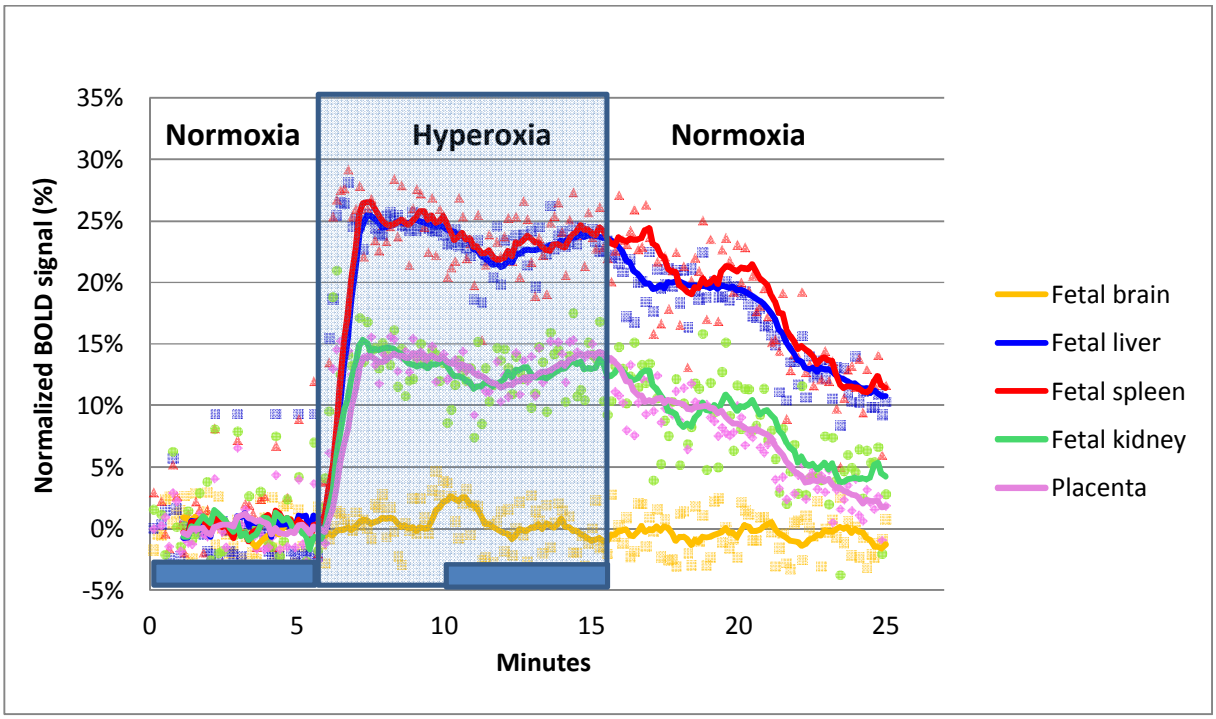

Figure 24 Changes in normalized BOLD signal during maternal hyperoxia. Each organ is identified by the color of the curve. The blue bars indicate the value obtained for calculation of the hyperoxic BOLD response (ΔBOLD) (28)**.**

During hyperoxia the BOLD signal of the fetal liver, spleen and kidney as well as the placenta was increased. However, the BOLD signal of the fetal brain remained constant. A consistent pattern was demonstrated in the 8 individuals as the BOLD signal of the fetal liver and spleen was doubled when compared to the placenta, and the fetal kidney. In all individuals the BOLD signal of the fetal brain did not change during hyperoxia.

The hyperoxic BOLD response (ΔBOLD) was calculated for the fetal organs and the placenta and data are shown in Figure 24.

Fetus Number	Gestational age (weeks + days)	Fetal weight UL estimated (gram)	ΔBOLD Fetal Liver (%)	ΔBOLD Fetal Spleen (%)	ΔBOLD Fetal Kidney (%)	ΔBOLD Placenta (%)	ΔBOLD Fetal Brain (%)
1	28+2	1381	14.6	15.3	5.2	5.5	-0.3
2	28+0	1350	-0.6	2.2	0.5	0.5	-0.01
3	28+6	1555	33.3	33.2	14.4	13.1	0.8
4	27+4	1038	13.9	16.0	5.3	4.7	0.7
5	34+1	2227	22.9	23.2	12.7	12.9	-0.3
6	33+6	2392	4.8	5.6	0.3	2.2	0.1
7	33+2	2190	9.1	9.0	3.8	4.6	1.5
8	33+6	2273	16.0	17.4	7.3	8.5	0.3
Mean (±SEM)			14.3 (±3.7)	15.2 (±3.5)	6.2 (±1.8)	6.5 (±1.6)	0.3 (±0.2)
P-value			0.006	0.003	0.006	0.005	n.s.

Figure 25 The hyperoxic BOLD response (ΔBOLD) of the fetal organs and the placenta in each individual and organ specific mean. For each organ the increased in BOLD signal is tested by a paired t-test, and the p-value is demonstrated in the Figure (28)**.**

During maternal hyperoxia the BOLD signal was significantly increased in the placental and all fetal organs except for the fetal brain.

The human placental study (Papers 4+5)

In this study the placental response to maternal hyperoxia was investigated by the BOLD MRI technique. During hyperoxia a rather dramatic visual change occurred in the BOLD image (Figure 26)

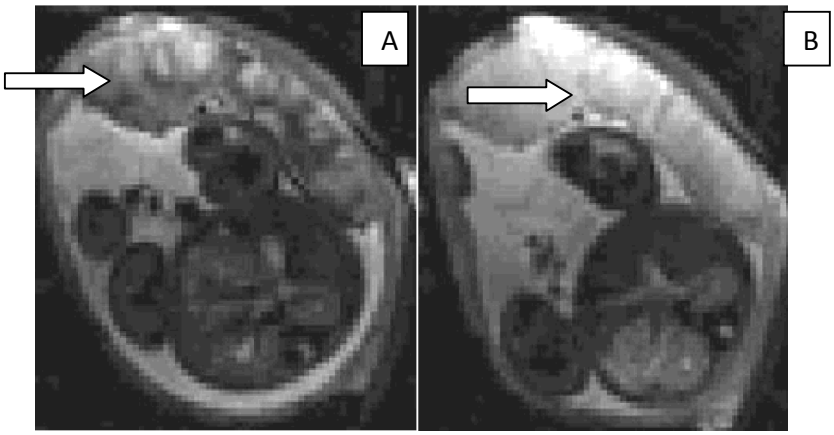

Figure 26 BOLD image demonstrating a cross section of the placenta and fetus during normoxia (A) and hyperoxia (B). White arrows indicate the placenta (27)**.**

During normoxia the placenta appeared heterogeneous. Dark areas were located to the fetal side of the placenta and brighter areas were located to the maternal side. During hyperoxia however, placenta became brighter. The tissue appeared homogeneous, and the dark areas were no longer visible.

The visual changes were quantified by estimating the increase in BOLD signal of the total placenta during hyperoxia. ROIs were drawn covering the entire placenta, and the absolute BOLD signal was normalized using the normoxic BOLD signal as a reference in each ROI. The normalized BOLD signal versus time curves were drawn for each ROI (Figure 27).

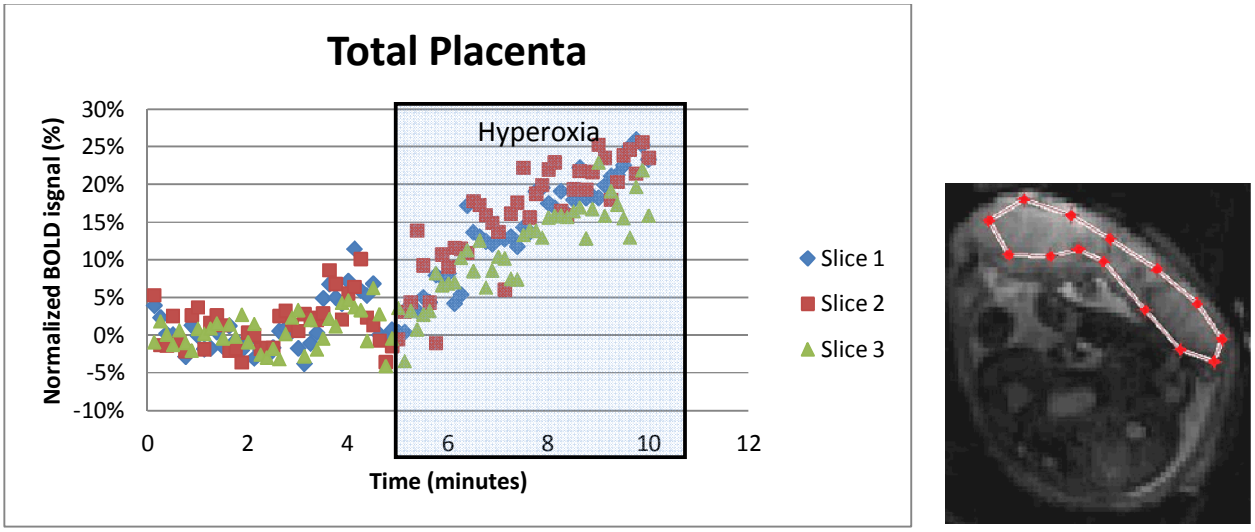

Figure 27 The normalized BOLD signal versus time curves the total placenta. The ROI is demonstrated in the BOLD image in the lower right corner. Three central slices within the same placenta are demonstrated (27)**.**

Data from one individual is shown in Figure 27. The three curves represent three different slices within the same placenta. The curves are very similar, indicating a high reproducibility of the hyperoxic BOLD response within the same placenta. Data from the 8 individuals are presented in Table 1.

Table 1 The hyperoxic BOLD response of the total placenta ($\Delta BOLD_{tot}$), the fetal placenta ($\Delta BOLD_{fet}$), and the maternal placenta ($\Delta BOLD_{mat}$) for the eight individuals included in paper 4.

ID number	Gestational age (weeks + days)	Total placenta $\Delta BOLD_{tot}$ (%) Mean±SD (3 slices)	Dark placental area Fetal side $\Delta BOLD_{fet}$ (%) Mean±SD (3 slices)	Bright placental area Maternal side $\Delta BOLD_{mat}$ (%) Mean±SD (3 slices)
1	30+5	19.4 ± 5.4	48.3 ± 19.2	10.9 ± 0.8
2	28+2	12.6 ± 2.2	30.6 ± 15.6	4.4 ± 1.4
3	32+1	19.1 ± 2.5	43.1 ± 16.4	6.8 ± 8.4
4	35+1	12.9 ± 3.4	27.5 ± 8.5	3.2 ± 6.4
5	35+5	12.3 ± 4.4	27.9 ± 11.1	1.8 ± 3.3
6	33+0	12.1 ± 1.3	34.4 ± 20.9	2.1 ± 5.5
7	36+3	17.9 ± 3.6	23.2 ± 12.5	4.3 ± 8.6
8	35+2	15.4 ± 1.0	22.2 ± 7.8	10.0 ± 6.5
Mean± SD		15.2 ± 3.2	32.1 ± 9.3	5.4 ± 3.5
P-value		p<0.0001	p<0.0001	p<0.003

For the total group of 8 individuals the mean hyperoxic increase in the placental BOLD signal was significantly increased 15.2% ± 3.2 (mean ± SD), ($p<0.0001$). A curve demonstrating the mean normalized BOLD signal ± SD of the total placenta can be drawn as shown in Figure 28.

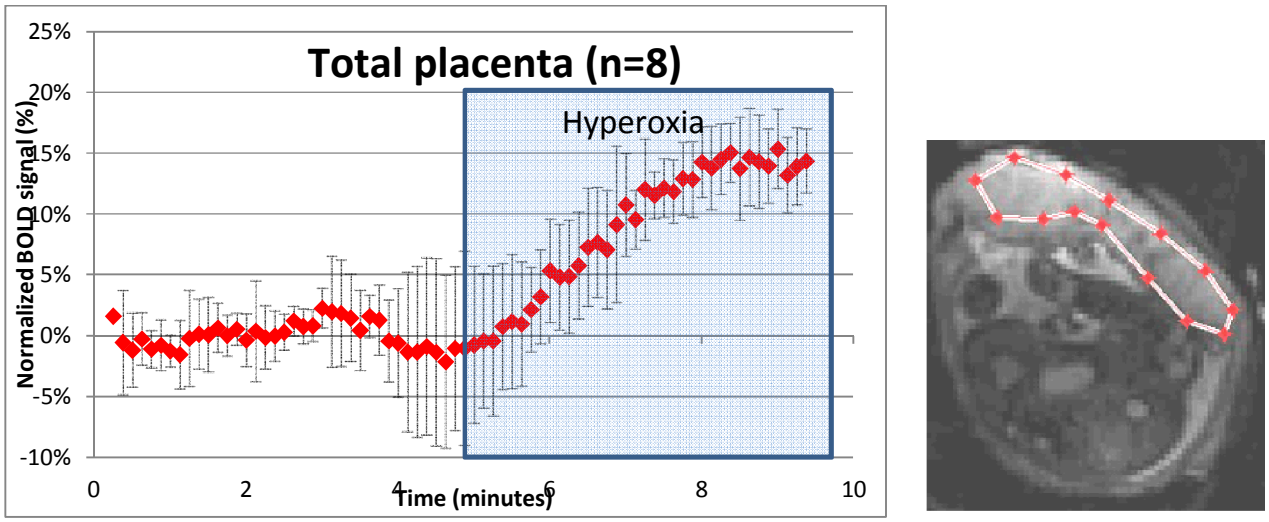

Figure 28 The mean value of the normalized placental BOLD signal of the 8 individuals. Error bars indicate the standard deviation. (Unpublished)

Within each placenta, the hyperoxic response of the dark and the bright regions were investigated separately by drawing a small ROI in the bright and the dark placental regions.

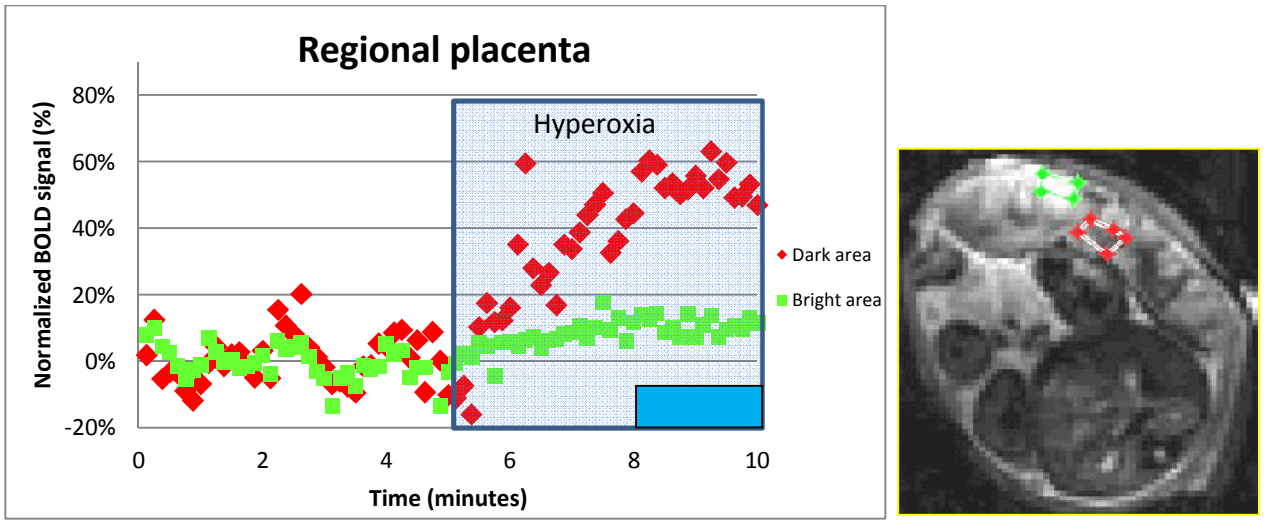

Figure 29 Changes in the normalized BOLD signal of two different placental regions during maternal hyperoxia in one case. The placenta ROIs are demonstrated by the BOLD image in the lower right corner. Blue bar indicated the values of the 2 last minutes of the hyperoxic episode included for calculation of ΔBOLD (27)**.**

The hyperoxic BOLD response of the two regions was quite different; the hyperoxic increase in the BOLD signal was predominantly seen in the darker region of the placenta. This difference between the two regions was a consistent finding in each of the 8 individuals. Based on all individuals mean values were calculated for both regions; $\Delta BOLD_{dark}$=32.1% ± 9.3 and $\Delta BOLD_{bright}$=5.4% ± 3.5 (mean ±SD). The difference between ΔBOLD of the two regions was highly significant, when tested by a paired t-test, p<0.0001.

After the publication of paper 4, 16 more women were included. Because of difficulties in identifying the steady state level of the hyperoxic placental BOLD signal three individuals were excluded from the calculation of ΔBOLD. In total the group of 21 individuals ΔBOLD was 14.4% ± 6.0, which is very similar to the findings of the first 8 individuals. Figure 30 shows the relation between the placental ΔBOLD and gestational age and a significant linear correlation was found as the placental BOLD response is increased by 0.6% per gestational week.

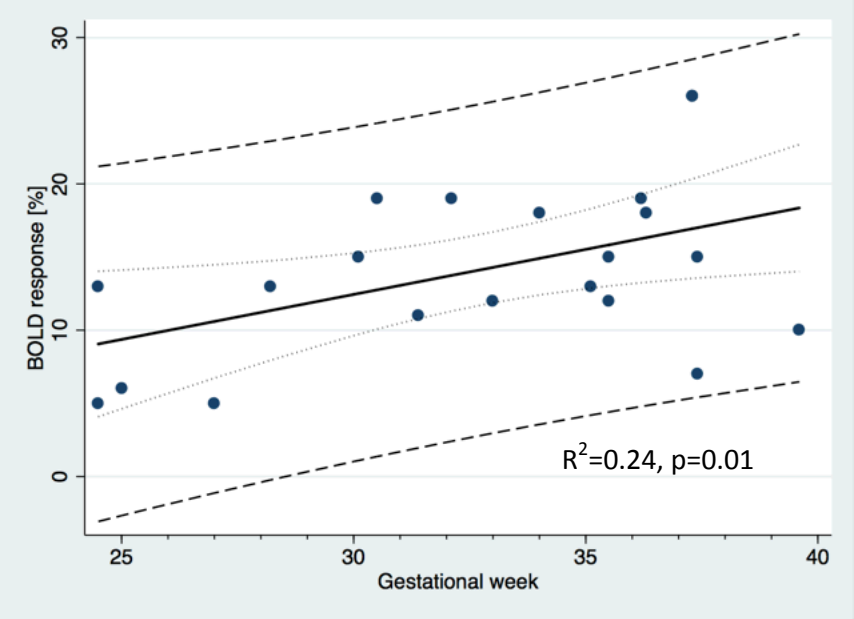

Figure 30 The relation between the hyperoxic placental response (ΔBOLD) and gestational age (n=21). A linear regression analysis is performed (the thick line), and Pearson coefficient (R) and p-value are presented in the figure. Dotted lines indicate the 95% confidence interval and dashed lines indicate the 95% prediction interval. (Unpublished)

In the total group of 24 women the placental T2* relaxation time was investigated. Initially the reproducibility of the placental T2* measurement was assessed regarding three levels of variation: (1) the slice-to-slice variation, (2) the scan-to-scan variation and (3) the session-to-session variation. For each of the three levels the reproducibility is estimated by bar plots, Bland-Altman plots and identity plots as shown in Figure 31.

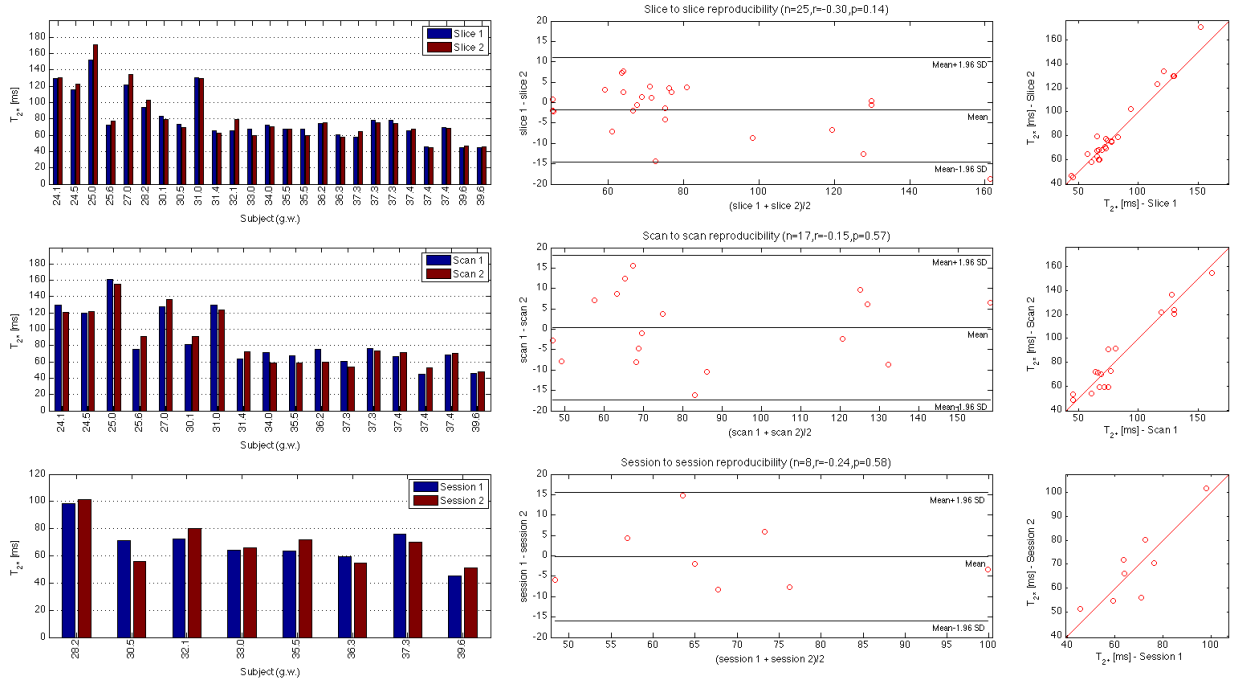

Figure 31 The reproducibility of placental T2* measurements demonstrated by bar plots, Bland-Altman plots and identity plots. Three levels of variation are investigated slice-to-slice (top), scan-to-scan (middle) and session-to-session (bottom).(Paper 5)

For each of the three levels, no systematic differences were demonstrated between the two measurements of placental T2*. The 95% limits of agreement indicates, that the reproducibility is best when the placental T2* is measured in two slices of the same placenta as it has the narrowest limits of agreement (-1.8±13.1 ms). The reproducibility between scans and between sessions is almost the same -0.1±17.8 ms and -0.3±15.7 ms, respectively.

The mean placental T2* value was 81.3 ms ± 28.1 (mean ± SD) and a significant linear relation was demonstrated between placental T2* and gestational age. The placental T2* value was found to decrease by 4.84 ms per gestational week (Figure 32).

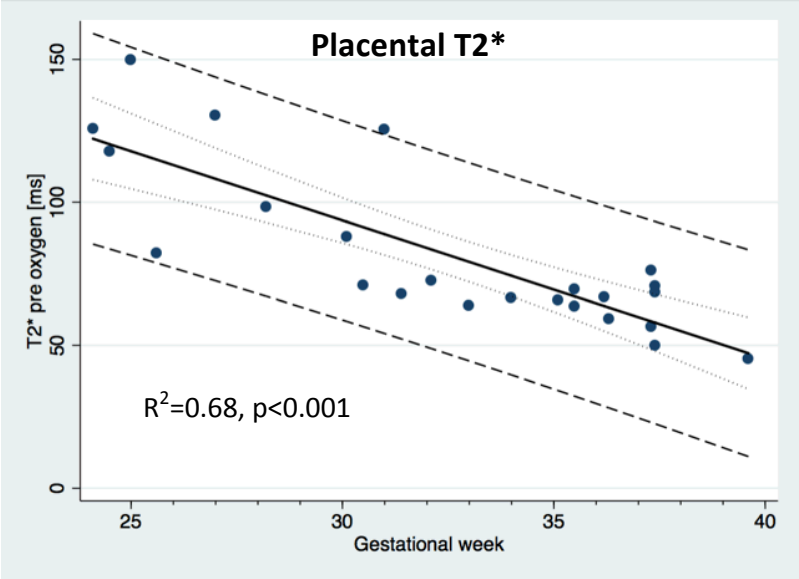

Figure 32 The relation between placental T2* and gestational age. The thick line indicates the linear correlation and Pearsons coefficient (R) and p-value are presented in the figure. Dotted lines indicate 95% confidence interval and dashed lines indicate 95% prediction interval. (Paper 5)

The hyperoxic placental response (ΔT2*) was investigated, and the findings are demonstrated in Figure 33

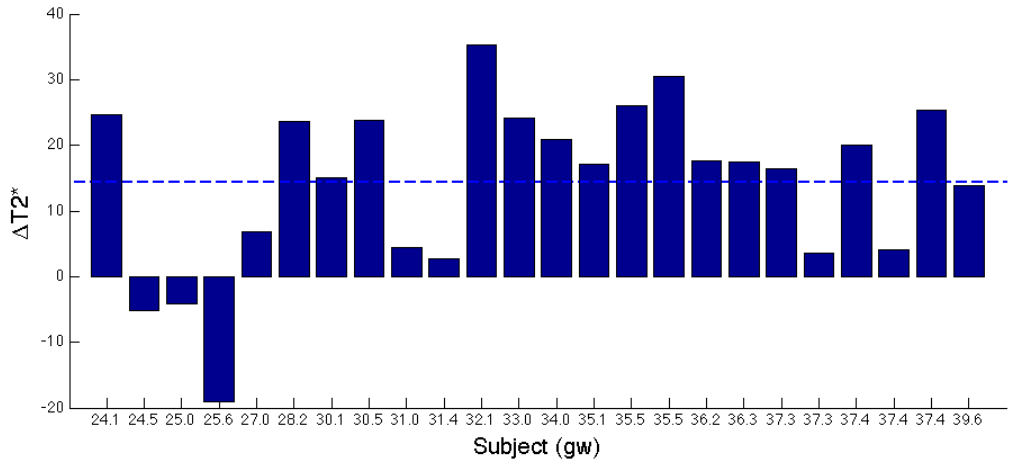

Figure 33 Each column represents the hyperoxic placental T2* response (ΔT2*) in one individual. The individuals are arranged according to gestational age. The dashed line indicates the mean ΔT2* of the 24 individuals.(Paper 5)

In the group of 24 individuals the mean ΔT2* was 14.4 ms ±12.8 (p=0.00002). The increase was statistically significant when tested by a paired t-test, but ΔT2* tended to vary between individuals as shown in Figure 33.

Discussion

First, the general methodological aspects of fetal BOLD MRI are discussed. The limitations of the method are presented including the experience we have had working with this method over the years to assess fetal and placental oxygenation. Following is a discussion of the main findings of each of the individual studies. Possible physiological explanations are offered for the BOLD MRI findings, as the BOLD findings are related to previous studies based on ultrasound Doppler examination of fetal and placental circulation and previous studies in BOLD MRI.

General aspects

There are several general aspects of the BOLD MRI method that need to be considered when interpreting the BOLD findings.

The qualitative BOLD scan versus the quantitative T2* measurement

The BOLD signal provides dynamic information about changes in tissue oxygenation; however, absolute oxygenation cannot be estimated by the BOLD scan. The baseline BOLD signal depends not only on tissue oxygenation but also on technical parameters and tissue physiology (172). Only relative changes, as estimated by the normalized BOLD signal, can be directly compared between individuals. The T2* measurement is a quantitative method. It is directly comparable between individuals. It is tissue specific and depends on several factors such as tissue morphology and tissue oxygenation (173,174). In our data we observed that the distance between the placenta and the receiver coil had a strong influence on the absolute BOLD signal. The absolute BOLD signal of an anterior placenta is almost doubled when compared to a posterior placenta, however the normalized BOLD response and the placental T2* value is not affected by the distance to the receiver coil. This finding highlights the important difference between the qualitative BOLD scan and the quantitative T2* measurement.

The magnitude of the BOLD response

Tissue physiology

The changes in the BOLD signal reflect changes in the amount of dexohgb present in the region of interest. The amount of deoxyHgb present will depend on local tissue metabolism, blood

perfusion, blood volume and the oxygen content of the blood (10). In its traditional use BOLD MRI provides information about brain activation by detecting changes in tissue metabolism and cerebral blood flow (12,13). In our studies of the fetus and placenta, we assume that the tissue metabolism is constant and we estimate the effect of altered maternal oxygen supply. However, changing the maternal oxygen supply might affect the blood volume and blood flow of the fetal organs and the placenta. These changes need to be taken into consideration as they influence the BOLD response. In previous studies, the fetal and placental circulatory changes during hypoxia and hyperoxia have been extensively investigated by Doppler flow measurements of fetal, umbilical and uterine vessels (see the background section). In our studies, we have related the fetal BOLD MRI findings to well described circulatory changes of the fetal brain and the fetal liver based on previous ultrasound studies. However, we did not estimate these parameters directly in our experiments. The magnitude of the BOLD response also relies on baseline tissue physiology such as baseline tissue oxygenation, and as the BOLD response is supposed to increase when baseline tissue oxygenation is decreased (172). In our data we found that the hyperoxic BOLD response was increased with increasing gestational age. This finding might be explained by the well described decrease in placental oxygenation with increasing gestational age (175).

Technical factors

Furthermore, the magnitude of the BOLD response also depends on technical parameters. In our studies, we increased the echo time in order to increase the hyperoxic BOLD response of the placental tissue. This change was based on the T2* decay curves of the normoxic and the hyperoxic placenta. Following this change in TE the hyperoxic placental BOLD response was increased from 6.2% to 15.2%. However, the two studies were performed in two different locations and at two different MRI systems (Philips versus GE), which might also have influenced the magnitude of the BOLD response. Shimming differences between the two MRI systems might contribute to some of the difference between the scans.

Fetal versus adult hemoglobin

The hgb molecule consists of 2 pairs of polypeptide globin chains and four heme groups. The globulin chains determine the type of hgb formed. Fetal hgb consist of two alpha chains and two

gamma chains, this is in contrast to adult hgb in which the gamma chains are replaced by beta chains (96). The paramagnetic effect of deoxyHgb depends on the electrons of the heme groups which are similar in fetal and adult hgb (1). Therefore it is expected, that the magnetic susceptibility of fetal and adult blood should be the same. Actually, the BOLD method is very suitable for estimating changes in the oxygenation in fetal blood in particular, because at normoxia fetal blood has a rather low saturation (80%) when compared to adult blood (100%)(92). Because of the sigmoid shape of the hgb dissociation curve, the curve is steeper at lower saturation levels. This means that at lower hgb saturation any given increase in pO_2 would make a more pronounced increase in hgb saturation. This explains why a stronger BOLD response would be expected in fetal blood when compared to maternal blood. The placenta contains a mixture of fetal and maternal blood, but the hyperoxic BOLD response (ΔBOLD) is predominantly derived from an increase in the saturation of fetal blood as maternal blood is already fully saturated at normoxia. Therefore the magnitude of ΔBOLD reflects placental oxygen transport capacity (27).

Fetal movement artifacts

One major limitation of the BOLD MRI method is that it is very sensitive to fetal movements. In our human studies we experienced a transient increase in fetal movement during the initial two or three minutes of each BOLD MRI scan. This finding is well known (44), and it is explained as a fetal response to noise during the MRI scan. Because the echo planar imaging (EPI) sequence used in the study the images are acquired very fast, and the quality of the BOLD image is therefore not severely affected by fetal movements. However, when moving the ROI in the BOLD image in order to keep the ROI within the selected organ during fetal movements the distance to the coil is influenced. As mentioned earlier, the absolute BOLD signal is decreased when the distance to the coil is increased. Therefore the fetal movements affect the absolute BOLD signal, and the changes in the BOLD signal due to moving the ROI exceeds the changes induced by oxygenation changes. In the sheep model, the fetal movements were reduced because of the use of anesthesia; however, in the human studies the fetal movements were greatly increased. The first software used by our group was capable of reducing the movement artifacts; however, with the second MATLAB software it was impossible for us to estimate the hyperoxic BOLD response from any fetal organs

because of movements. Because of this software problem (se the method section), we changed focus towards placental BOLD MRI while we are trying to develop an adequate motion correction tool for the new software. To date only a few papers have been published in human fetal BOLD MRI (16-21,28). In all of these publications the method has been limited because of fetal movements. The most successful study was published by our group when using the old software (28); unfortunately, it has not been possible to reproduce these results with the MATLAB software.

The hyperoxic placental response: ΔBOLD and ΔT2*

The hyperoxic placental response was estimated by 1) the change in placental BOLD signal (ΔBOLD) and 2) the difference between placental T2* measured in the hyperoxic and the normoxic episode (ΔT2*). The mean value of placental ΔBOLD was 14.4% ± 6.0 and in placental ΔT2* was 14.4ms ± 12.8. The inter-individual variation is quite different in the two estimates and placental ΔBOLD seems more robust. When looking at the corresponding BOLD scan of each individual a sudden dip in the placental BOLD signal was observed in some cases. One of these cases is demonstrated in Figure 34.

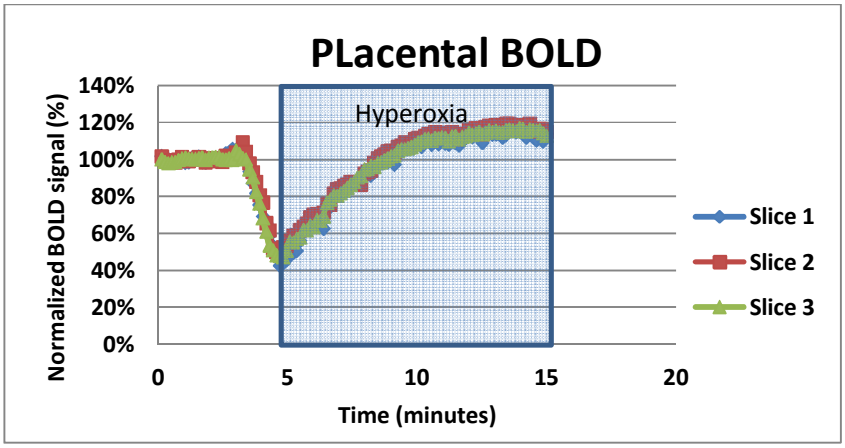

Figure 34 A sudden unexplained drop in the placental BOLD signal. Data from one case. Each curve represents one slice within the same placenta (Unpublished).

The depth of the drop in the BOLD signal varied between cases, however in each case the drop was identical in all placental slices, and the timing of the drop was independent of maternal hyperoxia. Any decrease in the placental BOLD signal reflects an increase in the amount of

deoxyHgb. A possible explanation of this sudden change could be reduced placental perfusion caused by either maternal aorto-caval compression (176) or uterine contractions (177). In the dynamic BOLD scan some of these cases demonstrated signs of uterine contractions such as altered shape of the uterus and transient thickening of the uterine wall according to the drop in BOLD signal. However, this finding needs to be investigated in another study including CTG for monitoring uterine contractions. In some of the cases the drop in placental BOLD signal interferes with the steady-state levels of either the normoxic or the hyperoxic episodes, which complicates the calculation of the ΔBOLD. When we identified this problem we increased the hyperoxic episode from 5 to 10 minutes for better identification of the hyperoxic placental BOLD steady state level. In most cases the steady state level could be identified, however 3 individuals were excluded from the calculation of ΔBOLD. Furthermore, in 9 cases the drop in placental BOLD signal extended into the hyperoxic placental T2* measurements, and so the ΔT2* measurement could be biased. Therfore we re-analyzed placental T2* data excluding the 9 individuals. Figure 35 is a reproduction of Figure 33, in which the 9 individuals excluded from the analysis are marked by red columns.

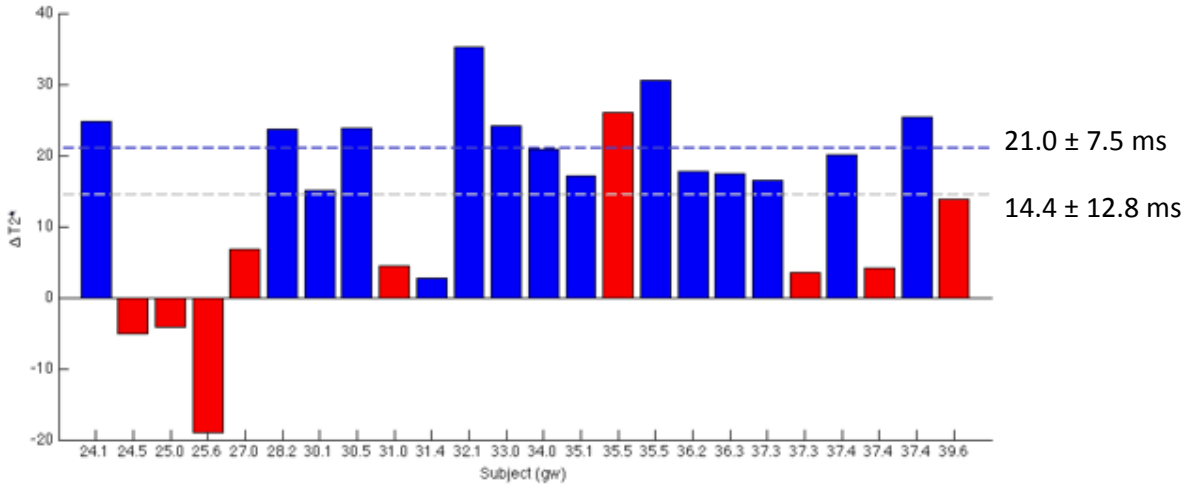

Figure 35 The placental T2* difference (hyperoxic T2* - normoxic T2*). Figure 33 re-analyzed. The red columns indicate the individuals excluded from the analysis. The bright dashed line indicates the original mean increase in placental T2* of all individuals. The dark dashed line indicates the re-analysed mean increase in placental T2* value of the remaining 13 individuals. (Unpublished)

When re-analyzing data the hyperoxic placental T2* response increased from 14.4ms ± 12.8 to 21.0 ms ± 7.5 (mean± SD) as demonstrated in Figure 35. By excluding the 9 cases the variation was decreased. This finding highlight the importance of including the dynamic BOLD scan when estimating placental T2*measurements. Another explanation of the ΔBOLD being more robust than ΔT2* in estimation placental hyperoxic response is that the calculation of ΔT2* is based on two single measurements of placental T2*, which is in contrast to the multiple time points included for the calculation of ΔBOLD.

The discussion of each study

The sheep study (Paper 1+2)

The main finding of the sheep study was the close relationship between the changes in the BOLD signal of the fetal liver and the direct measurements of fetal liver oxygenation. This finding is in accordance with other studies demonstrating a close correlation between the BOLD signal of several fetal organs and fetal oxygenation when estimated by the saturation of the fetal carotid artery blood (22-24).

Unlike most other studies we included not only maternal hypoxia, but also maternal hyperoxia, and we demonstrated a close relationship between maternal oxygenation and the BOLD signal of several fetal organs except for the fetal brain. However, we did not find a linear relationship as previous suggested by Wedegärtner et al (22). Our data demonstrated a flattening of the curve at higher oxygenation levels. This finding could be explained by the sigmoid shape of the hgb dissociation curve. At higher oxygenation levels any given increase in pO_2 leads to a less marked increase in hgb saturation. During maternal hyperoxia we demonstrated a consistent increase in the oxygenation of the fetal liver, spleen and kidney. This finding is in accordance with other publications having demonstrated that fetal oxygenation is increased during maternal hyperoxia (148-151)(153). A possible physiological explanation for this finding is the increase in maternal arterial pO_2 which increases the trans-placental pO_2 gradient and thereby improves the placental oxygen transfer to the fetus (87,128).(128)

We demonstrated that the BOLD signal of the fetal brain did not change during varying maternal oxygenation levels. This finding is likely explained by the autoregulation of fetal cerebral blood flow – also known as the brain sparing mechanism. It is well described by ultrasound Doppler flow measurements that during hypoxia the blod flow to the fetal brain is increased to maintain a normal cerebral oxygenation (128). Interestingly, this protective brain sparing mechanism might also be demonstrated during hyperoxia, because the BOLD signal of the fetal brain also remained constant during maternal hyperoxia. This mechanism is less well known; nevertheless, ultrasound Doppler studies of sheep (149,160) as well as of human fetuses (159,161) have demonstrated that the resistance of the cerebral vessels was increased during fetal hyperoxia. Our BOLD findings are in contrast with previous studies published by Wedegärtner et al (22,178,179), in the studies published by Wedegärtner the BOLD signal of the fetal brain was decreased during maternal hypoxia. However, these studies are not directly comparable with our studies. The first study of Wedegärtner was performed during short extreme maternal hypoxia (179), and the following two studies were performed on a 3Tesla MRI system (178,179), which is expected to be more sensitive in measuring oxygenation changes (24). However, in both studies the BOLD signal of the fetal liver and heart was decreased to a greater extent than that of the fetal brain.

Another interesting finding of the sheep study was the increasing left-right difference in fetal liver oxygenation during hypoxia. The reason why the left-right difference is increased during hypoxia, could be explained by increased ductus venosus shunting. During hypoxia an increasing amount of oxygen rich umbilical vein blood is shunted away from the fetal liver, especially the right side of the live, towards the fetal heart and brain to improve the oxygenation of these important central organs, and the degree of shunting is related to the degree of hypoxia (122). This is in accordance with our findings, demonstrating an increasing left-right oxygenation difference with decreasing maternal pO_2. In this study only the relative changes in fetal liver oxygenation were estimated as the BOLD method provides no information about absolute oxygenation.

A limitation of the study was that the degree of maternal and fetal hypoxia was not standardized in each animal experiment. The oxygen content of maternal ventilated gas was varied between

10% and 100% in each animal. Even at a certain level of oxygen the maternal oxygenation varied among individuals. These differences could be explained by maternal lung athelectasis due to the long duration of the experiment. Therefore, maternal oxygenation was estimated by arterial blood samples rather than the oxygen supply of the ventilation gas. Another limitation of the study was the use of general anesthesia. The cardiovascular depressant effects of anesthetic drugs used for induction might have affected the fetal vascular reactivity transiently. However, as these drugs were introduced at least 90 minutes prior to the BOLD MRI scan, it is unlikely that they affected the BOLD findings. The anesthesia was maintained by isoflurane inhalation which has a known cardiovascular depressant effect (180). Thus, isoflurane might have reduced the fetal vascular response, leading us to underestimate the effect of hypoxia on the left-right fetal liver oxygenation difference.

Extrapolation of data from animal to human physiology should be performed with caution. However, the sheep is a well known model of the human fetus and placenta (109). The sheep placenta has been extensively investigated, and there are known differences between the human and the sheep placenta. First, in the sheep placenta the oxygen transport is less effective, and so the pO_2 difference between the maternal and fetal blood is increased when compared to humans. This difference can be explained by the sheep placenta being epithelio-chorial and by the arrangement of the fetal and maternal vessels in a concurrent pattern (74). The fetal sheep physiology, the neuro-endocrine and cardiovascular response on altered oxygenation is well documented and very similar to the human fetus (24,181,182). For fetal imaging the sheep fetus has an appropriate size, and the number of fetuses can be restricted to singletons. However, when it comes to placental imaging, the sheep placenta is not a very suitable model because the sheep placenta consists of separate cotyledons, which is in contrast to the discoid shape of the human placenta.

The human fetal study (Paper 3)

This study demonstrated a significant increase in the normalized BOLD signal of several fetal organs during maternal hyperoxia. According to the sheep study, an increase in the BOLD signal reflects an increase in fetal oxygenation (25). In agreement with the findings of the sheep study

(25), the BOLD signal of the human fetal brain did not change during maternal hyperoxia, and this finding is likely explained by autoregulation of the fetal cerebral blood flow as discussed in the previous section.

To date, only a few studies have been published in human fetal BOLD MRI. Brain activation has been demonstrated following in utero visual and acoustic stimulation (16-18). Furthermore, fetal liver T2* was increased in 5 out of 9 fetuses during maternal hyperoxia (20); however, in a larger study of 80 human fetuses this finding could not be reproduced (21). A possible explanation could be inaccuracy of the fetal T2* measurement due to fitting inaccuracy or fetal movement artifacts which, in accordance with our experience, is an important limitation of this method. Because of this problem we focused on placental rather than fetal oxygenation in the study to follow.

The magnitude of ΔBOLD varied between the eight individuals included in this study. In fetuses number 2 and 6 ΔBOLD of all organs was decreased when compared to the rest of the group. A possible explanation of this finding could be differences in maternal oxygen supply by the facial mask as the mask is not perfectly tight. Maternal blood is already fully saturated at room air; therefore, maternal pulse-oximetry would not provide any information in regards to maternal hyperoxygenation. In a group of 5 pregnant women, the efficacy of the facial mask was investigated by maternal arterial blood gas analysis, and it was demonstrated that during a 10 minute period of oxygen breathing (100%O2, 12l/min.), maternal arterial pO_2 was increased to 45.0 ±8 kPa (not published). Another explanation of the differences in ΔBOLD among individuals could be differences in placental oxygen transport capacity. However, as these are uncomplicated pregnancies with documented normal fetal weight and normal Doppler flow measurements, this explanation is rather unlikely.

In each fetus we demonstrated a fixed relationship between ΔBOLD of the different fetal organs. ΔBOLD of the fetal liver and spleen was doubled when compared to the ΔBOLD of the placenta and fetal kidney. This finding might be explained by organ-specific differences such as differences in blood volume and blood flow. Biological differences will affect the baseline BOLD signal and, thus, the magnitude of the BOLD response in each organ. Furthermore, imaging parameters,

especially the echo-time (TE), are important determinants of the magnitude of the BOLD response. The TE=40 ms selected in this study might favor the BOLD contrast of the fetal liver and spleen over the placenta and the kidney.

The human placental study (Paper 4+5)

In a group of 8 healthy pregnant women the changes in placental oxygenation were investigated during maternal hyperoxia. In the BOLD image the hyperoxic placental response could be visualized as the darker placental regions located to the fetal side became brighter and the placenta appeared more homogeneous. During hyperoxia the normalized BOLD signal of the total placenta was significantly increased, and the increase was predominantly seen in the darker regions of the placenta. We hypothesize that the dark placental regions represent the fetal part of the placenta. This hypothesis is based on the anatomic location of the dark placental regions on the fetal side of the placenta, and the stronger increase in ΔBOLD of the darker placental regions when compared to the brighter placental regions. It is expected that ΔBOLD is increased in the fetal part of the placenta when compared to the maternal part of the placenta, because of a lower saturation of fetal blood (80%) when compared to maternal blood (100%). Hyperoxia increases the saturation predominantly in fetal blood, and this is the reason why ΔBOLD of the total placenta is predominantly derived from the fetal blood, and therefore ΔBOLD reflects the transplacental oxygen transport.

In the interpretation of ΔBOLD possible changes in placental perfusion and placental blood volume during hyperoxia should be taken into consideration. A possible vaso-constriction of the umbilical vessels due to hyperoxia was suggested based on in-vitro studies (166,167); however, these findings were never reproduced in vivo. Furthermore, any vaso-constriction of either the umbilical or the uterine vessels would tend to reduce the placental BOLD response, so we would underestimate the placental BOLD response demonstrated in this study.

When comparing the hyperoxic BOLD response in three central slices of each placenta, the technical reproducibility of the method seems rather high as demonstrated by Table 3. Unfortunately, there are no repeated scan sessions of the same individual available; therefore, the

reproducibility of the placental BOLD response cannot be properly addressed by this study. The mean ΔBOLD among the first 8 individuals was 15.0% ± 3.2, and in a larger group of 21 individuals is was 14.14% ± 6.0. The variation between individuals can be explained by factors such as inaccurate maternal oxygen supply, uterus contractions, and differences in placental perfusion and blood volume.

A positive linear correlation was demonstrated between the placental ΔBOLD and gestational age, with an increase in ΔBOLD of 0.6% per gestational week. The influence of the baseline oxygenation on the magnitude of ΔBOLD has previously been demonstrated for the cerebral cortex, showing that ΔBOLD decreases with higher baseline oxygenation levels (172). It is well described that baseline placental oxygenation decreases with gestation age (175), and this might explain our findings. Another explanation of the increasing ΔBOLD could be an increase in transplacental oxygen transport at later gestation. The normal placental maturation includes an increase in the total villous surface area and a thinning of the placental membrane, which increases the placental oxygen transport by approximately 40% (72).

In a larger group of 24 individuals the mean normoxic placental T2* was 81.3 ±28.1 ms, and the placental T2* was linearly correlated to gestational age with a decrease of 4.8 ms per gestational week. These findings are in conflict with a previous publication by Huen et al (21), who found the mean normoxic placental T2* value to be only 54.6 ± 15.9ms without any correlation with gestational age. The placental T2* values of the two studies were estimated by using the same fitting method. However in the study published by Huen et al. a multiple gradient–recalled echo sequence using only 10 echo-times (TE=5 – 50ms) was used, which, is in contrast to the protocol of our study using 16 echo-times (TE=3 – 67.5ms). By using a higher number of echo-times including longer echo-times the estimate of placental T2* should be more precise. Another possible explanation of the difference in placental T2* value could be differences in the mean gestational age of the two groups of women studied.

The correlation between the placental T2* value and gestational age is in accordance with previous studies investigating placental T2 value (174,183,184). In these studies a linear

correlation between the placental T2 and gestational age was demonstrated with a decrease in placenta T2 value of 4.0 ms per week in a 0.5 Tesla system (183,184) and 2.4 ms per week in a 1.5 Tesla system (174). Furthermore it was demonstrated that placental T2 was correlated to the amount of fibrin deposition indicating a morphological explanation for its relation with gestational age (174). It is well known that specific tissue characteristics determine tissue relaxation times. In general T2 relaxation time is increased with increasing tissue water content (173), decreasing surface area, and an increasing amount of macromolecular deposition (174). The normal placental maturation is known to include an equivalent increase in the total volume of villi and intervillous space; furthermore, the total placental membrane surface area is increased (72,185). The exact relation between these morphological changes and the T2 relaxation time still needs to be investigated. The T2* relaxation time depends on the T2 relaxation time, but it is also influenced by the local magnetic field inhomogeneties as created by the presence of deoxyHgb. We therefore suggest that the decrease in placental T2* value demonstrated in our study can be explained partly by the morphological changes in normal placental maturation, and partly by the well described decrease in placental oxygenation with increasing gestational age (175).

The reproducibility of the placental T2* value was investigated on three levels: 1) the slice-to-slice variation, 2) the scan-to-scan variation and 3) the session-to-session variation. For all levels the 95% limits of agreement were estimated. As expected we demonstrated that the reproducibility was the best between slices (-1.8 ± 13.1 ms), but surprisingly, the scan-to-scan and session-to-session variation was only slightly lower (-0.1 ± 17.8 ms) and (-0.3 ± 15.7 ms), respectively. These findings suggest that the variation of the method relies mainly on technical variation (such as fitting inaccuracy, movement artifacts and scanner calibration) rather than biological variation; otherwise, the variation should have been increased when comparing the two sessions. The reproducibility of placental T2* needs to be evaluated in a clinical perspective, taking the potential difference between normal and pathological placenta T2* into consideration. If the difference between normal and pathological placenta T2* is very small the reproducibility needs to be high, and likewise if the difference in placental T2* is large, then a lower reproducibility is clinically accepted. Currently, the difference in T2* between normal and FGR placenta is unknown, but it

should be revealed by future studies of the FGR placenta. The method is not very sensitive in detecting the hyperoxic placental ΔT2*, because the expected mean ΔT2* is only 14.4±12.8 ms, and 21.0 ± 7.5 ms when the cases demonstrating possible contractions were excluded. Unfortunately, ΔT2* is only slightly larger than the 95% limits of agreement in session-to-session variation of -0.3 ± 15.7 ms.

Conclusions

The overall conclusion of this thesis is that it is feasible to estimate fetal and placental oxygenation changes non-invasively by using the BOLD MRI method.

The main conclusions of each of the 5 papers included in the thesis are as follows

Paper 1

In the sheep fetus changes in the BOLD signal of the total fetal liver reflect changes in fetal liver oxygenation directly estimated by internal oxygen sensors. During hyperoxia fetal oxygenation was increased and during hypoxia it is decreased. However, the oxygenation of the fetal brain remained constant. This finding could be explained by the auto-regulation of fetal cerebral blood flow.

Paper 2

In the sheep fetus the left-right oxygenation difference of the fetal liver was increased during hypoxia. This finding could be explained by increased ductus venosus shunting.

Paper 3

Human fetal and placental oxygenation was significantly increased during hyperoxia. However, as demonstrated in the sheep study, the oxygenation of the fetal brain remained constant.

Paper 4

Human placental oxygenation was increased during hyperoxia. The dark placental regions represent the fetal parts of the placenta. The hyperoxic BOLD response of the total placenta is derived predominantly from the fetal blood and it reflects the transplacental oxygen transport.

Paper 5

The reproducibility of human placental T2* is described. Placental T2* is decreased during pregnancy, and it is increased during hyperoxia. Placental T2* reflects placental tissue morphology and oxygenation.

Perspective

The fetal and placental findings presented in this thesis are the result of research conducted in healthy pregnancies. Future studies should focus on pathological pregnancies such as FGR due to placental insufficiency.

The clinical perspective of the method is a non-invasive test of placental function based on a combination of the following two parameters

- Placental T2* measurement, which reflects placental morphology and oxygenation
- Placental hyperoxic BOLD response (ΔBOLD), which reflects the transplacental oxygen transport

In the growth restricted fetus assessment of the placental function is of major importance, as impaired placental function is associated with fetal hypoxia, acidosis and still birth. As previously mentioned, current methods in fetal surveillance estimate fetal well being rather than placental function.

Previous publications have suggested maternal oxygen challenge as a test of placental function. In FGR pregnancies oxygen challenge was evaluated by either an increase in umbilical pO_2 (153) or a normalization of fetal brain sparing (158). And no response was suggested as an indicator of severely impaired placental oxygen transport, which predicted a poor neonatal outcome. In accordance with these studies placental ΔBOLD might be a predictor of poor neonatal outcome. This theory is supported by a rat model of FGR. In this model the ΔBOLD of the feto-placental unit is reduced when compared to healthy controls (29,30).

Previous publications have demonstrated that placental T2 is reduced in FGR pregnancies when compared to normal pregnancies (183,184,186). Placental T2 was reduced even before clinical signs of FGR (186), which is very important for the clinical perspective of this method. Morphological changes of the FGR placenta, such as increased necrosis and infarction, might explain the lower T2 value in the FGR placenta. T2* relaxation is the sum of T2 relaxation and the effect of local magnetic field inhomogeneities such as created by deoxyHgb, and therefore it is

expected that T2* is also reduced in the FGR placenta. Actually, T2* might be even more sensitive than T2 to detect placental pathology because it is more sensitive to tissue hypoxia. However this still needs to be investigated.

There are several limitations of this method. Some limitations can be controlled in future studies. These limitations include inaccurate maternal oxygen supply, which can be controlled by maternal non-invasive transcutaneous pO_2 sensors, and uterine contractions, which can be monitored by MRI compatible CTGs. Furthermore, we hope to develop an additional software tool to deal with the changes in BOLD signal because of varying distance between the ROI and the receiver coil during fetal movements. By introducing these improvements, the reproducibility of the method should be increased. However general limitations of the method such as altered baseline tissue oxygenation, hyperoxic changes in placental blood volume and blood flow are difficult to control for. These limitations should always be considered when interpreting BOLD findings.

Several aspects of the fetal and placental BOLD MRI method need further investigation. In the group of normal pregnancies the reproducibility of placental ΔBOLD still needs to be addressed. The main focus for future placental BOLD MRI is pregnancies complicated by FGR because of impaired placental function. Placental ΔBOLD and T2* measurements should be performed in FGR pregnancies, and in each case longitudinal data should be obtained to demonstrate the timeline of progression in placental impairment. Another interesting perspective of BOLD MRI is the opportunity to investigate placental oxygenation changes during uterine contractions.

Placental BOLD MRI has the potential to become an important non-invasive test of placental function in selected cases of FGR. In these cases, BOLD MRI might provide the obstetrician valuable knowledge of placental function in order to decide how to monitor and when to deliver extremely high-risk fetuses.

English summary

Placental function is crucial for fetal growth and development. Fetal growth restriction (FGR) due to impaired placental function is associated with an increased risk of neonatal morbidity and mortality because of reduced supply of oxygen. The aim of fetal monitoring is to identify the growth restricted fetus to ensure rational monitoring intervals and timely delivery. Fetal monitoring is based on various methods, such as CTG, biophysical profile and ultrasound Doppler measurements of fetal and umbilical blood flow. Current methods focus on fetal wellbeing and thus only indirectly estimate placental function. Today, the only method available for direct assessment of placental oxygen transport is cordocentesis. This invasive procedure is associated with an increased risk of fetal loss and is therefore not used. In neuroscience Blood Oxygen Level Dependent (BOLD) magnetic resonance imaging (MRI) provides non-invasive information about brain oxygenation as changes in BOLD signal reflect changes in the saturation of hemoglobin. Furthermore, the transversal relaxation time (T2*) reflect tissue morphology and tissue oxygenation. Over the last decade BOLD MRI has become the main method in mapping brain function in cognitive studies; however, in fetal medicine the method is only briefly described. In this thesis the feasibility of BOLD MR as a non-invasive method for estimating fetal and placental oxygenation is investigated in healthy pregnancies.

In a sheep model fetal oxygenation changes were induced by changing the oxygen content of the maternal breathing air, and the corresponding changes in the BOLD signal were measured in selected fetal organs. In the fetal liver the tissue oxygenation was estimated directly by internal oxygen sensors, and a close association was demonstrated between changes in the BOLD signal and changes in tissue oxygenation. In healthy human pregnancies fetal and placental hyperoxia was induced by increasing the oxygen content of maternal breathing air. In the fetus the oxygenation of the spleen, liver and kidney was increased. The placental oxygenation was also increased; however, this increase was predominantly seen in the fetal part of the placenta. Thus, from this thesis it can be concluded, that BOLD MRI is a feasible method to estimate fetal and placental oxygenation non-invasively.

The future perspective of this method is a non invasive test of placental function in cases of FGR. Placental BOLD MRI might be an additional tool to support obstetricians in the very difficult decision of when to deliver these high risk fetuses.

Dansk resumé

Moderkagens og fosterets oxygenering målt ved hjælp af BOLD MRI

Moderkagens funktion har afgørende betydning for fosterets vækst og udvikling. Væksthæmning på grund af nedsat funktion af moderkagen er forbundet med en øget risiko for permanent fosterskade og fosterdød på grund af nedsat ilt tilførsel via moderkagen. Fosterovervågning sigter blandt andet mod at identificer væksthæmning for at sikre rettidig forløsning. Overvågningen baseres primært på ultralydsskanning inklusiv måling af blodets strømning i navlesnoren og fosterets blodkar samt registrering af fosterets hjertefrekvens, fostervandsmængde og fosterbevægelser. Disse metoder vurderer primært fosterets tilstand, og estimerer derved kun indirekte moderkagens funktion. Moderkagens evne til at transportere ilt kan idag udelukkende vurderes ved hjælp af en blodprøve fra navlesnoren. Dette invasive indgreb udføres dog ikke, idet det er fundet med en øget risko for fosteret. Ved Blood Oxygen Level Dependent (BOLD) MR skanning af hjernen udføres i dag non-invasive målinger af iltmætning til kortlægning af hjernen kognitive funktion. Ændringer i BOLD MR signalet afspejler ændringer i hæmoglobins iltmætning,, og den den transverselle relaxationstid (T2*) er relateret til både vævs struktur og vævs oxygenering. Indenfor foster overvågning er metoden endnu ganske lidt beskrevet, hvorfor formålet med dette PhD studie er at undersøge teknikkens evne til at måle ændringer i iltmætning hos fostre og i moderkagen.

Studiets første BOLD MR undersøgelser blev udført på fårefostre. Ved at ændre iltindholdet i moderens ventilationsluft ændredes fosterets oxygenering, og ved samtidig BOLD MR skanning kunne signalændringer i udvalgte fosterorganer registreres. Iltmætningen i fosterets lever blev målt direkte ved hjælp af invasive ilt sensorer, og der blev påvist en tæt sammenhæng mellem ændringer i BOLD signalet og ændringer i iltmætning. Ved BOLD MR skanning af raske humane fostre i forbindelse med at moderen indånder 100% ilt på maske fandtes en øget iltmætning af fosterets lever, milt og nyre. Ved skanning af moderkagen fandtes også en øget iltmætning dog primært i den føtale del. Konklusionen på PhD studiet er således, at BOLD MR kan anvendes son en non-invasiv metode til at estimere ændret iltmætning i foster og moderkage. Det fremtidige perspektiv ved denne metode er en non-invasiv test af moderkagens funktion i forbindelse med fostervæksthæmning. BOLD MR skanning af moderkagen kan herved blive et ekstra redskab, som kan støtte obstetrikeren i den svære beslutning om forløsningstidspunktet for ekstremt væksthæmmede fostre.

References

(1) Currie S, Hoggard N, Craven IJ, Hadjivassiliou M, Wilkinson ID. Understanding MRI: basic MR physics for physicians. Postgrad Med J 2013 Apr;89(1050):209-223.

(2) Ogawa S, Lee TM. Magnetic resonance imaging of blood vessels at high fields: in vivo and in vitro measurements and image simulation. Magn Reson Med 1990 Oct;16(1):9-18.

(3) Ogawa S, Lee TM, Nayak AS, Glynn P. Oxygenation-sensitive contrast in magnetic resonance image of rodent brain at high magnetic fields. Magn Reson Med 1990 Apr;14(1):68-78.

(4) Belliveau JW, Kennedy DN,Jr, McKinstry RC, Buchbinder BR, Weisskoff RM, Cohen MS, et al. Functional mapping of the human visual cortex by magnetic resonance imaging. Science 1991 Nov 1;254(5032):716-719.

(5) Fox MD, Raichle ME. Spontaneous fluctuations in brain activity observed with functional magnetic resonance imaging. Nat Rev Neurosci 2007 Sep;8(9):700-711.

(6) Bandettini PA. Twenty years of functional MRI: the science and the stories. Neuroimage 2012 Aug 15;62(2):575-588.

(7) Pauling L, Coryell CD. The Magnetic Properties and Structure of Hemoglobin, Oxyhemoglobin and Carbonmonoxyhemoglobin. Proc Natl Acad Sci U S A 1936 Apr;22(4):210-216.

(8) Cohen ER, Ugurbil K, Kim SG. Effect of basal conditions on the magnitude and dynamics of the blood oxygenation level-dependent fMRI response. J Cereb Blood Flow Metab 2002 Sep;22(9):1042-1053.

(9) Gustard S, Williams EJ, Hall LD, Pickard JD, Carpenter TA. Influence of baseline hematocrit on between-subject BOLD signal change using gradient echo and asymmetric spin echo EPI. Magn Reson Imaging 2003 Jul;21(6):599-607.

(10) Blockley NP, Griffeth VE, Simon AB, Buxton RB. A review of calibrated blood oxygenation level-dependent (BOLD) methods for the measurement of task-induced changes in brain oxygen metabolism. NMR Biomed 2012 Sep 4.

(11) Norris DG. Principles of magnetic resonance assessment of brain function. J Magn Reson Imaging 2006 Jun;23(6):794-807.

(12) Logothetis NK, Pfeuffer J. On the nature of the BOLD fMRI contrast mechanism. Magn Reson Imaging 2004 Dec;22(10):1517-1531.

(13) Logothetis NK. What we can do and what we cannot do with fMRI. Nature 2008 Jun 12;453(7197):869-878.

(14) Buxton RB, Uludag K, Dubowitz DJ, Liu TT. Modeling the hemodynamic response to brain activation. Neuroimage 2004;23 Suppl 1:S220-33.

(15) Boxerman JL, Bandettini PA, Kwong KK, Baker JR, Davis TL, Rosen BR, et al. The intravascular contribution to fMRI signal change: Monte Carlo modeling and diffusion-weighted studies in vivo. Magn Reson Med 1995 Jul;34(1):4-10.

(16) Hykin J, Moore R, Duncan K, Clare S, Baker P, Johnson I, et al. Fetal brain activity demonstrated by functional magnetic resonance imaging. Lancet 1999 Aug 21;354(9179):645-646.

(17) Moore RJ, Vadeyar S, Fulford J, Tyler DJ, Gribben C, Baker PN, et al. Antenatal determination of fetal brain activity in response to an acoustic stimulus using functional magnetic resonance imaging. Hum Brain Mapp 2001 Feb;12(2):94-99.

(18) Fulford J, Vadeyar SH, Dodampahala SH, Moore RJ, Young P, Baker PN, et al. Fetal brain activity in response to a visual stimulus. Hum Brain Mapp 2003 Dec;20(4):239-245.

(19) Fulford J, Vadeyar SH, Dodampahala SH, Ong S, Moore RJ, Baker PN, et al. Fetal brain activity and hemodynamic response to a vibroacoustic stimulus. Hum Brain Mapp 2004 Jun;22(2):116-121.

(20) Semple SI, Wallis F, Haggarty P, Abramovich D, Ross JA, Redpath TW, et al. The measurement of fetal liver T(*)(2) in utero before and after maternal oxygen breathing: progress towards a non-invasive measurement of fetal oxygenation and placental function. Magn Reson Imaging 2001 Sep;19(7):921-928.

(21) Morris DM, Ross JA, McVicar A, Semple SI, Haggarty P, Gilbert FJ, et al. Changes in foetal liver T2* measurements by MRI in response to maternal oxygen breathing: application to diagnosing foetal growth restriction. Physiol Meas 2010 Sep;31(9):1137-1146.

(22) Wedegartner U, Tchirikov M, Schafer S, Priest AN, Kooijman H, Adam G, et al. Functional MR imaging: comparison of BOLD signal intensity changes in fetal organs with fetal and maternal oxyhemoglobin saturation during hypoxia in sheep. Radiology 2006 Mar;238(3):872-880.

(23) Wedegartner U, Kooijman H, Andreas T, Beindorff N, Hecher K, Adam G. T2 and T2* measurements of fetal brain oxygenation during hypoxia with MRI at 3T: correlation with fetal arterial blood oxygen saturation. Eur Radiol 2009 Jul 18.

(24) Wedegartner U, Popovych S, Yamamura J, Kooijman H, Adam G. DeltaR2* in fetal sheep brains during hypoxia: MR imaging at 3.0 T versus that at 1.5 T. Radiology 2009 Aug;252(2):394-400.

(25) Sorensen A, Pedersen M, Tietze A, Ottosen L, Duus L, Uldbjerg N. BOLD MRI in sheep fetuses: a non-invasive method for measuring changes in tissue oxygenation. Ultrasound Obstet Gynecol 2009 Dec;34(6):687-692.

(26) Huen I, Morris DM, Wright C, Parker GJ, Sibley CP, Johnstone ED, et al. R(1) and R(2) * changes in the human placenta in response to maternal oxygen challenge. Magn Reson Med 2012 Dec 27.

(27) Sorensen A, Peters D, Frund E, Lingman G, Christiansen O, Uldbjerg N. Changes in human placental oxygenation during maternal hyperoxia as estimated by BOLD MRI. Ultrasound Obstet Gynecol 2013 Jan 10.

(28) Sorensen A, Peters D, Simonsen C, Pedersen M, Stausbol-Gron B, Christiansen OB, et al. Changes in human fetal oxygenation during maternal hyperoxia as estimated by BOLD MRI. Prenat Diagn 2013 Feb;33(2):141-145.

(29) Aimot-Macron S, Salomon LJ, Deloison B, Thiam R, Cuenod CA, Clement O, et al. In vivo MRI assessment of placental and foetal oxygenation changes in a rat model of growth restriction using blood oxygen level-dependent (BOLD) magnetic resonance imaging. Eur Radiol 2013 May;23(5):1335-1342.

(30) Chalouhi GE, Alison M, Deloison B, Thiam R, Autret G, Balvay D, et al. Fetoplacental Oxygenation in an Intrauterine Growth Restriction Rat Model by Using Blood Oxygen Level-Dependent MR Imaging at 4.7 T. Radiology 2013 May 21.

(31) Kanal E, Barkovich AJ, Bell C, Borgstede JP, Bradley WG,Jr, Froelich JW, et al. ACR guidance document for safe MR practices: 2007. AJR Am J Roentgenol 2007 Jun;188(6):1447-1474.

(32) International Commission on Non-Ionizing Radiation Protection. Guidelines on limits of exposure to static magnetic fields. Health Phys 2009 Apr;96(4):504-514.

(33) Hoyer C, Vogt MA, Richter SH, Zaun G, Zahedi Y, Maderwald S, et al. Repetitive exposure to a 7 Tesla static magnetic field of mice in utero does not cause alterations in basal emotional and cognitive behavior in adulthood. Reprod Toxicol 2012 Aug;34(1):86-92.

(34) Abramowicz JS, Barnett SB, Duck FA, Edmonds PD, Hynynen KH, Ziskin MC. Fetal thermal effects of diagnostic ultrasound. J Ultrasound Med 2008 Apr;27(4):541-59; quiz 560-3.

(35) Ziskin MC, Morrissey J. Thermal thresholds for teratogenicity, reproduction, and development. Int J Hyperthermia 2011;27(4):374-387.

(36) Schroder HJ, Power GG. Engine and radiator: fetal and placental interactions for heat dissipation. Exp Physiol 1997 Mar;82(2):403-414.

(37) Gowland PA, De Wilde J. Temperature increase in the fetus due to radio frequency exposure during magnetic resonance scanning. Phys Med Biol 2008 Nov 7;53(21):L15-8.

(38) Edwards MJ. Hyperthermia as a teratogen: a review of experimental studies and their clinical significance. Teratog Carcinog Mutagen 1986;6(6):563-582.

(39) Hand JW, Li Y, Thomas EL, Rutherford MA, Hajnal JV. Prediction of specific absorption rate in mother and fetus associated with MRI examinations during pregnancy. Magn Reson Med 2006 Apr;55(4):883-893.

(40) International Commission on Non-Ionizing Radiation Protection. Medical magnetic resonance (MR) procedures: protection of patients. Health Phys 2004 Aug;87(2):197-216.

(41) Price DL, De Wilde JP, Papadaki AM, Curran JS, Kitney RI. Investigation of acoustic noise on 15 MRI scanners from 0.2 T to 3 T. J Magn Reson Imaging 2001 Feb;13(2):288-293.

(42) Glover P, Hykin J, Gowland P, Wright J, Johnson I, Mansfield P. An assessment of the intrauterine sound intensity level during obstetric echo-planar magnetic resonance imaging. Br J Radiol 1995 Oct;68(814):1090-1094.

(43) Noise: a hazard for the fetus and newborn. American Academy of Pediatrics. Committee on Environmental Health. Pediatrics 1997 Oct;100(4):724-727.

(44) Gagnon R, Hunse C, Carmichael L, Fellows F, Patrick J. Human fetal responses to vibratory acoustic stimulation from twenty-six weeks to term. Am J Obstet Gynecol 1987 Dec;157(6):1375-1381.

(45) Baschat AA. Arterial and venous Doppler in the diagnosis and management of early onset fetal growth restriction. Early Hum Dev 2005 Nov;81(11):877-887.

(46) Westgate JA, Wibbens B, Bennet L, Wassink G, Parer JT, Gunn AJ. The intrapartum deceleration in center stage: a physiologic approach to the interpretation of fetal heart rate changes in labor. Am J Obstet Gynecol 2007 Sep;197(3):236.e1-236.11.

(47) Aldrich CJ, D'Antona D, Spencer JA, Wyatt JS, Peebles DM, Delpy DT, et al. Late fetal heart decelerations and changes in cerebral oxygenation during the first stage of labour. Br J Obstet Gynaecol 1995 Jan;102(1):9-13.

(48) Schifrin BS, Ater S. Fetal hypoxic and ischemic injuries. Curr Opin Obstet Gynecol 2006 Apr;18(2):112-122.

(49) Grivell RM, Alfirevic Z, Gyte GM, Devane D. Antenatal cardiotocography for fetal assessment. Cochrane Database Syst Rev 2010 Jan 20;(1)(1):CD007863.

(50) Sameshima H, Ikenoue T, Ikeda T, Kamitomo M, Ibara S. Unselected low-risk pregnancies and the effect of continuous intrapartum fetal heart rate monitoring on umbilical blood gases and cerebral palsy. Am J Obstet Gynecol 2004 Jan;190(1):118-123.

(51) Rosen KG, Amer-Wahlin I, Luzietti R, Noren H. Fetal ECG waveform analysis. Best Pract Res Clin Obstet Gynaecol 2004 Jun;18(3):485-514.

(52) Baskett TF, Liston RM. Fetal movement monitoring: clinical application. Clin Perinatol 1989 Sep;16(3):613-625.

(53) Yoshimura S, Masuzaki H, Gotoh H, Ishimaru T. Fetal redistribution of blood flow and amniotic fluid volume in growth-retarded fetuses. Early Hum Dev 1997 Feb 20;47(3):297-304.

(54) Lalor JG, Fawole B, Alfirevic Z, Devane D. Biophysical profile for fetal assessment in high risk pregnancies. Cochrane Database Syst Rev 2008 Jan 23;(1):CD000038. doi(1):CD000038.

(55) Cruz-Martinez R, Figueras F. The role of Doppler and placental screening. Best Pract Res Clin Obstet Gynaecol 2009 Dec;23(6):845-855.

(56) Alfirevic Z, Stampalija T, Gyte GM. Fetal and umbilical Doppler ultrasound in normal pregnancy. Cochrane Database Syst Rev 2010 Aug 4;(8):CD001450. doi(8):CD001450.

(57) Alfirevic Z, Stampalija T, Gyte GM. Fetal and umbilical Doppler ultrasound in high-risk pregnancies. Cochrane Database Syst Rev 2010 Jan 20;(1):CD007529. doi(1):CD007529.

(58) When do obstetricians recommend delivery for a high-risk preterm growth-retarded fetus? The GRIT Study Group. Growth Restriction Intervention Trial. Eur J Obstet Gynecol Reprod Biol 1996 Aug;67(2):121-126.

(59) Thornton JG, Hornbuckle J, Vail A, Spiegelhalter DJ, Levene M, GRIT study group. Infant wellbeing at 2 years of age in the Growth Restriction Intervention Trial (GRIT): multicentred randomised controlled trial. Lancet 2004 Aug 7-13;364(9433):513-520.

(60) Walker DM, Marlow N, Upstone L, Gross H, Hornbuckle J, Vail A, et al. The Growth Restriction Intervention Trial: long-term outcomes in a randomized trial of timing of delivery in fetal growth restriction. Am J Obstet Gynecol 2011 Jan;204(1):34.e1-34.e9.

(61) Lees C, Baumgartner H. The TRUFFLE study--a collaborative publicly funded project from concept to reality: how to negotiate an ethical, administrative and funding obstacle course in the European Union. Ultrasound Obstet Gynecol 2005 Feb;25(2):105-107.

(62) Turan OM, Turan S, Berg C, Gembruch U, Nicolaides KH, Harman CR, et al. Duration of persistent abnormal ductus venosus flow and its impact on perinatal outcome in fetal growth restriction. Ultrasound Obstet Gynecol 2011 Sep;38(3):295-302.

(63) Bilardo CM, Wolf H, Stigter RH, Ville Y, Baez E, Visser GH, et al. Relationship between monitoring parameters and perinatal outcome in severe, early intrauterine growth restriction. Ultrasound Obstet Gynecol 2004 Feb;23(2):119-125.

(64) Baschat AA, Gembruch U, Reiss I, Gortner L, Weiner CP, Harman CR. Relationship between arterial and venous Doppler and perinatal outcome in fetal growth restriction. Ultrasound Obstet Gynecol 2000 Oct;16(5):407-413.

(65) Baschat AA. Neurodevelopment following fetal growth restriction and its relationship with antepartum parameters of placental dysfunction. Ultrasound Obstet Gynecol 2011 May;37(5):501-514.

(66) Gude NM, Roberts CT, Kalionis B, King RG. Growth and function of the normal human placenta. Thromb Res 2004;114(5-6):397-407.

(67) Everett TR, Lees CC. Beyond the placental bed: placental and systemic determinants of the uterine artery Doppler waveform. Placenta 2012 Nov;33(11):893-901.

(68) Sibley CP, Turner MA, Cetin I, Ayuk P, Boyd CA, D'Souza SW, et al. Placental phenotypes of intrauterine growth. Pediatr Res 2005 Nov;58(5):827-832.

(69) Enders AC, Carter AM. Review: The evolving placenta: different developmental paths to a hemochorial relationship. Placenta 2012 Feb;33 Suppl:S92-8.

(70) Kingdom J, Huppertz B, Seaward G, Kaufmann P. Development of the placental villous tree and its consequences for fetal growth. Eur J Obstet Gynecol Reprod Biol 2000 Sep;92(1):35-43.

(71) Huppertz B, Peeters LL. Vascular biology in implantation and placentation. Angiogenesis 2005;8(2):157-167.

(72) Burton GJ, Jauniaux E. Sonographic, stereological and Doppler flow velocimetric assessments of placental maturity. Br J Obstet Gynaecol 1995 Oct;102(10):818-825.

(73) Schroder HJ. Comparative aspects of placental exchange functions. Eur J Obstet Gynecol Reprod Biol 1995 Nov;63(1):81-90.

(74) Wilkening RB, Meschia G. Current topic: comparative physiology of placental oxygen transport. Placenta 1992 Jan-Feb;13(1):1-15.

(75) Pardi G, Marconi AM, Cetin I, Baggiani AM, Lanfranchi A, Bozzetti P. Fetal oxygenation and acid base balance during pregnancy. J Perinat Med 1991;19 Suppl 1:139-144.

(76) Kingdom JC, Burrell SJ, Kaufmann P. Pathology and clinical implications of abnormal umbilical artery Doppler waveforms. Ultrasound Obstet Gynecol 1997 Apr;9(4):271-286.

(77) Morrow RJ, Adamson SL, Bull SB, Ritchie JW. Effect of placental embolization on the umbilical arterial velocity waveform in fetal sheep. Am J Obstet Gynecol 1989 Oct;161(4):1055-1060.

(78) Morrow RJ, Adamson SL, Bull SB, Ritchie JW. Acute hypoxemia does not affect the umbilical artery flow velocity waveform in fetal sheep. Obstet Gynecol 1990 Apr;75(4):590-593.

(79) Burrell SJ, Kingdom JC. The use of umbilical artery Doppler ultrasonography in modern obstetrics. Curr Opin Obstet Gynecol 1997 Dec;9(6):370-374.

(80) Lin S, Shimizu I, Suehara N, Nakayama M, Aono T. Uterine artery Doppler velocimetry in relation to trophoblast migration into the myometrium of the placental bed. Obstet Gynecol 1995 May;85(5 Pt 1):760-765.

(81) Madazli R, Somunkiran A, Calay Z, Ilvan S, Aksu MF. Histomorphology of the placenta and the placental bed of growth restricted foetuses and correlation with the Doppler velocimetries of the uterine and umbilical arteries. Placenta 2003 May;24(5):510-516.

(82) Urban G, Vergani P, Ghidini A, Tortoli P, Ricci S, Patrizio P, et al. State of the art: non-invasive ultrasound assessment of the uteroplacental circulation. Semin Perinatol 2007 Aug;31(4):232-239.

(83) Hernandez-Andrade E, Brodszki J, Lingman G, Gudmundsson S, Molin J, Marsal K. Uterine artery score and perinatal outcome. Ultrasound Obstet Gynecol 2002 May;19(5):438-442.

(84) Malassine A, Cronier L. Hormones and human trophoblast differentiation: a review. Endocrine 2002 Oct;19(1):3-11.

(85) Carter AM. Placental oxygen transfer and the oxygen supply to the fetus. Fetal Matern Med Rev 1999;11(3-4):151-161.

(86) Carter AM. Placental oxygen consumption. Part I: in vivo studies--a review. Placenta 2000 Mar-Apr;21 Suppl A:S31-7.

(87) Carter AM. Factors affecting gas transfer across the placenta and the oxygen supply to the fetus. J Dev Physiol 1989 Dec;12(6):305-322.

(88) Desforges M, Sibley CP. Placental nutrient supply and fetal growth. Int J Dev Biol 2010;54(2-3):377-390.

(89) Cetin I, Alvino G. Intrauterine growth restriction: implications for placental metabolism and transport. A review. Placenta 2009 Mar;30 Suppl A:S77-82.

(90) Cetin I, Ronzoni S, Marconi AM, Perugino G, Corbetta C, Battaglia FC, et al. Maternal concentrations and fetal-maternal concentration differences of plasma amino acids in normal and intrauterine growth-restricted pregnancies. Am J Obstet Gynecol 1996 May;174(5):1575-1583.

(91) Pardi G, Marconi AM, Cetin I. Placental-fetal interrelationship in IUGR fetuses--a review. Placenta 2002 Apr;23 Suppl A:S136-41.

(92) Goplerud JM, Delivoria-Papadopoulos M. Physiology of the placenta--gas exchange. Ann Clin Lab Sci 1985 Jul-Aug;15(4):270-278.

(93) Gregg AR, Weiner CP. "Normal" umbilical arterial and venous acid-base and blood gas values. Clin Obstet Gynecol 1993 Mar;36(1):24-32.

(94) Longo LD, Meschia G. Elizabeth M. Ramsey and the evolution of ideas of uteroplacental blood flow and placental gas exchange. Eur J Obstet Gynecol Reprod Biol 2000 Jun;90(2):129-133.

(95) Martin CB,Jr. Normal fetal physiology and behavior, and adaptive responses with hypoxemia. Semin Perinatol 2008 Aug;32(4):239-242.

(96) Bell SG. An introduction to hemoglobin physiology. Neonatal Netw 1999 Mar;18(2):9-15.

(97) Chaddha V, Viero S, Huppertz B, Kingdom J. Developmental biology of the placenta and the origins of placental insufficiency. Semin Fetal Neonatal Med 2004 Oct;9(5):357-369.

(98) Redline RW. Disorders of placental circulation and the fetal brain. Clin Perinatol 2009 Sep;36(3):549-559.

(99) Nicolaides KH, Economides DL, Soothill PW. Blood gases, pH, and lactate in appropriate- and small-for-gestational-age fetuses. Am J Obstet Gynecol 1989 Oct;161(4):996-1001.

(100) Cetin I. Placental transport of amino acids in normal and growth-restricted pregnancies. Eur J Obstet Gynecol Reprod Biol 2003 Sep 22;110 Suppl 1:S50-4.

(101) Kingdom JC, Kaufmann P. Oxygen and placental villous development: origins of fetal hypoxia. Placenta 1997 Nov;18(8):613-21; discussion 623-6.

(102) Sebire NJ. Umbilical artery Doppler revisited: pathophysiology of changes in intrauterine growth restriction revealed. Ultrasound Obstet Gynecol 2003 May;21(5):419-422.

(103) Raio L, Ghezzi F, Cromi A, Nelle M, Durig P, Schneider H. The thick heterogeneous (jellylike) placenta: a strong predictor of adverse pregnancy outcome. Prenat Diagn 2004 Mar;24(3):182-188.

(104) Elchalal U, Ezra Y, Levi Y, Bar-Oz B, Yanai N, Intrator O, et al. Sonographically thick placenta: a marker for increased perinatal risk--a prospective cross-sectional study. Placenta 2000 Mar-Apr;21(2-3):268-272.

(105) Rudolph AM, Heymann MA. The circulation of the fetus in utero. Methods for studying distribution of blood flow, cardiac output and organ blood flow. Circ Res 1967 Aug;21(2):163-184.

(106) Edelstone DI, Rudolph AM. Preferential streaming of ductus venosus blood to the brain and heart in fetal lambs. Am J Physiol 1979 Dec;237(6):H724-9.

(107) Edelstone DI, Rudolph AM, Heymann MA. Effects of hypoxemia and decreasing umbilical flow liver and ductus venosus blood flows in fetal lambs. Am J Physiol 1980 May;238(5):H656-63.

(108) Junno J, Bruun E, Gutierrez JH, Erkinaro T, Haapsamo M, Acharya G, et al. Fetal sheep left ventricle is more sensitive than right ventricle to progressively worsening hypoxemia and acidemia. Eur J Obstet Gynecol Reprod Biol 2012 Dec 21.

(109) Kiserud T. Physiology of the fetal circulation. Semin Fetal Neonatal Med 2005 Dec;10(6):493-503.

(110) Brezinka C. Fetal hemodynamics. J Perinat Med 2001;29(5):371-380.

(111) Arbeille P. Fetal arterial Doppler-IUGR and hypoxia. Eur J Obstet Gynecol Reprod Biol 1997 Dec;75(1):51-53.

(112) Baschat AA, Hecher K. Fetal growth restriction due to placental disease. Semin Perinatol 2004 Feb;28(1):67-80.

(113) Bonnin P, Guyot B, Bailliart O, Benard C, Blot P, Martineaud JP. Relationship between umbilical and fetal cerebral blood flow velocity waveforms and umbilical venous blood gases. Ultrasound Obstet Gynecol 1992 Jan 1;2(1):18-22.

(114) Baschat AA. Doppler application in the delivery timing of the preterm growth-restricted fetus: another step in the right direction. Ultrasound Obstet Gynecol 2004 Feb;23(2):111-118.

(115) DAWES GS. The umbilical circulation. Am J Obstet Gynecol 1962 Dec 1;84:1634-1648.

(116) Johnson P, Maxwell DJ, Tynan MJ, Allan LD. Intracardiac pressures in the human fetus. Heart 2000 Jul;84(1):59-63.

(117) Mielke G, Benda N. Cardiac output and central distribution of blood flow in the human fetus. Circulation 2001 Mar 27;103(12):1662-1668.

(118) Baschat AA. The fetal circulation and essential organs-a new twist to an old tale. Ultrasound Obstet Gynecol 2006 Apr;27(4):349-354.

(119) Haugen G, Kiserud T, Godfrey K, Crozier S, Hanson M. Portal and umbilical venous blood supply to the liver in the human fetus near term. Ultrasound Obstet Gynecol 2004 Nov;24(6):599-605.

(120) Kessler J, Rasmussen S, Kiserud T. The fetal portal vein: normal blood flow development during the second half of human pregnancy. Ultrasound Obstet Gynecol 2007 Jul;30(1):52-60.

(121) Kessler J, Rasmussen S, Godfrey K, Hanson M, Kiserud T. Fetal growth restriction is associated with prioritization of umbilical blood flow to the left hepatic lobe at the expense of the right lobe. Pediatr Res 2009 Jul;66(1):113-117.

(122) Tchirikov M, Eisermann K, Rybakowski C, Schroder HJ. Doppler ultrasound evaluation of ductus venosus blood flow during acute hypoxemia in fetal lambs. Ultrasound Obstet Gynecol 1998 Jun;11(6):426-431.

(123) Kiserud T, Rasmussen S, Skulstad S. Blood flow and the degree of shunting through the ductus venosus in the human fetus. Am J Obstet Gynecol 2000 Jan;182(1 Pt 1):147-153.

(124) Acharya G, Tronnes A, Rasanen J. Aortic isthmus and cardiac monitoring of the growth-restricted fetus. Clin Perinatol 2011 Mar;38(1):113-25, vi-vii.

(125) Makowski EL, Hertz RH, Meschia G. Effects of acute maternal hypoxia and hyperoxia on the blood flow to the pregnant uterus. Am J Obstet Gynecol 1973 Mar 1;115(5):624-631.

(126) Wilkening RB, Meschia G. Fetal oxygen uptake, oxygenation, and acid-base balance as a function of uterine blood flow. Am J Physiol 1983 Jun;244(6):H749-55.

(127) Bennet L, Gunn AJ. The fetal heart rate response to hypoxia: insights from animal models. Clin Perinatol 2009 Sep;36(3):655-672.

(128) Wladimiroff JW, Tonge HM, Stewart PA. Doppler ultrasound assessment of cerebral blood flow in the human fetus. Br J Obstet Gynaecol 1986 May;93(5):471-475.

(129) Wladimiroff JW, vd Wijngaard JA, Degani S, Noordam MJ, van Eyck J, Tonge HM. Cerebral and umbilical arterial blood flow velocity waveforms in normal and growth-retarded pregnancies. Obstet Gynecol 1987 May;69(5):705-709.

(130) Makikallio K, Jouppila P, Rasanen J. Retrograde aortic isthmus net blood flow and human fetal cardiac function in placental insufficiency. Ultrasound Obstet Gynecol 2003 Oct;22(4):351-357.

(131) Kiserud T, Kessler J, Ebbing C, Rasmussen S. Ductus venosus shunting in growth-restricted fetuses and the effect of umbilical circulatory compromise. Ultrasound Obstet Gynecol 2006 Aug;28(2):143-149.

(132) Kiserud T. The ductus venosus. Semin Perinatol 2001 Feb;25(1):11-20.

(133) Reuss ML, Rudolph AM. Distribution and recirculation of umbilical and systemic venous blood flow in fetal lambs during hypoxia. J Dev Physiol 1980 Feb-Apr;2(1-2):71-84.

(134) Kiserud T. Hemodynamics of the ductus venosus. Eur J Obstet Gynecol Reprod Biol 1999 Jun;84(2):139-147.

(135) Tchirikov M, Schroder HJ, Hecher K. Ductus venosus shunting in the fetal venous circulation: regulatory mechanisms, diagnostic methods and medical importance. Ultrasound Obstet Gynecol 2006 Apr;27(4):452-461.

(136) Makikallio K, Acharya G, Erkinaro T, Kavasmaa T, Haapsamo M, Huhta JC, et al. Ductus venosus velocimetry in acute fetal acidemia and impending fetal death in a sheep model of increased placental vascular resistance. Am J Physiol Heart Circ Physiol 2010 Apr;298(4):H1229-34.

(137) Hecher K, Campbell S, Doyle P, Harrington K, Nicolaides K. Assessment of fetal compromise by Doppler ultrasound investigation of the fetal circulation. Arterial, intracardiac, and venous blood flow velocity studies. Circulation 1995 Jan 1;91(1):129-138.

(138) Richardson BS, Bocking AD. Metabolic and circulatory adaptations to chronic hypoxia in the fetus. Comp Biochem Physiol A Mol Integr Physiol 1998 Mar;119(3):717-723.

(139) Rizzo G, Capponi A, Rinaldo D, Arduini D, Romanini C. Ventricular ejection force in growth-retarded fetuses. Ultrasound Obstet Gynecol 1995 Apr;5(4):247-255.

(140) Cohn HE, Sacks EJ, Heymann MA, Rudolph AM. Cardiovascular responses to hypoxemia and acidemia in fetal lambs. Am J Obstet Gynecol 1974 Nov 15;120(6):817-824.

(141) Bahtiyar MO, Copel JA. Cardiac changes in the intrauterine growth-restricted fetus. Semin Perinatol 2008 Jun;32(3):190-193.

(142) Godfrey ME, Messing B, Cohen SM, Valsky DV, Yagel S. Functional assessment of the fetal heart: a review. Ultrasound Obstet Gynecol 2012 Feb;39(2):131-144.

(143) Kitanaka T, Alonso JG, Gilbert RD, Siu BL, Clemons GK, Longo LD. Fetal responses to long-term hypoxemia in sheep. Am J Physiol 1989 Jun;256(6 Pt 2):R1348-54.

(144) Barker DJ. The developmental origins of well-being. Philos Trans R Soc Lond B Biol Sci 2004 Sep 29;359(1449):1359-1366.

(145) Barker DJ, Gluckman PD, Godfrey KM, Harding JE, Owens JA, Robinson JS. Fetal nutrition and cardiovascular disease in adult life. Lancet 1993 Apr 10;341(8850):938-941.

(146) Morrison JL, Duffield JA, Muhlhausler BS, Gentili S, McMillen IC. Fetal growth restriction, catch-up growth and the early origins of insulin resistance and visceral obesity. Pediatr Nephrol 2010 Apr;25(4):669-677.

(147) Neerhof MG, Thaete LG. The fetal response to chronic placental insufficiency. Semin Perinatol 2008 Jun;32(3):201-205.

(148) Myers RE, Stange L, Joelsson I, Huzell B, Wussow C. Effects upon the fetus of oxygen administration to the mother. A study in monkey. Acta Obstet Gynecol Scand 1977;56(3):195-203.

(149) Sonesson SE, Fouron JC, Teyssier G, Bonnin P. Effects of increased resistance to umbilical blood flow on fetal hemodynamic changes induced by maternal oxygen administration: a Doppler velocimetric study on the sheep. Pediatr Res 1993 Dec;34(6):796-800.

(150) VASICKA A, QUILLIGAN EJ, AZNAR R, LIPSITZ PJ, BLOOR BM. Oxygen tension in maternal and fetal blood, amniotic fluid, and cerebrospinal fluid of the mother and the baby. Am J Obstet Gynecol 1960 Jun;79:1041-1047.

(151) Tomimatsu T, Pena JP, Longo LD. Fetal cerebral oxygenation: the role of maternal hyperoxia with supplemental CO2 in sheep. Am J Obstet Gynecol 2007 Apr;196(4):359.e1-359.e5.

(152) Willcourt RJ, King JC, Queenan JT. Maternal oxygenation administration and the fetal transcutaneous PO2. Am J Obstet Gynecol 1983 Jul 15;146(6):714-715.

(153) Nicolaides KH, Campbell S, Bradley RJ, Bilardo CM, Soothill PW, Gibb D. Maternal oxygen therapy for intrauterine growth retardation. Lancet 1987 Apr 25;1(8539):942-945.

(154) Rizzo G, Arduini D, Romanini C, Mancuso S. Effects of maternal hyperoxygenation on atrioventricular velocity waveforms in healthy and growth-retarded fetuses. Biol Neonate 1990;58(3):127-132.

(155) Caforio L, Caruso A, Testa AC, Pompei A, Ciampelli M. Short-term maternal oxygen administration in fetuses with absence or reversal of end-diastolic velocity in umbilical artery: pathophysiological and clinical considerations. Acta Obstet Gynecol Scand 1998 Aug;77(7):707-711.

(156) Arduini D, Rizzo G, Mancuso S, Romanini C. Short-term effects of maternal oxygen administration on blood flow velocity waveforms in healthy and growth-retarded fetuses. Am J Obstet Gynecol 1988 Nov;159(5):1077-1080.

(157) Arduini D, Rizzo G, Romanini C, Mancuso S. Doppler assessment of fetal blood flow velocity waveforms during acute maternal oxygen administration as predictor of fetal outcome in post-term pregnancy. Am J Perinatol 1990 Jul;7(3):258-262.

(158) Arduini D, Rizzo G, Romanini C, Mancuso S. Hemodynamic changes in growth retarded fetuses during maternal oxygen administration as predictors of fetal outcome. J Ultrasound Med 1989 Apr;8(4):193-196.

(159) Almstrom H, Sonesson SE. Doppler echocardiographic assessment of fetal blood flow redistribution during maternal hyperoxygenation. Ultrasound Obstet Gynecol 1996 Oct;8(4):256-261.

(160) Sonesson SE, Fouron JC, Teyssier G, Bonnin P. Doppler echocardiographic assessment of changes in the central circulation of the fetal sheep induced by maternal oxygen administration. Acta Paediatr 1994 Oct;83(10):1007-1011.

(161) Simchen MJ, Tesler J, Azami T, Preiss D, Fedorko L, Goldszmidz E, et al. Effects of maternal hyperoxia with and without normocapnia in uteroplacental and fetal Doppler studies. Ultrasound Obstet Gynecol 2005 Oct;26(5):495-499.

(162) Tomimatsu T, Pereyra Pena J, Hatran DP, Longo LD. Maternal oxygen administration and fetal cerebral oxygenation: studies on near-term fetal lambs at both low and high altitude. Am J Obstet Gynecol 2006 Aug;195(2):535-541.

(163) Soregaroli M, Rizzo G, Danti L, Arduini D, Romanini C. Effects of maternal hyperoxygenation on ductus venosus flow velocity waveforms in normal third-trimester fetuses. Ultrasound Obstet Gynecol 1993 Mar 1;3(2):115-119.

(164) Bekedam DJ, Mulder EJ, Snijders RJ, Visser GH. The effects of maternal hyperoxia on fetal breathing movements, body movements and heart rate variation in growth retarded fetuses. Early Hum Dev 1991 Dec;27(3):223-232.

(165) Bartnicki J, Saling E. Influence of maternal oxygen administration on the computer-analysed fetal heart rate patterns in small-for-gestational-age fetuses. Gynecol Obstet Invest 1994;37(3):172-175.

(166) Mildenberger E, Siegel G, Versmold HT. Oxygen-dependent regulation of membrane potential and vascular tone of human umbilical vein. Am J Obstet Gynecol 1999 Sep;181(3):696-700.

(167) McGrath JC, MacLennan SJ, Mann AC, Stuart-Smith K, Whittle MJ. Contraction of human umbilical artery, but not vein, by oxygen. J Physiol 1986 Nov;380:513-519.

(168) Battaglia FC, Meschia G, Makowski EL, Bowes W. The effect of maternal oxygen inhalation upon fetal oxygenation. J Clin Invest 1968 Mar;47(3):548-555.

(169) Polvi HJ, Pirhonen JP, Erkkola RU. The hemodynamic effects of maternal hypo- and hyperoxygenation in healthy term pregnancies. Obstet Gynecol 1995 Nov;86(5):795-799.

(170) Mahutte CK. On-line arterial blood gas analysis with optodes: current status. Clin Biochem 1998 Apr;31(3):119-130.

(171) Sorensen A, Holm D, Pedersen M, Tietze A, Stausbol-Gron B, Duus L, et al. Left-right difference in fetal liver oxygenation during hypoxia estimated by BOLD MRI in a fetal sheep model. Ultrasound Obstet Gynecol 2011 Dec;38(6):665-672.

(172) Lu H, Zhao C, Ge Y, Lewis-Amezcua K. Baseline blood oxygenation modulates response amplitude: Physiologic basis for intersubject variations in functional MRI signals. Magn Reson Med 2008 Aug;60(2):364-372.

(173) Cameron IL, Ord VA, Fullerton GD. Characterization of proton NMR relaxation times in normal and pathological tissues by correlation with other tissue parameters. Magn Reson Imaging 1984;2(2):97-106.

(174) Wright C, Morris DM, Baker PN, Crocker IP, Gowland PA, Parker GJ, et al. Magnetic resonance imaging relaxation time measurements of the placenta at 1.5 T. Placenta 2011 Dec;32(12):1010-1015.

(175) Soothill PW, Nicolaides KH, Rodeck CH, Campbell S. Effect of gestational age on fetal and intervillous blood gas and acid-base values in human pregnancy. Fetal Ther 1986;1(4):168-175.

(176) Lee SW, Khaw KS, Ngan Kee WD, Leung TY, Critchley LA. Haemodynamic effects from aortocaval compression at different angles of lateral tilt in non-labouring term pregnant women. Br J Anaesth 2012 Dec;109(6):950-956.

(177) Li H, Gudmundsson S, Olofsson P. Uterine artery blood flow velocity waveforms during uterine contractions. Ultrasound Obstet Gynecol 2003 Dec;22(6):578-585.

(178) Wedegartner U, Tchirikov M, Schafer S, Priest AN, Walther M, Adam G, et al. Fetal sheep brains: findings at functional blood oxygen level-dependent 3-T MR imaging--relationship to maternal oxygen saturation during hypoxia. Radiology 2005 Dec;237(3):919-926.

(179) Wedegartner U, Tchirikov M, Koch M, Adam G, Schroder H. Functional magnetic resonance imaging (fMRI) for fetal oxygenation during maternal hypoxia: initial results. Rofo 2002 Jun;174(6):700-703.

(180) Okutomi T, Whittington RA, Stein DJ, Morishima HO. Comparison of the effects of sevoflurane and isoflurane anesthesia on the maternal-fetal unit in sheep. J Anesth 2009;23(3):392-398.

(181) Kiserud T, Jauniaux E, West D, Ozturk O, Hanson MA. Circulatory responses to maternal hyperoxaemia and hypoxaemia assessed non-invasively in fetal sheep at 0.3-0.5 gestation in acute experiments. BJOG 2001 Apr;108(4):359-364.

(182) Gudmundsson S, Gunnarsson GO, Hokegard KH, Ingemarsson J, Kjellmer I. Venous Doppler velocimetry in relationship to central venous pressure and heart rate during hypoxia in the ovine fetus. J Perinat Med 1999;27(2):81-90.

(183) Duncan KR, Gowland P, Francis S, Moore R, Baker PN, Johnson IR. The investigation of placental relaxation and estimation of placental perfusion using echo-planar magnetic resonance imaging. Placenta 1998 Sep;19(7):539-543.

(184) Gowland PA, Freeman A, Issa B, Boulby P, Duncan KR, Moore RJ, et al. In vivo relaxation time measurements in the human placenta using echo planar imaging at 0.5 T. Magn Reson Imaging 1998 Apr;16(3):241-247.

(185) Mayhew TM, Wadrop E. Placental morphogenesis and the star volumes of villous trees and intervillous pores. Placenta 1994 Feb-Mar;15(2):209-217.

(186) Derwig I, Barker GJ, Poon L, Zelaya F, Gowland P, Lythgoe DJ, et al. Association of placental T2 relaxation times and uterine artery Doppler ultrasound measures of placental blood flow. Placenta 2013 Jun;34(6):474-479.

(187) Girsh E, Plaks V, Gilad AA, Nevo N, Schechtman E, Neeman M, et al. Cloprostenol, a prostaglandin F(2alpha) analog, induces hypoxia in rat placenta: BOLD contrast MRI. NMR Biomed 2007 Feb;20(1):28-39.

Appendix

The Review Table

Paper 1

Sørensen A, Pedersen M, Tietze A, Ottosen L, Duus L, Uldbjerg N.

BOLD MRI in sheep fetuses: a non-invasive method for measuring changes in tissue oxygenation.

Ultrasound Obstet Gynecol. 2009 Dec;34(6):687-92.

Paper 2

Sørensen A, Holm D, Pedersen M, Tietze A, Stausbøl-Grøn B, Duus L, Uldbjerg N.

Left-right difference in fetal liver oxygenation during hypoxia estimated by BOLD MRI in a fetal sheep model.

Ultrasound Obstet Gynecol. 2011 Dec;38(6):665-72

Paper 3

Sørensen A, Peters D, Simonsen C, Pedersen M, Stausbøl-Grøn B, Christiansen OB, Lingman G, Uldbjerg N.

Changes in human fetal oxygenation during maternal hyperoxia as estimated by BOLD MRI..

Prenat Diagn. 2013 Feb;33(2):141-5

Paper 4

Sørensen A, Peters D, Fründ E, Lingman G, Christiansen O, Uldbjerg N.

Changes in human placental oxygenation during maternal hyperoxia as estimated by BOLD MRI.

Ultrasound Obstet Gynecol. 2013 Sep;42(3):310-4

Paper 5

Peters D, Sørensen A, Simonsen C, M. Sinding, Uldbjerg N.

The reproducibility of human placental T2* measurements and the hyperoxic response.

Radiology 2013 (Submitted)

Review Table

First Author (Reference) Year	Studied cases Number	MRI system	Reference of fetal saturation	Stimulus	Target organ
Hykin (16) **1999**	Human fetus n=4 (14)	0.5T		Auditory stimulus	ΔBOLD fetal brain
Semple (20) **2001**	Human fetus n=9	0.95T (Siemens)		Hyperoxia	ΔT2* liver
Moore (17) **2001**	Human fetus n=7 (12)	0.5T		Auditory stimulus	ΔBOLD fetal brain
Wedegärtner (179) **2002**	Sheep fetus n=2	1.5T (Siemens)		Hypoxia	ΔBOLD fetal brain, heart, liver
Fulford (18) **2003**	Human fetus n=9 (12)	0.5T		Light stimulus	ΔBOLD fetal brain
Fulford (19) **2004**	Human fetus n=15 (17)	0.5T		Vibroacoustic stimulus	ΔBOLD fetal brain
Wedegärtner (178) **2005**	Sheep fetus n=5	3.0T (Philips)		Hypoxia	ΔBOLD fetal brain
Wedegärtner (22) **2006**	Sheep fetus n=6	3.0T (Philips)	Fetal hemoglobin saturation. (Carotid artery)	Hypoxia	ΔBOLD fetal brain, lung, liver, heart ΔBOLD placenta
Girsh (187) **2006**	Rat placenta n=6 (4)	4.7T (Bruker)		Hypoxia (Prostaglandin $F_{2\alpha}$)	ΔBOLD placenta
Wedegärtner (23) **2009**	Sheep fetus n=5	3T (Philips)	Fetal hemoglobin saturation (Carotid artery)	Hypoxia	ΔT2* fetal brain (MR-sO_2)
Wedegärtner (24) **2009**	Sheep fetus n=5 + n=5	1.5T (Philips) 3.0T (Philips)	Fetal hemoglobin saturation (Carotid artery)	Hypoxia	ΔT2* fetal brain
Sørensen (25) **2009**	Sheep fetus n=7	1.5T (Philips)	Fetal liver oxygenation (oxygen sensor)	Hyperoxia /Hypoxia	ΔBOLD fetal brain, liver, spleen, kidney.
Morris (21) **2010**	Human fetus n=41 AGA n=39 SGA	1.5T (GE)		Hyperoxia	ΔT2* fetal liver

Sørensen (171,171) **2011**	Sheep fetus n=8	1.5T (Philips)		Hyperoxia/Hypoxia	ΔBOLD fetal liver (left-right)
Huen (26) **2012**	Human placenta n=14	1.5T (Philips)		Hyperoxia	ΔT2* placenta
Aimot-Macron (29) **2013**	Rat fetus and placenta n=18 (FGR)	1.5T (GE)		Hyperoxia	ΔBOLD placenta ΔBOLD rat fetus
Sørensen (28) **2013**	Human fetus n=8	1.5T (Philips)		Hyperoxia	ΔBOLD fetal liver, spleen, kidney, brain
Sørensen (27) **2013**	Human placenta n=8	1.5T (GE)		Hyperoxia	ΔBOLD placenta
Chalouhi (30) **2013**	Rat fetus and placenta n=16 (19) (FGR)	4.7T (Bruker)		Hyperoxia	ΔT2* placenta ΔT2* fetal liver ΔT2* fetal brain

Paper 1

Ultrasound Obstet Gynecol 2009; **34**: 687–692
Published online 21 September 2009 in Wiley InterScience (www.interscience.wiley.com). **DOI:** 10.1002/uog.7322

BOLD MRI in sheep fetuses: a non-invasive method for measuring changes in tissue oxygenation

A. SØRENSEN*, M. PEDERSEN†, A. TIETZE‡, L. OTTOSEN*, L. DUUS* and N. ULDBJERG*

**Department of Gynecology and Obstetrics, †MR Research Center and ‡Department of Radiology, Institute of Clinical Medicine, Aarhus University Hospital, Skejby, Aarhus, Denmark*

KEYWORDS: BOLD MRI; brain sparing; fetal sheep; fetus; hypoxia; oxygen; tissue oxygenation

ABSTRACT

Objective *The purpose of this descriptive study was to correlate changes in the blood oxygen level-dependent (BOLD) magnetic resonance imaging (MRI) signal with direct measurements of fetal tissue oxygenation.*

Methods *Seven anesthetized ewes carrying singleton fetuses at 125 days' gestation (term 145 days) underwent BOLD MRI, covering the entire fetus in a multislice approach. The fetuses were subjected to normoxic, hypoxic and hyperoxic conditions by changing the O_2/N_2O ratio in the maternal ventilated gas supply. The partial pressure of oxygen (pO_2) in the fetal liver was measured using an oxygen-sensitive optode. Maternal arterial blood samples were simultaneously withdrawn for blood gas analysis. These measurements were compared with BOLD MRI signals in the fetal liver, kidney, spleen and brain.*

Results *We demonstrated a consistent increase in the BOLD MRI signal with increasing tissue pO_2. For the fetal liver, spleen and kidney we observed a clear association between changes in maternal arterial blood pO_2 and changes in BOLD MRI signal. Interestingly, we found that the BOLD signal of the fetal brain remained unchanged during hypoxic, normoxic and hyperoxic conditions.*

Conclusions *This experimental study demonstrated that BOLD MRI is a reliable non-invasive method for measuring changes in tissue oxygenation in fetal sheep. The unchanged signal in the fetal brain during altered maternal oxygen conditions is probably explained by the brain-sparing mechanism. Copyright © 2009 ISUOG. Published by John Wiley & Sons, Ltd.*

INTRODUCTION

Monitoring fetal well-being, identifying fetuses at high risk of poor perinatal outcome and timing of delivery are the main challenges in obstetrics. Doppler ultrasonography and cardiotocography are the preferred diagnostic tools for this purpose, providing immediate information about the fetal heart rate and blood flow[1]. These methods, however, do not offer direct information about the oxygen supply to the fetus nor the oxygen levels in the fetal organs. The only current method for obtaining this direct information is cordocentesis, which is a procedure associated with a risk of miscarriage. In this experimental study we introduce a non-invasive method for the direct measurement of changes in fetal tissue oxygenation.

The blood oxygen level-dependent (BOLD) effect in magnetic resonance imaging (MRI) is based on the magnetic properties of hemoglobin. Oxyhemoglobin has diamagnetic properties whereas deoxyhemoglobin has paramagnetic properties[2]. Changes in the blood saturation level will therefore affect the apparent transversal relaxation time ($T2^*$) of the surrounding water molecules, providing a measurable change in the MRI signal using a $T2^*$-weighted sequence. The content of deoxyhemoglobin is inversely related to $T2^*$[3], and a signal reduction in $T2^*$-weighted images therefore corresponds to an increased deoxyhemoglobin content. Thus, assuming that the pO_2 of capillary blood is in equilibrium with the pO_2 in tissue, changes in BOLD signal relate to changes in tissue oxygenation[4].

BOLD MRI provides an opportunity to monitor tissue oxygenation *in vivo*. This technique has allowed investigation of the fetal response following maternal hyperoxygenation[5] as well as audio and visual fetal stimuli[6–8]. In an experimental study in pregnant sheep, Wedegärtner *et al.* showed a reduced BOLD signal in fetal organs suffering from hypoxia[9–11]. Although these observations justify the use of BOLD MRI as a novel diagnostic tool to identify critical changes in the fetal oxygenation level, the exact tissue oxygen content cannot be established. Hence, the aim of this study was to investigate the relationship between changes in BOLD

Correspondence to: Dr A. Sørensen, Aarhus University Hospital, Skejby, Department of Gynecology and Obstetrics, 8200 Aarhus N, Denmark (e-mail: anne.soerensen@ki.au.dk)

Accepted: 3 June 2009

MRI signal and direct tissue oxygen measurements in the fetal liver during hyperoxic, normoxic and hypoxic conditions. In addition, BOLD MRI signals in fetal organs were compared to maternal arterial pO_2 in response to changes in the ventilated oxygen supply.

METHODS

Seven healthy ewes (Gotland sheep) carrying singleton fetuses at 125 days' gestation (term 145 days) were included in the study. Prior to the experimental procedures, the ewes were cared for at our animal farm (Påskehøjgård, Aarhus University Hospital, Denmark), where they had free access to water and food. On the day of the experiment the ewe was sedated with atropine (Nycomed, Taastrup, Denmark) 2 mg and Rompun (Bayer Schering Pharma, Berlin, Germany) 2.5 mg and transported to the surgical unit. Anesthesia was induced with Ketamine (Pfizer, New York, NY, USA) 2 mg/kg and Dormicum (Roche, Basel, Switzerland) 0.25 mg/kg and maintained by Isoflurane (Baxter, Deerfield, IL, USA) 1.5% in an O_2/N_2O mixture. Orotracheal intubation (tube diameter 9 mm) was followed by artificial ventilation using a servoventilator (Abott, Solna, Sweden; tidal volume 600–800 mL, 18 breaths/min). Catheterization of the left common carotid artery was performed for withdrawal and blood gas analysis (Radiometer, Brønshøj, Denmark), a pulse oximeter sensor was attached to an ear, and a capnograph was used for end-tidal CO_2 measurement.

By changing the O_2/N_2O ratio in ventilated gas, the fetus was subjected to normoxic, hypoxic and hyperoxic conditions. The oxygen content varied between 10% and 100%. Each ventilation level was maintained for 30 min to allow steady-state oxygenation conditions. In four ewes, the tissue oxygenation in the fetal liver was successfully measured using an oxygen sensitive optode. The experimental protocol was approved by the local animal ethics committee.

The invasive tissue oxygenation measurements were performed with an MRI-compatible optical oxygen-sensitive optode (Presens, Regensburg, Germany). The optodes used in this study consisted of a 15-m long, 0.9-mm thick fiber-optic cable, exposed and coated with oxygen-sensitive fluorescent sensor material at the tip, which was 0.1 mm in diameter. The principle of measurement is based on the effect of dynamic luminescence quenching of the fluorescent sensor material by molecular oxygen. The dynamic quenching is directly related to the local tissue pO_2 and is measured in real time. The 90% response time of the optode was approximately 10 s[12]. Compared to conventional oxygen-sensitive (Clark-type) electrodes, optodes have the advantage of not consuming oxygen during measurements, such that long-term pO_2 measurements *in vivo* can be performed in tissue, without depleting oxygen around the optode tip, even in regions where oxygen supply is mainly limited to molecular diffusion. One previous study has been published applying this fluorescent technique to fetal tissue oxygen measurement *in vivo*[13]. In this study a 1.2-mm diameter trocar was placed in the fetal liver using sonographic guidance and the optode was firmly inserted through it.

MRI was performed with a 1.5 T clinical system (Philips Medical Systems, Best, The Netherlands). The anesthetized ewe was examined in a left lateral position. The acquisitions were obtained with a phased-array abdominal radio-frequency coil. Fast axial and coronal scans of the fetus were initially performed to locate organs of interest. Next, a sequence was employed, sensitive to changes in magnetic susceptibility using strong $T2^*$-weighting, allowing one to assess changes in the BOLD contrast. This was performed as a dynamic sequence, in which $T2^*$-weighting was accomplished using a two-dimensional gradient-echo sequence with sequential echo-planar encoding. The sequence parameters included: eight slices with 3 mm of thickness; field of view 250×250 mm^2; acquired spatial resolution 256×256 voxels; repetition time (TR) 1500 ms; flip angle 90°; and an echo time of 40 ms optimized for the average $T2^*$ value *in vivo*. Six transients were acquired for optimal signal-to-noise ratio, giving a single-frame scan time of 300 s. A total of 150 dynamic frames were recorded with an interval of 112 s.

The MRI data were transferred to an external workstation equipped with the Mistar software (Apollo Imaging Technology, Melbourne, Australia). All images displayed an adequate signal-to-noise ratio and did not show substantial artifacts. The signal intensity of the $T2^*$-weighted images was examined in regions of interest (ROIs) as shown in Figure 1. Placement of ROIs in the fetal kidney, liver, spleen and brain was performed by a clinical radiologist, and movements were adjusted manually in each dynamic image. For each ROI, the mean ($\pm$ SD) signal versus time curve was calculated.

From a theoretical point of view the local magnetic susceptibility is the degree of magnetization of a material in response to a magnetic field, but the inherent differences

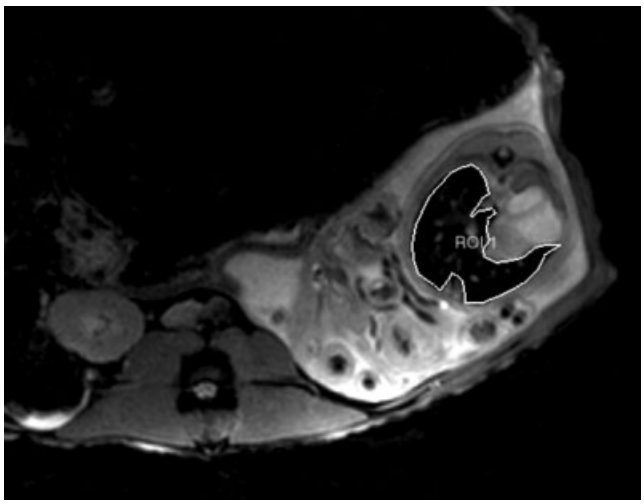

Figure 1 Blood oxygen level-dependent magnetic resonance image showing an axial view of the fetus with the fetal liver selected as the region of interest (ROI).

in local magnetic field mean that it is not possible to directly compare the acquired BOLD signal between animals. Furthermore inter-animal variations are expected in hydration, fetal size, temperature, distance to the receiver coil etc. Owing to these expected inter-animal variations and the modest size of the dataset, we have taken a descriptive approach to data analysis.

Optode measurements of fetal pO_2 were compared with levels of BOLD MRI of the fetal liver during different maternal ventilation oxygenation levels, and the BOLD MRI signals of all fetal organs were compared with maternal arterial pO_2 levels and graphically presented.

RESULTS

All the animals underwent BOLD MRI during normoxic, hyperoxic and hypoxic conditions. In four out of seven animals an oxygen-sensitive optode was successfully inserted into the fetal liver for direct measurement of tissue oxygen. For the fetal liver, changes in the BOLD signal were associated with changes in the direct optode measurements of tissue pO_2 (Figures 2 and 3). Within a few min after changing the maternal oxygen supply (performed by changing the ventilated O_2/N_2O ratio), we observed a corresponding response in the optode measurements as well as in the acquired BOLD signal of the fetal liver. Because of progressive lung atelectasis, the maternal arterial pO_2 did not return to the starting level when the maternal ventilation was returned to normoxic conditions (O_2/N_2O ratio $= 1.0$) at the end of the experiment, and consequently the BOLD signal of the fetal liver and the optode measurements also remained at a lower level in the last period of the experiment.

Figure 4 demonstrates a linear relationship between maternal arterial pO_2 and optode measurements of tissue oxygen levels, justifying the use of maternal arterial pO_2 as a reference for organs without optode measurements. Figure 5 illustrates the BOLD signal in one of the seven fetuses during periods of different maternal arterial pO_2 level. The BOLD signal of the fetal kidney and the spleen changed in patterns similar to the one seen in the liver. In contrast to this, the signal of the brain remained constant during normoxic, hypoxic and hyperoxic conditions.

In all the animals we observed that changes in the BOLD signal of the fetal spleen, kidney and liver were closely associated with changes in maternal arterial oxygenation (Figure 6). As shown in Figures 3 and 6, the BOLD MRI data from each organ in relation to optode/maternal arterial measurements seem to describe a curved graph, which is steeper at lower oxygen levels and flattens at higher oxygen levels. The only exception to this pattern is the BOLD response from the brain, the BOLD signal of which remained constant.

The BOLD MRI signal response was expected to vary between the animals. However, as shown in Figures 3 and 6 there was only a small amount of variation between the different animals, thus the data seem to be reproducible.

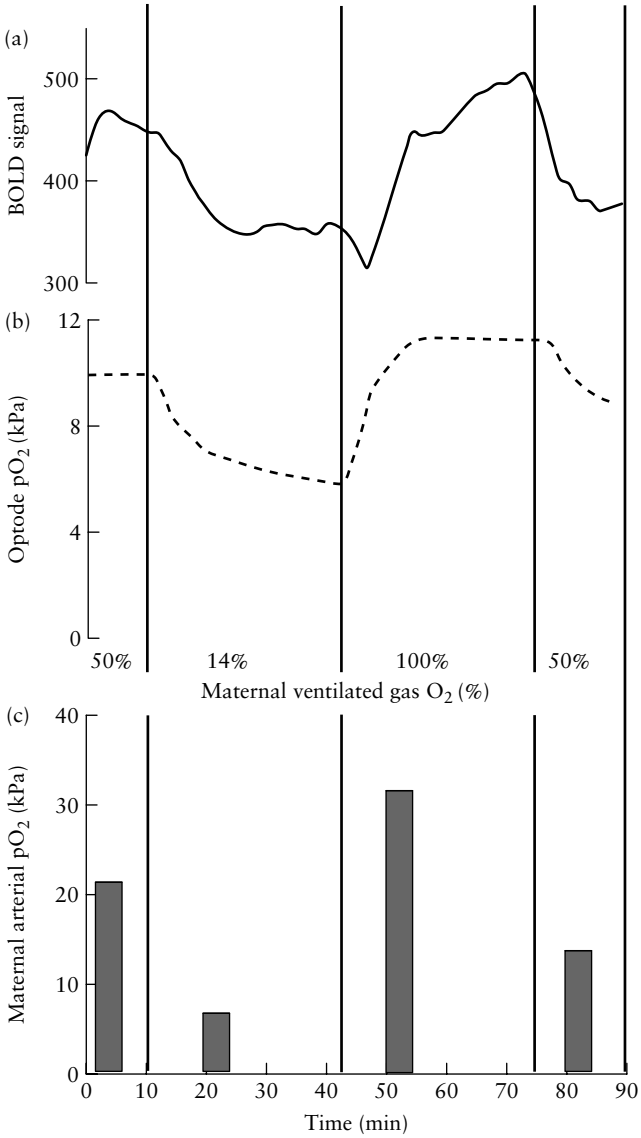

Figure 2 Changes in fetal liver blood oxygen level-dependent (BOLD) magnetic resonance signal (a), fetal liver optode oxygen measurement (b) and maternal arterial pO_2 (c) over time for one sheep (Animal 8) during varying oxygen levels (14–100%) in maternal ventilated gas.

DISCUSSION

This experimental study in pregnant sheep demonstrated that changes in the BOLD MRI signal of the fetal liver were closely related to changes in tissue oxygenation determined by an oxygen-sensitive fluorescence optode. We also observed that changes in BOLD MRI signal were reproducible among animals. Thus, BOLD MRI seems to constitute a reliable non-invasive technique for the determination of short-term changes in fetal tissue oxygenation.

The sensitivity of BOLD MRI is enhanced by the relative hypoxic conditions of the normal fetus. Despite the left shift of the dissociation curve of fetal hemoglobin, as compared to adult hemoglobin, the hemoglobin saturation in the umbilical vein is only 80%[14]. The fetal arterial, mid-capillary and venous oxygen concentrations

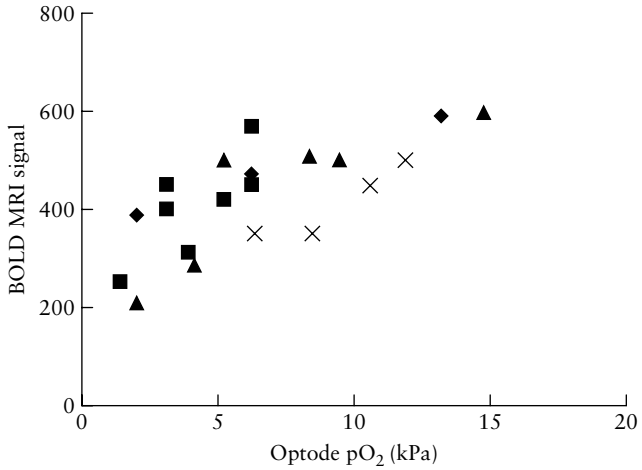

Figure 3 Association between the blood oxygen level-dependent (BOLD) magnetic resonance imaging (MRI) signal of the fetal liver and the direct optode measurements from the fetal liver in four animals. ♦, Animal 2; ■, Animal 3; ▲, Animal 5; ×, Animal 8.

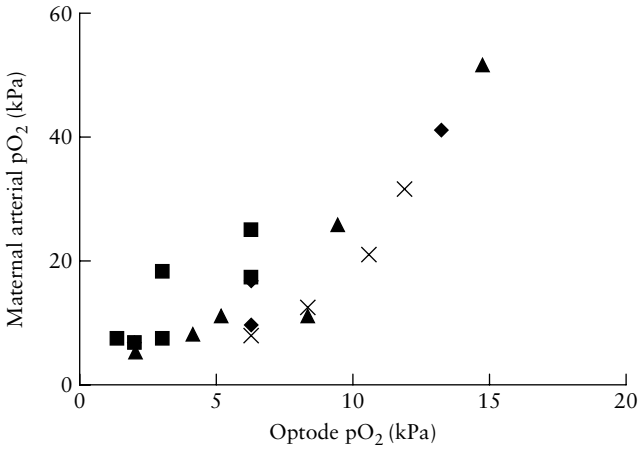

Figure 4 Association between optode measurements of pO_2 in the fetal liver and pO_2 measured in maternal arterial blood samples in four animals. ♦, Animal 2; ■, Animal 3; ▲, Animal 5; ×, Animal 8.

correspond with the steeper part of the hemoglobin dissociation curve. Therefore, with any given change in oxygen concentration, a more pronounced change in the BOLD signal is expected in the fetus as compared to the adult. Keeping the sigmoidal shape of the dissociation curve in mind, one should expect a more pronounced change in BOLD signal during lower oxygen levels and the opposite effect for higher oxygen levels. Our work supports this theory, as the BOLD data from each organ in relation to optode/maternal arterial measurements seem to describe a curved graph that is steep at lower oxygen levels and flattens at higher levels. This is in conflict with a study by Wedegärtner *et al.*[9] that suggested a linear association between maternal arterial saturation and the BOLD signal of selected fetal organs. This difference is probably explained by the different experimental designs of the two studies, as we, unlike Wedegärtner *et al.*, also performed experimental measurements during hyperoxic conditions.

Another variable of importance is the 'fractional blood volume'. As the BOLD MRI signal reflects the deoxyhemoglobin concentration, it depends not only on hemoglobin saturation but also on the fractional blood volume, i.e. if the vessels dilate the amounts of both oxyhemoglobin and deoxyhemoglobin increase within the voxel even in case of unchanged hemoglobin saturation[15]. The oxygen-sensitive optodes used in this study, however, operate independently of changes in fractional blood volume. This indicates that the changes in BOLD MRI signal truly reflect oxygenation changes.

As we only succeeded in inserting oxygen-sensitive optodes into the fetal liver of four animals, we used

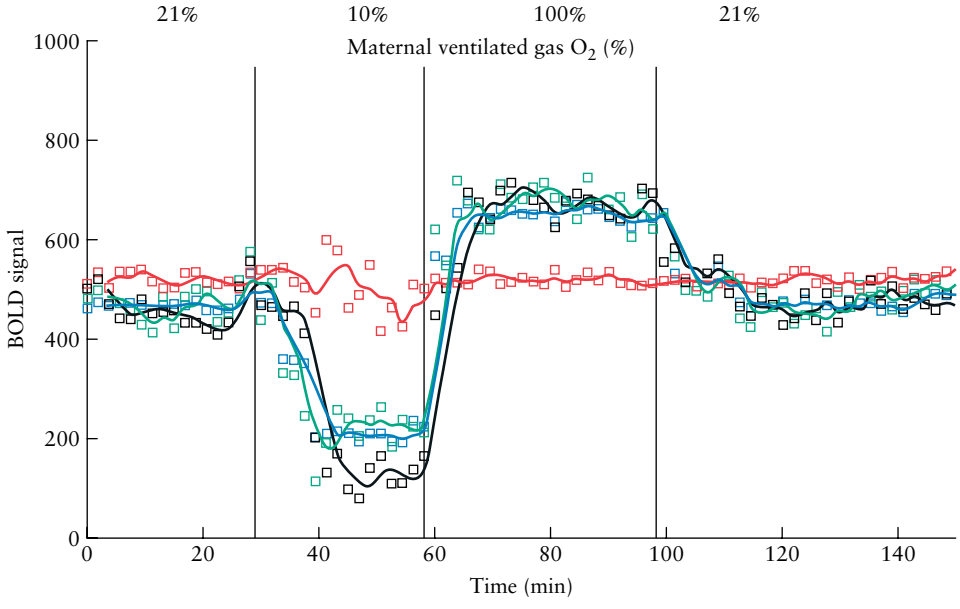

Figure 5 Blood oxygen level-dependent (BOLD) magnetic resonance signals from the fetal brain (□), spleen (□), liver (□) and kidneys (□) in one animal (Animal 5) during varying oxygen levels in maternal ventilated gas (10–100%).

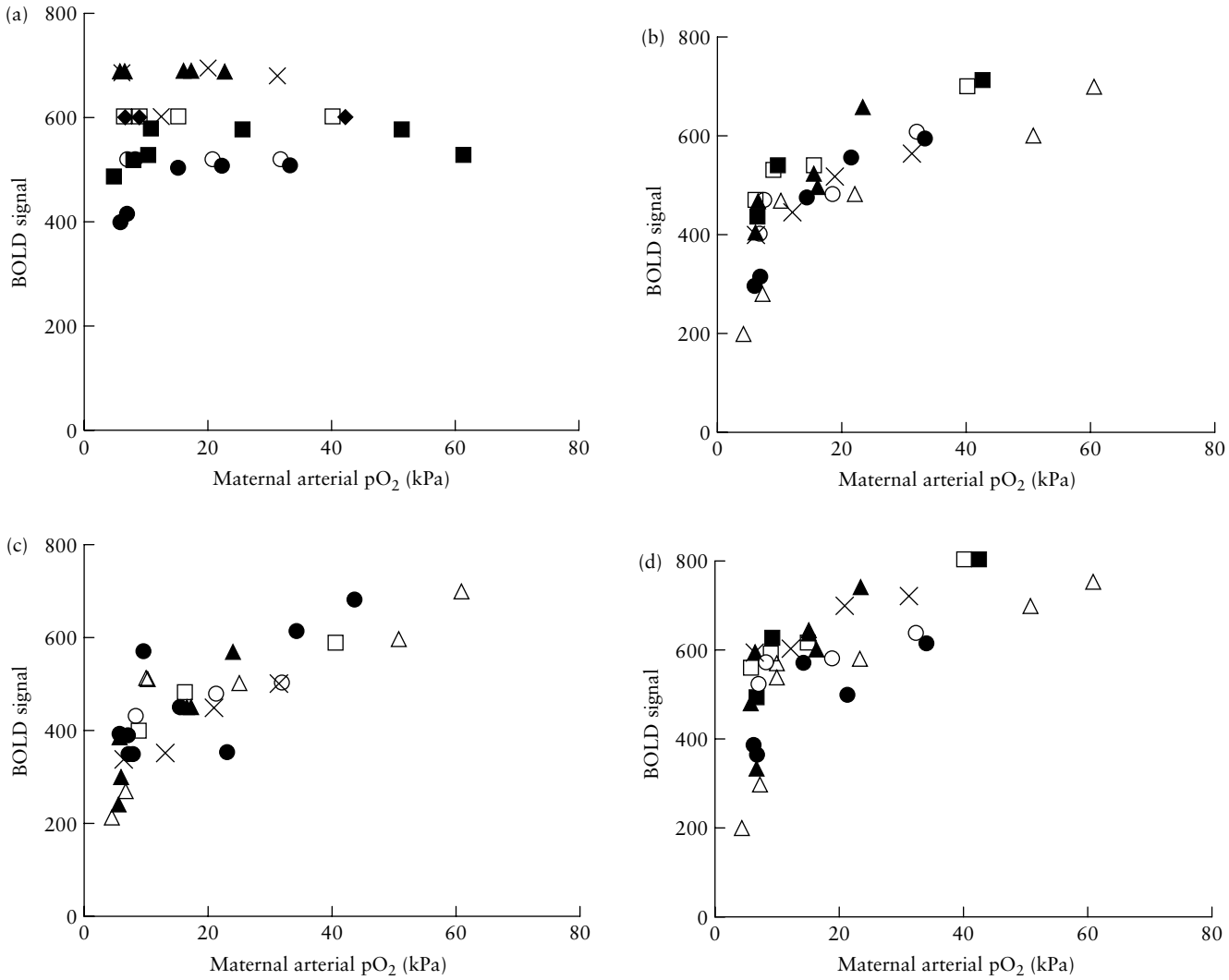

Figure 6 Association between blood oxygen level-dependent (BOLD) magnetic resonance signals from the fetal brain (a), spleen (b), liver (c) and kidney (d) and maternal arterial pO_2. ■, Animal 1; □, Animal 2; ▲, Animal 3; △, Animal 5; ●, Animal 6; ○, Animal 7; ×, Animal 8.

the maternal arterial pO_2 as a reference for the remaining fetal organs. This was justified by the observed linear relationship between the optode measurements and the maternal arterial pO_2. In the fetal liver, spleen and kidney we found a clear association between changes in the BOLD signal and changes in maternal arterial pO_2. In contrast to this, the BOLD signal of the fetal brain remained unchanged during the normoxic, hypoxic and hyperoxic conditions – a consistent finding in all our experiments. We explain this interesting phenomenon as a result of the brain-sparing mechanism, characterized by increased blood flow to the brain during hypoxic conditions, thus compensating for the reduced oxygen content of the circulating blood. This autoregulation is very efficient, and protects the brain from extreme conditions. Our results indicate that the brain was also spared from hyperoxic conditions.

Apart from the fetal brain, fetal oxygenation increased during hyperoxic maternal conditions. This consistent finding is supported by other studies. Semple *et al.*[5] performed BOLD MRI during hyperoxia in normal pregnancies, showing an increase in BOLD signal in five out of nine pregnancies. The lack of response in four pregnancies was probably due to fetal movements interfering with the MRI signal[5]. In growth-restricted fetuses maternal hyperoxygenation seems to improve umbilical pO_2 as determined by cordocentesis[16], normalize brain sparing demonstrated by Doppler flow[17] and increase fetal movements[18]. The 'oxygen test' was introduced by Arduini *et al.*[19]; if fetal brain sparing is normalized by maternal hyperoxygenation the test is positive, and if brain sparing remains unaffected the oxygen test is negative. A negative test has been reported to be a strong predictor of adverse perinatal outcome[19,20]. A positive oxygen test cannot be explained by increased oxygenation of maternal hemoglobin as the arterial saturation is close to 100% even during normoxic conditions. Therefore, an increased oxygen partial pressure gradient across the placental membrane is likely to be of importance, as the hemoglobin saturation of venous umbilical blood is only 80%[14].

Differences between the human placenta and the sheep placenta complicate extrapolation of our experimental findings to the human situation. The histological

structure of the human placenta can be represented by the multivillous model, in contrast to the sheep placenta, which is represented by the venous equilibration exchange model[21]. The sheep placenta is less effective at transporting oxygen to the fetus than is the human placenta. As a consequence of the reduced O_2 extraction coefficient the sheep fetus is slightly more hypoxic (umbilical vein, 4.7 kPa; umbilical artery, 2.7 kPa) compared to the human fetus (umbilical vein, 5.5 kPa; umbilical artery, 3.9 kPa). The neuroendocrine and cardiovascular responses in hypoxia are very similar in sheep and human fetuses, including the brain-sparing mechanism[22]. The long duration of anesthesia might have affected our results, but not the conclusions drawn from them.

In conclusion, BOLD MRI is a reliable non-invasive method for measuring regional changes in tissue oxygenation in fetal organs *in vivo*. This method provides new opportunities for fetal monitoring and fetal testing.

ACKNOWLEDGMENTS

This work was supported by Forskningsinitiativet, Aarhus University Hospital. Thanks to Peter Årslev Nielsen for support and advice in anesthesiological matters.

REFERENCES

1. Baschat AA. Pathophysiology of fetal growth restriction: implications for diagnosis and surveillance. *Obstet Gynecol Surv* 2004; **59**: 617–627.
2. Prasad PV. Functional MRI of the kidney: tools for translational studies of pathophysiology of renal disease. *Am J Physiol Renal Physiol* 2006; **290**: F958–F974.
3. Prasad PV, Edelman RR, Epstein FH. Noninvasive evaluation of intrarenal oxygenation with BOLD MRI. *Circulation* 1996; **94**: 3271–3275.
4. Pedersen M, Dissing TH, Mørkenborg J, Stødkilde-Jorgensen H, Hansen LH, Pedersen LB, Grenier N, Frøkiær J. Validation of quantitative BOLD MRI measurements in kidney: application to unilateral ureteral obstruction. *Kidney Int* 2005; **67**: 2305–2312.
5. Semple SI, Wallis F, Haggarty P, Abramovich D, Ross JA, Redpath TW, Gilbert FJ. The measurement of fetal liver T(*)(2) in utero before and after maternal oxygen breathing: progress towards a non-invasive measurement of fetal oxygenation and placental function. *Magn Reson Imaging* 2001; **19**: 921–928.
6. Fulford J, Vadeyar SH, Dodampahala SH, Ong S, Moore RJ, Baker PN, James DK, Gowland P. Fetal brain activity and hemodynamic response to a vibroacoustic stimulus. *Hum Brain Mapp* 2004; **22**: 116–121.
7. Fulford J, Vadeyar SH, Dodampahala SH, Moore RJ, Young P, Baker PN, James DK, Gowland P. Fetal brain activity in response to a visual stimulus. *Hum Brain Mapp* 2003; **20**: 239–245.
8. Moore RJ, Vadeyar S, Fulford J, Tyler DJ, Gribben C, Baker PN, James DK, Gowland P. Antenatal determination of fetal brain activity in response to an acoustic stimulus using functional magnetic resonance imaging. *Hum Brain Mapp* 2001; **12**: 94–99.
9. Wedegärtner U, Tchirikov M, Schafer S, Priest AN, Kooijman H, Adam G, Schröder HJ. Functional MR imaging: comparison of BOLD signal intensity changes in fetal organs with fetal and maternal oxyhemoglobin saturation during hypoxia in sheep. *Radiology* 2006; **238**: 872–880.
10. Wedegärtner U, Tchirikov M, Schäfer S, Priest AN, Walther M, Adam G, Schröder HJ. Fetal sheep brains: findings at functional blood oxygen level-dependent 3-T MR imaging – relationship to maternal oxygen saturation during hypoxia. *Radiology* 2005; **237**: 919–926.
11. Wedegärtner U, Tchirikov M, Koch M, Adam G, Schröder H. Functional magnetic resonance imaging (fMRI) for fetal oxygenation during maternal hypoxia: initial results. *Rofo* 2002; **174**: 700–703.
12. Mahutte CK. On-line arterial blood gas analysis with optodes: current status. *Clin Biochem* 1998; **31**: 119–130.
13. Tomimatsu T, Pereyra Pena J, Hatran DP, Longo LD. Maternal oxygen administration and fetal cerebral oxygenation: studies on near-term fetal lambs at both low and high altitude. *Am J Obstet Gynecol* 2006; **195**: 535–541.
14. Carter AM. Placental oxygen transfer and the oxygen supply to the fetus. *Fetal Matern Med Rev* 1999; **11**: 151–161.
15. Kennan RP, Scanley BE, Gore JC. Physiologic basis for BOLD MR signal changes due to hypoxia/hyperoxia: separation of blood volume and magnetic susceptibility effects. *Magn Reson Med* 1997; **37**: 953–956.
16. Nicolaides KH, Campbell S, Bradley RJ, Bilardo CM, Soothill PW, Gibb D. Maternal oxygen therapy for intrauterine growth retardation. *Lancet* 1987; **25**: 942–945.
17. Arduini D, Rizzo G, Mancuso S, Romanini C. Short-term effects of maternal oxygen administration on blood flow velocity waveforms in healthy and growth-retarded fetuses. *Am J Obstet Gynecol* 1988; **159**: 1077–1080.
18. Bekedam DJ, Mulder EJ, Snijders RJ, Visser GH. The effects of maternal hyperoxia on fetal breathing movements, body movements and heart rate variation in growth retarded fetuses. *Early Hum Dev* 1991; **27**: 223–232.
19. Arduini D, Rizzo G, Romanini C, Mancuso S. Hemodynamic changes in growth retarded fetuses during maternal oxygen administration as predictors of fetal outcome. *J Ultrasound Med* 1989; **8**: 193–196.
20. Caforio L, Caruso A, Testa AC, Pompei A, Ciampelli M. Short-term maternal oxygen administration in fetuses with absence or reversal of end-diastolic velocity in umbilical artery: pathophysiological and clinical considerations. *Acta Obstet Gynecol Scand* 1998; **77**: 707–711.
21. Wilkening RB, Meschia G. Current topic: comparative physiology of placental oxygen transport. *Placenta* 1992; **13**: 1–15.
22. Morrison JL. Sheep models of intrauterine growth restriction: fetal adaptations and consequences. *Clin Exp Pharmacol Physiol* 2008; **35**: 730–743.

Paper 2

Ultrasound Obstet Gynecol 2011; **38**: 665–672
Published online in Wiley Online Library (wileyonlinelibrary.com). **DOI:** 10.1002/uog.9044

Left–right difference in fetal liver oxygenation during hypoxia estimated by BOLD MRI in a fetal sheep model

A. SØRENSEN*, D. HOLM†, M. PEDERSEN‡, A. TIETZE§, B. STAUSBØL-GRØN¶, L. DUUS** and N. ULDBJERG**

**Department of Gynecology and Obstetrics, Aarhus University Hospital, Aalborg, Denmark; †Department of Clinical Engineering, Aarhus University Hospital, Aarhus, Denmark; ‡Institute of Clinical Medicine, Aarhus University Hospital, Skejby, Denmark; §Department of Neuroradiology, Aarhus University Hospital, Aarhus, Denmark; ¶MRI Research Center, Aarhus University Hospital, Skejby, Denmark; **Department of Gynecology and Obstetrics, Aarhus University Hospital, Skejby, Denmark*

KEYWORDS: blood oxygen level-dependent; ductus venosus; oxygenation; functional MRI; hypoxia; liver circulation; magnetic resonance imaging

ABSTRACT

Objective *The purpose of this study was to measure differences in oxygenation between the left and right sides of the fetal liver during varying oxygenation levels.*

Methods *Eight ewes carrying singleton fetuses at gestational age 125 days (term, 145 days) were included in the study. Under anesthesia the ewes were ventilated with gas containing different levels of oxygen, thereby subjecting the fetuses to hyperoxia (mean ± SD maternal arterial partial pressure of oxygen (pO_2), 23.2 ± 8.2 kPa) and hypoxia (mean maternal arterial pO_2, 7.1 ± 0.5 kPa). Changes in oxygenation within the fetal liver were assessed by blood oxygen level-dependent (BOLD) magnetic resonance imaging (MRI).*

Results *During hyperoxia there was no difference between the BOLD signal in the left and right sides of the fetal liver; mean change in BOLD ($\Delta BOLD)_{hyperox}$, −0.9 ± 3.7%. During hypoxia, however, the decrease in the BOLD signal was more pronounced in the right side as compared with the left side, thereby creating a significant increase in the left–right difference in the BOLD signal; mean $\Delta BOLD_{hypox}$, 5.2 ± 2.2% (*$P = 0.002$*, paired* t*-test). The left–right difference was directly proportional to the degree of hypoxia (*$R^2 = 0.86$, $P = 0.007$*).*

Conclusions *To our knowledge, this is the first study demonstrating differences in oxygenation between the left and right sides of the fetal liver during hypoxia, a difference that can be explained by increased ductus venosus shunting. Thus, the BOLD MRI technique is a promising non-invasive tool that might be useful for the future monitoring of the human fetus. Copyright © 2011 ISUOG. Published by John Wiley & Sons, Ltd.*

INTRODUCTION

The fetal liver has a privileged position in the fetal circulation, as it is the first organ to receive blood directly from the placenta. Therefore the oxygen supply to this organ is better than to that of any other fetal organ. The fetal liver plays an important role in regulating fetal growth[1] and in programming adult metabolism[2]. The fetal circulation has been intensively investigated, initially using a radioactive microsphere technique[3,4] and later by ultrasound Doppler flow measurements[5–7]. The fetal liver has two main vascular sources. It receives about 75% of its blood supply from the well-oxygenated umbilical vein and 20% from the less-well-oxygenated portal vein[8]. The contributions of these sources are unevenly distributed in the fetal liver, as the left side receives primarily the well-oxygenated umbilical vein blood, while the right side receives an equal mixture from the two vascular sources[9]. The remainder is supplied by the hepatic artery, which makes a modest contribution of < 10% that is evenly distributed in the fetal liver[10]. The left portal vein has been identified as the means of communication between the umbilical vein and the portal circulation, as this vessel carries umbilical venous blood to the right side of the liver[11,12] (Figure 1). The contribution of umbilical vein blood to the right side of the liver is highly dependent on the ductus venosus shunting fraction, which in the third trimester is 20% in the healthy fetus. However, during acute hypoxia[13] and in the growth-restricted fetus[14–17] ductus venosus shunting is increased; consequently, blood flow in the left portal vein is reduced or even reversed[14]. This redistribution of umbilical vein blood increases the oxygen supply to the fetal heart and brain at the expense of the fetal liver, especially the right side of the fetal liver.

Correspondence to: Dr A. Sørensen, Department of Gynecology and Obstetrics, Aalborg Hospital, Region North, Reberbansgade, Postboks 561, 9100 Aalborg, Denmark (e-mail: ans@rn.dk)

Accepted: 18 April 2011

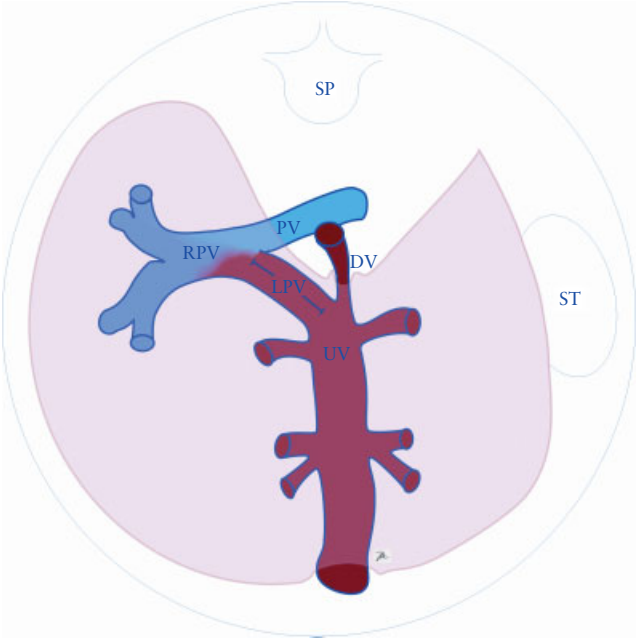

Figure 1 Main blood supply of the sheep fetal liver seen in transverse view. Red represents well-oxygenated and blue represents poorly oxygenated blood. DV, ductus venosus; LPV, left portal vein; PV, portal vein; RPV, right portal vein; SP, spine; ST, stomach; UV, umbilical vein. (Reproduced with permission[9].)

We hypothesized that during hypoxia the redistribution of umbilical vein blood would lead to lower oxygenation in the right side of the fetal liver than in the left side. The aim of this study was to evaluate the left–right difference in fetal liver oxygenation during hypoxia.

METHODS

Animal handling

Eight healthy ewes (Gotland sheep) carrying singleton fetuses at 125 days' gestation (term, 145 days, equivalent to 34 weeks' gestation in humans) were included in the study. Prior to the experimental procedures, the ewes were cared for at our animal farm (Påskehøjgård, Aarhus University Hospital, Denmark), with free access to water and food. On the day of the experiment, each ewe was sedated with atropine 2 mg (Nycomed, Taastrup, Denmark) and Rompun™ 2.5 mg (Bayer Schering Pharma, Berlin, Germany) and transported to the surgical unit. Anesthesia was induced with ketamine 2 mg/kg (Pfizer, New York, USA) and Dormicum™ 0.25 mg/kg (Roche, Basel, Switzerland) and maintained by isoflurane (Baxter, Deerfield, USA), 1.5% in an oxygen/nitrous oxide (O_2/N_2O) mixture. Orotracheal intubation (tube diameter, 9 mm) was followed by artificial ventilation using a servo-ventilator (Abott, Solna, Sweden) with a tidal volume of 600–800 mL at a rate of 18 breaths/min. Catheterization of the left common carotid artery was performed for withdrawal of blood and blood gas analysis (Radiometer, Brønshøj, Denmark). A pulse oximeter sensor was attached to an ear, and a capnograph was used for end-tidal carbon dioxide (CO_2) measurement. By sonographic guidance oxygen-sensitive optodes were placed in the fetal liver in four fetuses; these measurements were used for other purposes[18]. By changing the O_2/N_2O ratio in the maternal ventilated gas, the fetus was subjected to varying oxygenation levels. The oxygen content in the ventilated gas varied between 10% (hypoxia) and 100% (hyperoxia), and the corresponding mean maternal arterial partial pressure of oxygen (pO_2) was 7.1 ± 0.5 kPa (mean ± SD) during hypoxia and 23.2 ± 8.2 kPa during hyperoxia. In this study, we monitored maternal oxygenation not only by the oxygen content of the ventilation gas but also by maternal arterial blood samples. As a result, we discovered a discrepancy between the two, probably due to varying degrees of lung atelectasis in the ewes during our experiments. The experimental protocol was approved by the local animal ethics committee.

Anesthetics

The anesthetics used in this experiment and their potential effects on fetal circulation are discussed here. Rompun is an α_2-adrenoceptor agonist with known oxytocin-like effects on the uterus. In goat fetuses increased intrauterine pressure has been observed for 5–15 min following Rompun injection, thereby causing a mild and transient decrease in fetal pH and pO_2[19]. Ketamine has known sympathomimetic effects. In sheep fetuses a mild decrease in fetal pH has been noted following ketamine injection; however, no significant effects on fetal mean arterial blood pressure, fetal heart rate or uterine blood flow were seen[20]. Atropine is a non-selective muscarine receptor antagonist. In sheep fetuses near term a transient increase in heart rate and blood pressure has been seen following atropine injection, however no effects were seen on fetal arterial pH, pO_2 and partial pressure of CO_2 (pCO_2)[21]. Dormicum is a benzodiazepine derivate with sedative effects. In sheep fetuses a transient increase in heart rate has been noted following Dormicum injection, but no effects were seen on fetal blood pressure, uterine blood flow or fetal arterial pH, pO_2 or pCO_2[22]. By reducing fetal pH transiently Rompun and ketamine might have affected the ductus venosus shunting fraction initially. But as the magnetic resonance imaging (MRI) experiments were carried out at least 90 min after induction of anesthesia, these effects are unlikely to have influenced our results.

Isoflurane, used for maintaining anesthesia in this experiment, is a halogenated ether with known analgesic and muscle-relaxing effects. In fetal sheep reduced blood pressure has been noted following administration of isoflurane[23]. This cardiovascular depressant effect of isoflurane might have reduced the vascular response in the fetal liver, hence decreasing the changes in the right–left difference in fetal liver blood oxygen level-dependent (BOLD) signal–ΔBOLD – during hypoxia. Thus, we may have underestimated the effect of hypoxia on ΔBOLD in this study.

BOLD MRI

The absolute BOLD MRI signal is not a direct measure of fetal tissue oxygenation, but changes in the BOLD signal reflect changes in the proportion of oxygenated hemoglobin molecules in a given region. The BOLD effect is based on the magnetic properties of hemoglobin; oxyhemoglobin is diamagnetic whereas deoxyhemoglobin is paramagnetic. Changes in the oxygenation of hemoglobin, therefore, provide a change in the local magnetic field, and this leads to a corresponding change in the BOLD signal in the same region[24]. The BOLD MRI technique is now widely used in neuroscience, and it is the most important method for investigating brain function during cognitive and sensory stimuli[25]. BOLD MRI is also used for the non-invasive evaluation of changes in tissue oxygenation during physiological challenges such as hyperoxia and hypoxia in the following organs: the brain[26], the kidney[27] and the liver[28–30]. In fetal MRI the BOLD technique has been used for measuring changes in fetal oxygenation in the sheep fetus[18,31–33] during maternal hypoxia and the human fetus[34,35] during maternal hyperoxia. It has been shown that changes in the fetal BOLD MRI signal are closely related to changes in fetal arterial saturation[33] and changes in fetal tissue oxygenation as estimated by internal fetal oxygen sensors[18]. According to these studies BOLD MRI provides a reliable method for measuring changes in the overall oxygenation of selected fetal organs.

During our experiments BOLD scans were performed continuously at varying levels of maternal and fetal oxygenation. The BOLD signal inside certain regions of interest (ROIs) was obtained, and the changes in BOLD signal inside these ROIs reflected the changes in fetal oxygenation in these particular regions. One large ROI covering the entire liver was selected for overall oxygenation measurements (Figure 2a) and seven smaller ROIs, which were equidistantly distributed throughout the liver from the left to the right side, were used for regional oxygenation measurements (Figure 3a).

BOLD MRI was performed with a 1.5-T clinical system (Philips Medical Systems, Best, The Netherlands). The anesthetized ewe was examined in a left lateral position. Acquisitions were obtained with a phased-array abdominal radiofrequency coil. Fast axial and coronal scans of the fetus were initially performed to locate the fetal organ of interest. Next, a T2*-weighted sequence was performed, allowing assessment of changes in the BOLD signal. This was done using a dynamic multishot 2D-gradient-echo sequence with sequential echo-planar encoding. The sequence parameters included 10–17 slices 6 mm thick with an interslice gap of approximately 9 mm (depending on the orientation and position of the fetus); the field of view was 460 × 460 mm, acquired using a 256 × 256 matrix, resulting in an in-plane resolution of approximately 1.8 × 1.8 mm, TR = 2500 ms, flip angle = 90°, and an effective echo time of 40 ms optimized for the average T2* value *in vivo*. Each frame was averaged three times for the optimal signal-to-noise ratio. A total of 150 dynamic frames were recorded with an interval of 112 s.

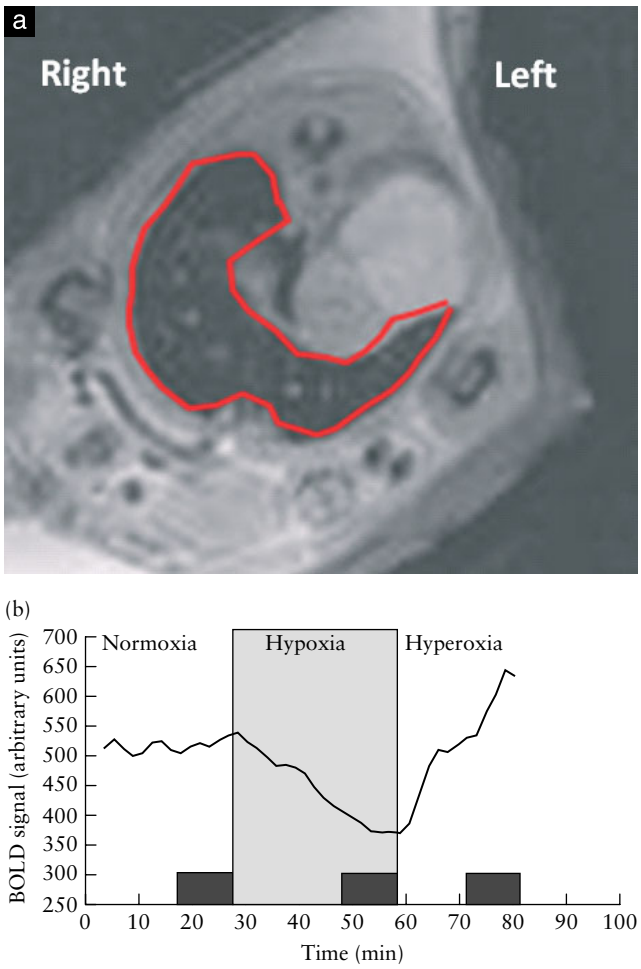

Figure 2 Change in overall fetal liver oxygenation in a sheep fetus (Fetus 1). (a) Blood oxygen level-dependent (BOLD) image of the fetal liver (transverse view) with one region of interest (ROI; red line) covering the entire fetal liver for overall fetal liver oxygenation assessment. (b) Changes in BOLD signal within the ROI during varying oxygenation levels presented as a signal/time curve. Such changes reflect changes in overall fetal liver oxygenation. ■, Signal values used for calculating mean value (see Table 1).

Data analysis

MRI data were transferred to an external workstation equipped with Mistar software (Apollo Imaging Technology, Melbourne, Australia). All images displayed adequate signal-to-noise ratio and did not show substantial artifacts. The signal intensity of the T2*-weighted BOLD images was obtained in the ROI as shown in Figures 2a and 3a. Placement of the ROIs within the fetal liver was performed by clinical radiologists (B.S.-G. and A.T.), and errors due to fetal movement were corrected by manually moving the ROI in each dynamic image. For each ROI, the mean signal vs. time curve was calculated. The BOLD signals from different regions were compared at different oxygenation levels. As we wanted to include only steady-state measurements, only the last 10 min of each oxygenation level were included. In each fetus the

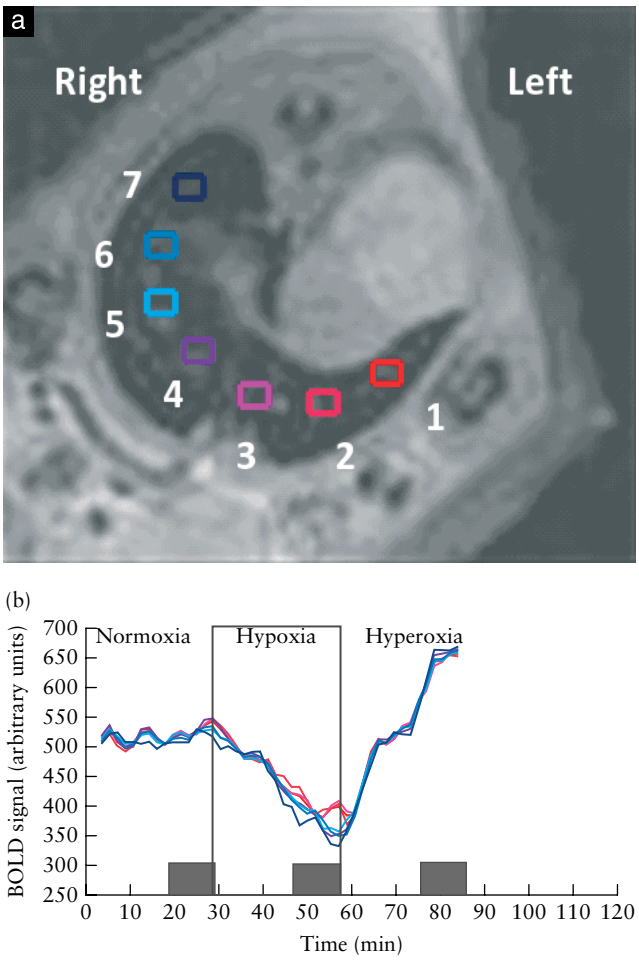

Figure 3 Change in regional fetal liver oxygenation in a sheep fetus (Fetus 1). (a) Blood oxygen level-dependent (BOLD) image of the fetal liver (transverse view), showing seven small regions of interest (ROIs) within the fetal liver for regional oxygenation assessment. ROIs are placed at regular intervals from left to right, with the blue-colored ROI (ROI-7) placed at the furthest right side and the red-colored ROI (ROI-1) placed at the furthest left side in the fetal liver. (b) Changes in BOLD signal within the seven ROIs during varying oxygenation levels presented as signal/time curves, each representing change in oxygenation in a different region of the fetal liver, identified by color. ▬, Signal values obtained for calculation of mean values (see Table 2) in each fetus. ——, ROI 1; ——, ROI 2; ——, ROI 3; ——, ROI 4; ——, ROI 5; ——, ROI 6; ——, ROI 7.

left–right difference in fetal liver oxygenation (ΔBOLD) was defined as the difference between the BOLD signal of the furthest left ROI (ROI-1) and the furthest right ROI (ROI-7) of the fetal liver. Using the starting normoxic overall BOLD signal as a reference ($BOLD_{ref}$) the relative ΔBOLD was calculated for each fetus during hyperoxia and hypoxia.

Statistical analysis

Absolute BOLD signal values were normalized, using the normoxic starting level as a reference in each fetus. Mean ± SD were calculated for the hyperoxic and hypoxic levels, reflecting changes in overall and regional fetal liver oxygenation (Tables 1 and 2). Using the paired *t*-test, we tested paired values of the BOLD signal from the left and the right regions of the fetal liver during hyperoxia as well as hypoxia. Our null hypothesis was that there was no left–right difference (ΔBOLD = 0). The relationship between ΔBOLD and the degree of hypoxia was tested using linear regression analysis, and for all tests $P < 0.05$ was considered statistically significant. Statistical analysis was performed using the Stata®11 (StataCorp LP, TX, USA) statistical package.

RESULTS

Eight animals were originally included in the study, but two were excluded from the analysis because fetus number 2 had a hepatic hematoma when the oxygen sensor was installed and animal number 4 had a cardiac arrest when anesthesia was induced, thus final data were only available for six animals.

For measuring changes in overall fetal liver oxygenation one ROI covering the entire fetal liver was drawn (Figure 2a). The corresponding changes in BOLD signal during different oxygenation levels are presented for one fetus (Fetus 1) in Figure 2b. Using the BOLD MRI technique we found the overall oxygenation of the fetal liver to be reduced to a mean ± SD of 75 ± 13% during hypoxia and increased to 121 ± 16% during hyperoxia when using the normoxic starting BOLD signal ($BOLD_{ref}$) as a reference (100%) for each fetus (Table 1).

Changes in regional oxygenation of the fetal liver were investigated using seven smaller ROIs, as shown in the BOLD image in Figure 3a. The red-colored ROI-1 was placed at the furthest left side of the liver, and the blue-colored ROI-7 was placed at the furthest right side of the liver. The corresponding changes in the BOLD signal at different oxygenation levels are presented for one fetus (Fetus 1) in Figure 3b. During hyperoxia the BOLD signal of every ROI increased to the same level. During hypoxia, however, the BOLD signal of the blue-colored ROIs of the right side was reduced to a lower level than the BOLD signal of the red-colored ROIs of the left side. This finding reflects lower oxygenation on the right side of the fetal liver as compared with the left side during hypoxia. Table 2 presents the absolute and normalized BOLD signals of the furthest left and furthest right ROIs in the fetal liver, and the calculated ΔBOLD during hyperoxia and hypoxia. ΔBOLD was significantly increased from a mean of −0.9 ± 3.7% during hyperoxia to 5.2 ± 2.2% during hypoxia ($P = 0.002$, paired *t*-test) (Table 2). For each fetus ΔBOLD increased during hypoxia, as illustrated in Figure 4.

Figure 5 illustrates the correlation between ΔBOLD and the maternal arterial pO_2 during hypoxia. ΔBOLD is directly proportional to the degree of hypoxia ($R^2 = 0.86$, $P = 0.007$). This correlation was not apparent during hyperoxia.

Table 1 Changes in overall liver oxygenation of sheep fetuses during hyperoxia and hypoxia

		Hyperoxia		*Hypoxia*	
Fetus	$BOLD_{ref}$	$BOLD_{hyperox}$	$BOLD_{hyperox}/BOLD_{ref}$ (%)	$BOLD_{hypox}$	$BOLD_{hypox}/BOLD_{ref}$ (%)
1	517 ± 18	678 ± 20	131	384 ± 22	74
3	401 ± 14	455 ± 25	113	344 ± 50	86
5	477 ± 16	563 ± 41	118	237 ± 48	50
6	440 ± 17	658 ± 16	150	375 ± 13	85
7	443 ± 23	492 ± 26	111	363 ± 31	82
8	431 ± 20	450 ± 57	104	315 ± 22	73
Mean (SD)			121 (16)		75 (13)

Only the last 10 min in each oxygenation episode were included. Values are given as mean ± SEM in arbitrary units except where indicated. BOLD, blood oxygen level-dependent magnetic resonance signal; $BOLD_{ref}$, BOLD of normoxic fetuses; $BOLD_{hyperox}$, BOLD of hyperoxic fetuses; $BOLD_{hypox}$, BOLD of hypoxic fetuses.

Table 2 Changes in regional liver oxygenation presented as blood oxygen level-dependent (BOLD) magnetic resonance signal and the left–right difference (ΔBOLD) of sheep fetuses during hyperoxia and hypoxia

		Hyperoxia			*Hypoxia*		
Fetus	$BOLD_{ref}$	$BOLD_{left}$	$BOLD_{right}$	$\Delta BOLD_{hyperox}$	$BOLD_{left}$	$BOLD_{right}$	$\Delta BOLD_{hypox}$
1	517 ± 18	627 ± 26 (121.3)	631 ± 27 (122.0)	−0.8	407 ± 65 (78.7)	390 ± 70 (75.4)	3.3
3	401 ± 14	439 ± 20 (109.5)	458 ± 25 (114.2)	−4.7	364 ± 31 (90.8)	339 ± 46 (84.5)	6.2
5	477 ± 16	606 ± 30 (127.0)	598 ± 28 (125.4)	1.7	247 ± 36 (51.8)	216 ± 20 (45.3)	6.5
6	440 ± 17	636 ± 53 (144.5)	641 ± 48 (145.7)	−1.1	382 ± 29 (86.8)	365 ± 41 (83.0)	3.9
7	443 ± 23	494 ± 41 (111.5)	516 ± 27 (116.5)	−5.0	368 ± 24 (83.1)	355 ± 32 (80.1)	2.9
8	431 ± 20	478 ± 38 (110.9)	458 ± 50 (106.3)	4.6	348 ± 18 (80.7)	312 ± 32 (72.4)	8.4
Mean (SD)				−0.9 (3.7)			5.2 (2.2)
P				0.6			0.002

For each fetus the absolute BOLD signal in arbitrary units was obtained from different regions of interest (ROIs) of the fetal liver during hyperoxia as well as hypoxia. Only the last 10 min in each oxygenation episode were included. Data are given as mean ± SEM in arbitrary units, mean ± SEM (%) or %. $BOLD_{ref}$, BOLD of normoxic fetuses; $BOLD_{left}$, BOLD of left side of liver i.e. region of interest (ROI)-1; $BOLD_{right}$, BOLD of right side of liver i.e. ROI-7; $\Delta BOLD_{hyperox}$, difference between ROI-1 and ROI-7 for hyperoxic fetuses; $\Delta BOLD_{hypox}$, difference between ROI-1 and ROI-7 for hypoxic fetuses. *P* according to paired *t*-test.

DISCUSSION

In this study we measured the difference in oxygenation between the left and right sides of the fetal liver (ΔBOLD) using the BOLD MRI technique. During hypoxia ΔBOLD was significantly increased and was found to be directly proportional to the degree of hypoxia. To our knowledge, this is the first study to describe changes in regional oxygenation within the fetal liver.

A limitation of the BOLD MRI technique is that the absolute BOLD signal depends not only on the proportion of paramagnetic deoxyhemoglobin but also on other variables including blood flow, blood volume in the fetal tissue, hematocrit and the hemoglobin concentration within fetal erythrocytes[36]. This could explain some of the interanimal variation in the normoxic $BOLD_{ref}$ signal presented in Table 1. Because of these variables only relative changes and not the absolute BOLD signal can be compared between animals.

Another limitation of this study involves the use of anesthesia. The possible fetal effects of the anesthetics used in this experiment are listed in the methods section. The cardiovascular depressant effect of isoflurane[23] might have reduced the vascular response in the fetal liver, hence decreasing the changes in ΔBOLD during hypoxia. Thus, we may have underestimated the effect of hypoxia on ΔBOLD in this study. The anesthetics used for induction of anesthesia might have affected the ductus venosus shunting fraction transiently, but as the MRI experiments were carried out at least 90 min after induction of anesthesia, these effects are unlikely to have influenced our results.

Our findings are in accordance with well-established theories about fetal liver circulation and fetal physiology based on Doppler ultrasound flow measurements. The increase in ΔBOLD in the fetal liver during hypoxia can be explained by increased ductus venosus shunting[37]. The direct proportion between ΔBOLD and the degree of hypoxia agrees with the results of a study by Kiserud *et al.*[16] showing increased ductus venosus shunting with an increasing degree of umbilical vein flow impairment in the growth-restricted fetus. The variation in maternal arterial pO_2 during hypoxia can be explained by varying degrees of lung atelectasis among the ewes during the experiment.

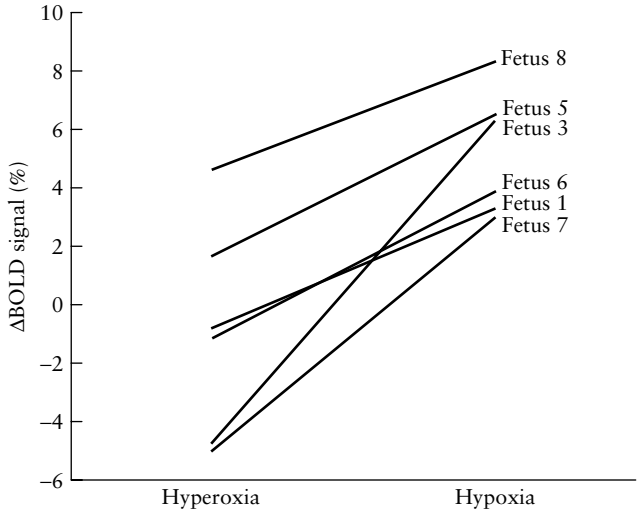

Figure 4 Increase in difference in left–right oxygenation (ΔBOLD) of the fetal sheep liver during hypoxia for each fetus.

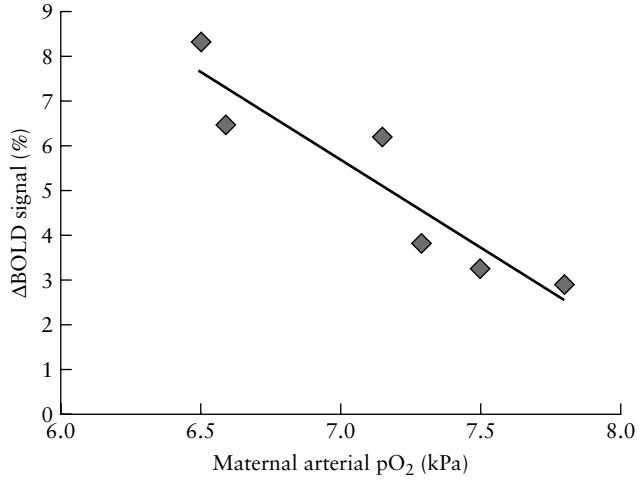

Figure 5 Correlation between difference in left–right oxygenation of the fetal sheep liver during hypoxia ($\Delta BOLD_{hypox}$) (see Table 1) and maternal arterial partial pressure of oxygen (pO_2). $R^2 = 0.86$.

According to our hypothesis, during hypoxia one would expect an increased ΔBOLD; this was confirmed by our experiment. During hyperoxia, however, we found no left–right difference in oxygenation. This was not expected. During hyperoxia the portal vein still contributes to the blood supply of the right side of the liver. Therefore, a left–right oxygenation difference should be expected at any oxygenation level, even during hyperoxia.

An explanation for this finding could be that the left–right oxygenation difference during hyperoxia was below the sensitivity for this method. A way to improve the sensitivity of the BOLD technique in fetal MRI would be to increase the magnetic field strength, as noted by Wedegärtner *et al.*[38]. When the magnetic field strength is doubled from 1.5 to 3 T the BOLD signal is more affected by the presence of deoxyhemoglobin, as the susceptibility effects are higher at 3 T than they are at 1.5 T. This leads to a higher signal-to-noise ratio for the BOLD response and a higher sensitivity in detecting signal changes. A negative aspect will be increased artifacts caused by fetal movements. From a clinical perspective 1.5 T is of greater interest because 3-T systems, as a safety precaution, are not currently used for human fetal MRI, although no harmful short- or long-term effects of prenatal MRI have ever been reported[39]. Further data about prenatal MRI in higher magnetic fields will probably change clinical practice in this field.

Fetal movements are known to interfere with MRI, causing artifacts on the images, thereby producing inaccuracy in measuring signal changes within selected fetal organs. In this study, however, the ewes and fetuses underwent general anesthesia, and fetal movements were therefore greatly reduced. A recent paper described no effects of maternal hyperoxia on human fetal liver oxygenation using quantitative $T2^*$ measurements in 80 human pregnancies (involving both healthy and growth-restricted fetuses)[35]. This might be caused by fetal movements between the acquisition of images at the different echo times or because the $T2^*$ mapping was not accurate or sensitive enough. The BOLD technique might not show the same susceptibility to fetal movements, and it might provide higher sensitivity to changes in susceptibility ($T2^*$). This needs to be investigated by further human studies in this field.

A study similar to this could not be conducted in human fetuses as it would not be ethical to induce acute hypoxia. However, fetuses subjected to chronic hypoxia, for example growth-restricted fetuses, might exhibit the same left–right differences in fetal liver oxygenation as seen during acute hypoxia. Examination of this group of human fetuses could provide the clinical protocol for this method. Moreover, in this particular group of fetuses we would not expect significant artifacts because of reduced fetal movements.

Before introducing ΔBOLD of the fetal liver for evaluating fetal wellbeing it should be remembered that the ductus venosus shunting fraction is influenced not only by hypoxia. Other factors such as fluid dynamics[40], neural and endocrine factors[37] and maternal diet[41] also play important roles. Furthermore, there are differences between the sheep and the human fetus regarding the fetal circulation and especially the ductus venosus shunting fraction. In the human fetus the ductus venosus shunting fraction is 20% in the third trimester[42] compared with 50% in the near-term sheep fetus[3,6]. However, during hypoxia the sheep fetus exhibits the same redistribution of umbilical vein blood as seen in the human fetus[3]. Therefore, changes in fetal liver oxygenation during hypoxia should be comparable in sheep and human fetuses.

In this study the BOLD MRI technique proved its potential as a non-invasive method for investigating changes in regional fetal oxygenation. Further research is needed in this field in healthy as well as growth-restricted human fetuses.

ACKNOWLEDGMENTS

The authors thank A.M. Carter, from the Department of Physiology and Pharmacology at the University of Southern Denmark, for inspiration and sharing his knowledge of fetal physiology with us. This work received financial support from Forskningsinitiativet, Aarhus University Hospital.

REFERENCES

1. Tchirikov M, Kertschanska S, Sturenberg HJ, Schroder HJ. Liver blood perfusion as a possible instrument for fetal growth regulation. *Placenta* 2002; **23** (Suppl A): S153–S158.
2. Morrison JL, Duffield JA, Muhlhausler BS, Gentili S, McMillen IC. Fetal growth restriction, catch-up growth and the early origins of insulin resistance and visceral obesity. *Pediatr Nephrol* 2010; **25**: 669–677.
3. Edelstone DI, Rudolph AM. Preferential streaming of ductus venosus blood to the brain and heart in fetal lambs. *Am J Physiol* 1979; **237**: H724–H729.
4. Edelstone DI. Regulation of blood flow through the ductus venosus. *J Dev Physiol* 1980; **2**: 219–238.
5. Baschat AA. The fetal circulation and essential organs – a new twist to an old tale. *Ultrasound Obstet Gynecol* 2006; **27**: 349–354.
6. Kiserud T. Physiology of the fetal circulation. *Semin Fetal Neonatal Med* 2005; **10**: 493–503.
7. Kiserud T. Hemodynamics of the ductus venosus. *Eur J Obstet Gynecol Reprod Biol* 1999; **84**: 139–147.
8. Haugen G, Kiserud T, Godfrey K, Crozier S, Hanson M. Portal and umbilical venous blood supply to the liver in the human fetus near term. *Ultrasound Obstet Gynecol* 2004; **24**: 599–605.
9. Kessler J, Rasmussen S, Kiserud T. The fetal portal vein: normal blood flow development during the second half of human pregnancy. *Ultrasound Obstet Gynecol* 2007; **30**: 52–60.
10. Edelstone DI, Rudolph AM, Heymann MA. Liver and ductus venosus blood flows in fetal lambs in utero. *Circ Res* 1978; **42**: 426–433.
11. Kessler J, Rasmussen S, Kiserud T. The left portal vein as an indicator of watershed in the fetal circulation: development during the second half of pregnancy and a suggested method of evaluation. *Ultrasound Obstet Gynecol* 2007; **30**: 757–764.
12. Kivilevitch Z, Gindes L, Deutsch H, Achiron R. In-utero evaluation of the fetal umbilical–portal venous system: two- and three-dimensional ultrasonic study. *Ultrasound Obstet Gynecol* 2009; **34**: 634–642.
13. Tchirikov M, Eisermann K, Rybakowski C, Schroder HJ. Doppler ultrasound evaluation of ductus venosus blood flow during acute hypoxemia in fetal lambs. *Ultrasound Obstet Gynecol* 1998; **11**: 426–431.
14. Kilavuz O, Vetter K, Kiserud T, Vetter P. The left portal vein is the watershed of the fetal venous system. *J Perinat Med* 2003; **31**: 184–187.
15. Kessler J, Rasmussen S, Godfrey K, Hanson M, Kiserud T. Fetal growth restriction is associated with prioritization of umbilical blood flow to the left hepatic lobe at the expense of the right lobe. *Pediatr Res* 2009; **66**: 113–117.
16. Kiserud T, Kessler J, Ebbing C, Rasmussen S. Ductus venosus shunting in growth-restricted fetuses and the effect of umbilical circulatory compromise. *Ultrasound Obstet Gynecol* 2006; **28**: 143–149.
17. Tchirikov M, Rybakowski C, Hüneke B, Schröder HJ. Blood flow through the ductus venosus in singleton and multifetal pregnancies and in fetuses with intrauterine growth retardation. *Am J Obstet Gynecol* 1998; **178**: 943–949.
18. Sørensen A, Pedersen M, Tietze A, Ottosen L, Duus L, Uldbjerg N. BOLD MRI in sheep fetuses: a non-invasive method for measuring changes in tissue oxygenation. *Ultrasound Obstet Gynecol* 2009; **34**: 687–692.
19. Sakamoto H, Misumi K, Nakama M, Aoki Y. The effects of xylazine on intrauterine pressure, uterine blood flow, maternal and fetal cardiovascular and pulmonary function in pregnant goats. *J Vet Med Sci* 1996; **58**: 211–217.
20. Strümper D, Gogarten W, Durieux ME, Hartleb K, Van Aken H, Marcus MA. The effects of S+-ketamine and racemic ketamine on uterine blood flow in chronically instrumented pregnant sheep. *Anesth Analg* 2004; **98**: 497–502, table of contents.
21. Zheng J, Yang W, Cao L, Li S, Zhang Y, Wan Z, Mao C. Muscarinic effects and foetal cardiovascular and hormonal responses in utero. *J Renin Angiotensin Aldosterone Syst* 2009; **10**: 138–146.
22. Conklin KA, Graham CW, Murad S, Randall FM, Katz RL, Cabalum T, Lieb SM, Brinkman CR, 3rd. Midazolam and diazepam: maternal and fetal effects in the pregnant ewe. *Obstet Gynecol* 1980; **56**: 471–474.
23. Okutomi T, Whittington RA, Stein DJ, Morishima HO. Comparison of the effects of sevoflurane and isoflurane anesthesia on the maternal–fetal unit in sheep. *J Anesth* 2009; **23**: 392–398.
24. Logothetis NK, Pfeuffer J. On the nature of the BOLD fMRI contrast mechanism. *Magn Reson Imaging* 2004; **22**: 1517–1531.
25. Logothetis NK, Wandell BA. Interpreting the BOLD signal. *Annu Rev Physiol* 2004; **66**: 735–769.
26. Rostrup E, Larsson HB, Toft PB, Garde K, Henriksen O. Signal changes in gradient echo images of human brain induced by hypo- and hyperoxia. *NMR Biomed* 1995; **8**: 41–47.
27. Boss A, Martirosian P, Jehs MC, Dietz K, Alber M, Rossi C, Claussen CD, Schick F. Influence of oxygen and carbogen breathing on renal oxygenation measured by T2*-weighted imaging at 3.0 T. *NMR Biomed* 2009; **22**: 638–645.
28. Barash H, Gross E, Matot I, Edrei Y, Tsarfaty G, Spira G, Vlodavsky I, Galun E, Abramovitch R. Functional MR imaging during hypercapnia and hyperoxia: noninvasive tool for monitoring changes in liver perfusion and hemodynamics in a rat model. *Radiology* 2007; **243**: 727–735.
29. Jin N, Deng J, Chadashvili T, Zhang Y, Guo Y, Zhang Z, Yang GY, Omary RA, Larson AC. Carbogen gas-challenge BOLD MR imaging in a rat model of diethylnitrosamine-induced liver fibrosis. *Radiology* 2010; **254**: 129–137.
30. Fan Z, Elzibak A, Boylan C, Noseworthy MD. Blood oxygen level-dependent magnetic resonance imaging of the human liver: preliminary results. *J Comput Assist Tomogr* 2010; **34**: 523–531.
31. Wedegärtner U, Tchirikov M, Koch M, Adam G, Schröder H. Functional magnetic resonance imaging (fMRI) for fetal oxygenation during maternal hypoxia: initial results. *Rofo* 2002; **174**: 700–703.
32. Wedegärtner U, Tchirikov M, Schäfer S, Priest AN, Kooijman H, Adam G, Schröder HJ. Functional MR imaging: comparison of BOLD signal intensity changes in fetal organs with fetal and maternal oxyhemoglobin saturation during hypoxia in sheep. *Radiology* 2006; **238**: 872–880.
33. Wedegärtner U, Kooijman H, Andreas T, Beindorff N, Hecher K, Adam G. T2 and T2* measurements of fetal brain oxygenation during hypoxia with MRI at 3T: correlation with fetal arterial blood oxygen saturation. *Eur Radiol* 2010; **20**: 121–127.
34. Semple SI, Wallis F, Haggarty P, Abramovich D, Ross JA, Redpath TW, Gilbert FJ. The measurement of fetal liver T(*)(2) in utero before and after maternal oxygen breathing: progress towards a non-invasive measurement of fetal oxygenation and placental function. *Magn Reson Imaging* 2001; **19**: 921–928.
35. Morris DM, Ross JA, McVicar A, Semple SI, Haggarty P, Gilbert FJ, Abramovich DR, Smith N, Redpath TW. Changes in foetal liver T2* measurements by MRI in response to

maternal oxygen breathing: application to diagnosing foetal growth restriction. *Physiol Meas* 2010; **31**: 1137–1146.
36. Lu H, Zhao C, Ge Y, Lewis-Amezcua K. Baseline blood oxygenation modulates response amplitude: Physiologic basis for intersubject variations in functional MRI signals. *Magn Reson Med* 2008; **60**: 364–372.
37. Tchirikov M, Schröder HJ, Hecher K. Ductus venosus shunting in the fetal venous circulation: regulatory mechanisms, diagnostic methods and medical importance. *Ultrasound Obstet Gynecol* 2006; **27**: 452–461.
38. Wedegärtner U, Popovych S, Yamamura J, Kooijman H, Adam G. DeltaR2* in fetal sheep brains during hypoxia: MR imaging at 3.0 T versus that at 1.5 T. *Radiology* 2009; **252**: 394–400.
39. Kok RD, de Vries MM, Heerschap A, van den Berg PP. Absence of harmful effects of magnetic resonance exposure at 1.5 T in utero during the third trimester of pregnancy: a follow-up study. *Magn Reson Imaging* 2004; **22**: 851–854.
40. Kiserud T, Stratford L, Hanson MA. Umbilical flow distribution to the liver and the ductus venosus: an in vitro investigation of the fluid dynamic mechanisms in the fetal sheep. *Am J Obstet Gynecol* 1997; **177**: 86–90.
41. Haugen G, Hanson M, Kiserud T, Crozier S, Inskip H, Godfrey KM. Fetal liver-sparing cardiovascular adaptations linked to mother's slimness and diet. *Circ Res* 2005; **96**: 12–14.
42. Kiserud T, Rasmussen S, Skulstad S. Blood flow and the degree of shunting through the ductus venosus in the human fetus. *Am J Obstet Gynecol* 2000; **182**: 147–153.

Paper 3

ORIGINAL ARTICLE

Changes in human fetal oxygenation during maternal hyperoxia as estimated by BOLD MRI

Anne Sørensen[1]*, David Peters[2], Carsten Simonsen[3], Michael Pedersen[4], Brian Stausbøl-Grøn[5], Ole Bjarne Christiansen[1], Göran Lingman[6] and Niels Uldbjerg[7]

[1]Department of Obstetrics and Gynecology, Aalborg Hospital, Aalborg, Denmark
[2]Department of Clinical Engineering, Aarhus University Hospital, Aarhus, Denmark
[3]Department of Radiology, Aalborg Hospital, Aalborg, Denmark
[4]Institute of Clinical Medicine, Aarhus University Hospital, Aarhus, Denmark
[5]MRI Research Center, Aarhus University Hospital, Aarhus, Denmark
[6]Department of Obstetrics and Gynecology, Lund University Hospital, Lund, Sweden
[7]Department of Obstetrics and Gynecology, Aarhus University Hospital, Aarhus, Denmark
*Correspondence to: Anne Sørensen. E-mail: annenoedgaard@hotmail.com

ABSTRACT

Objective Changes in blood oxygen level dependent (BOLD) magnetic resonance imaging (MRI) signal are closely related to changes in fetal oxygenation. In this study, we aimed to investigate the changes in human fetal oxygenation during maternal hyperoxia by using the non-invasive BOLD MRI technique.

Method Eight healthy pregnant women in gestational week 28 to 34 were included. With the use of a facial oxygen mask, we induced maternal hyperoxia and measured changes in the BOLD MRI signal of selected fetal organs.

Results In a number of fetal organs, the BOLD MRI signal increased significantly ($P < 0.01$) during maternal hyperoxia (mean change in % ± SEM): liver (14.3 ± 3.7%), spleen (15.2 ± 3.5%) and kidney (6.2 ± 1.8%) as well as the placenta (6.5 ± 1.6%). In the fetal brain, however, the BOLD MRI signal remained constant (0.3 ± 0.2%).

Conclusion During maternal hyperoxia, we demonstrated an increased oxygenation in a number of human fetal organs by using the non-invasive BOLD technique. The oxygenation of the fetal brain remained constant, thus a 'reversed' brain sparing mechanism could be considered in healthy fetuses subjected to hyperoxia.

Funding sources: None
Conflicts of interest: None declared

INTRODUCTION

The fetal effects of antepartum maternal hyperoxia in uncomplicated third trimester pregnancies have been investigated in several studies.[1–4] Cordocentesis performed during maternal hyperoxia showed the pO_2 in the umbilical vein to increase above the normal range.[1] Unfortunately, cordocentesis is associated with an increased risk of fetal mortality of 1%; therefore, it is not justified to perform it unless clinically indicated.[5] Furthermore, the oxygen content of the umbilical vein reflects the total oxygen supply to the fetus, but it does not provide information about the tissue oxygenation in individual fetal organs. By using the non-invasive blood oxygen level dependent (BOLD) technique, it is now possible to investigate oxygenation changes in different fetal organs.

BOLD magnetic resonance imaging (MRI) is widely used in clinical neuroimaging as it links brain anatomy and cognitive function.[6,7] This technique is based on the magnetic properties of hemoglobin. Deoxyhemoglobin is paramagnetic in contrast to oxyhemoglobin, which is diamagnetic. During hyperoxia, the concentration of deoxyhemoglobin decreases. Consequently, the local magnetic field changes thereby increasing the T2* relaxation time of the neighboring protons. This produces a measurable increase in the local BOLD MRI signal.[8] Studies in sheep fetuses have shown that changes in fetal BOLD MRI signal are closely related to changes in fetal oxygenation estimated by fetal arterial hemoglobin saturation[9,10] and by fluorescent oxygen sensors inserted into the fetal liver.[11]

The purpose of this present study was to investigate oxygenation changes in a number of fetal organs during maternal hyperoxia by using the non-invasive BOLD technique.

METHODS

The study was approved by the regional Committee on Biomedical Research Ethics (Journal number M-20090006). Oral and written informed consent was obtained from all

participating women. Eight healthy pregnant women carrying uncomplicated singleton pregnancies were included in the study. On the day of the examination, the fetal weight was estimated by ultrasound, and Doppler flow measurements of the umbilical artery, the middle cerebral artery and maternal uterine arteries were performed. All measurements were within the normal range. During the BOLD MRI scan, the maternal oxygen supply was controlled by a non-rebreather facial mask (Hudson Respiratory Care, Durham, NC, USA). Three consecutive maternal oxygenation episodes were induced: (1) a normoxic level (room air: 21% O_2) lasting 5 min, followed by (2) a hyperoxic level (12 L O_2/min corresponding to approximately 60% O_2) lasting 10 min, and finally (3) a normoxic level (air: 21% O_2) lasting10 min. The facial mask was applied without interfering with the BOLD MRI scan while the pregnant woman remained in the bore magnet in the left lateral position.

The BOLD MRI scan was performed with a 1.5 Tesla MRI System (Philips Medical Systems, Best, The Netherlands). A multi-receiver cardiac surface coil was placed over the abdomen covering the entire fetus. Data were acquired with a gradient echo-planar-imaging sequence with the following parameters: repetition time = 1800 ms, echo-time (effective) = 39.4 ms, number of averages = 3, flip angle = 30 and 15 slices of 6 mm with varying slice gap depending on the size of the fetus. The acquisition matrix was adjusted accordingly resulting in an in-plane spatial resolution of 2.8×2.8 mm, and spectral fat saturation was applied.

The BOLD MRI raw data were streamed to an external workstation and filtered by using dedicated custom software. Regions of interest (ROIs) were plotted in each dynamic BOLD image corresponding to the selected fetal organs and the placenta as presented in Figure 1. The ROI size depended on the size and shape of the investigated organ. In each organ, the ROI was drawn as big as possible, which meant that the placenta ROI was the biggest (approximately 670 pixels), and the kidney ROI was the smallest (approximately 45 pixels). The ROI was moved manually in each dynamic image to adjust for fetal movements, and less than 5% of the images were discarded because of severe movement artifacts. The change in BOLD signal during the entire 25-min BOLD MRI scan was obtained for each organ. For each ROI, the average BOLD signal of the initial normoxic episode (5 min) was used as a reference. The increase in BOLD signal was calculated as the average BOLD signal during the last 5 min of the hyperoxic episode. The values obtained for calculation are marked with blue bars in Figure 2.

The increase in the BOLD MRI signal during hyperoxia (ΔBOLD) was tested against the initial normoxic BOLD signal level for each organ by using a paired *t* test. A *P*-value <0.05 was considered statistically significant. The statistical analysis was performed with STATA®11 (StataCorp LP, College Station, TX, USA) statistical package.

RESULTS

Changes in the BOLD MRI signal during hyperoxia in one case (fetus number five) are shown in Figure 2. In Figure 3, data from the eight cases are pooled together, and each graph represents changes in BOLD signal (mean ± SEM) values of one fetal organ. During maternal hyperoxia, we observed an abrupt increase in the BOLD MRI signal of the fetal liver, spleen and kidney as well as the placenta; and within a few minutes, the MRI signal reached a steady-state plateau. During normoxia, the BOLD MRI signal returned to the initial reference level at a markedly slower pace. In contrast to the organs just mentioned, the BOLD MRI signal of the fetal brain remained constant during all three oxygenation periods.

Table 1 presents the eight cases and the ΔBOLD in all selected organs. The ΔBOLD was calculated for each organ. During hyperoxia, we found a significant increase in the BOLD MRI signal (ΔBOLD) of the three fetal organs (mean ± SEM): liver (14.3 ± 3.7%), spleen (15.2 ± 3.5%), kidney (6.2 ± 1.1%) and the placenta (6.5 ± 1.6%). Interestingly, the BOLD MRI signal of the fetal brain did not change during hyperoxia (0.3 ± 0.2%). We found, that the observed ΔBOLD in response to maternal hyperoxia varied among organs. For example, the

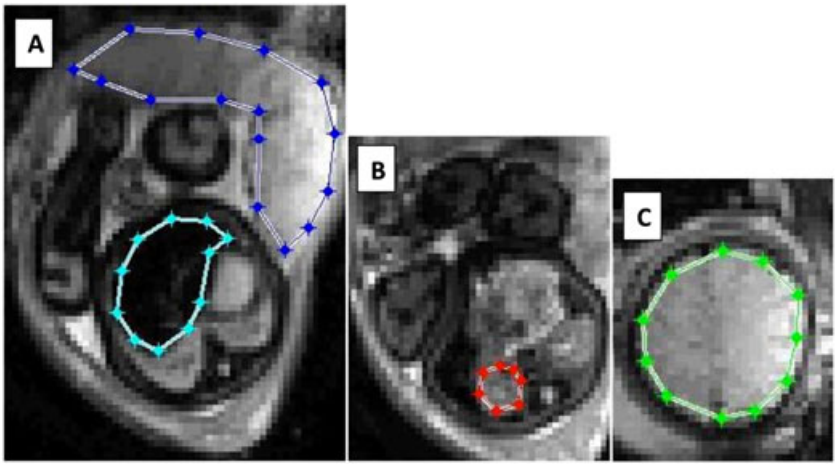

Figure 1 BOLD images of the fetus and the placenta (axial plane). Regions of interest (ROIs) are drawn in different locations. (A) the placenta (blue) and in the fetal liver (turquoise). (B) the fetal kidney, (C) the fetal brain

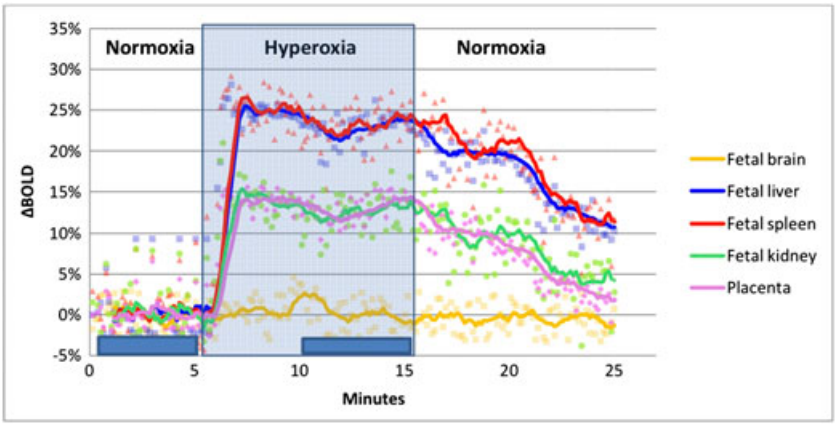

Figure 2 Changes in BOLD signal during maternal hyperoxia. Each fetal organ is represented by a different color. (Fetus number 5). The blue bars indicate the values obtained for calculation of ΔBOLD

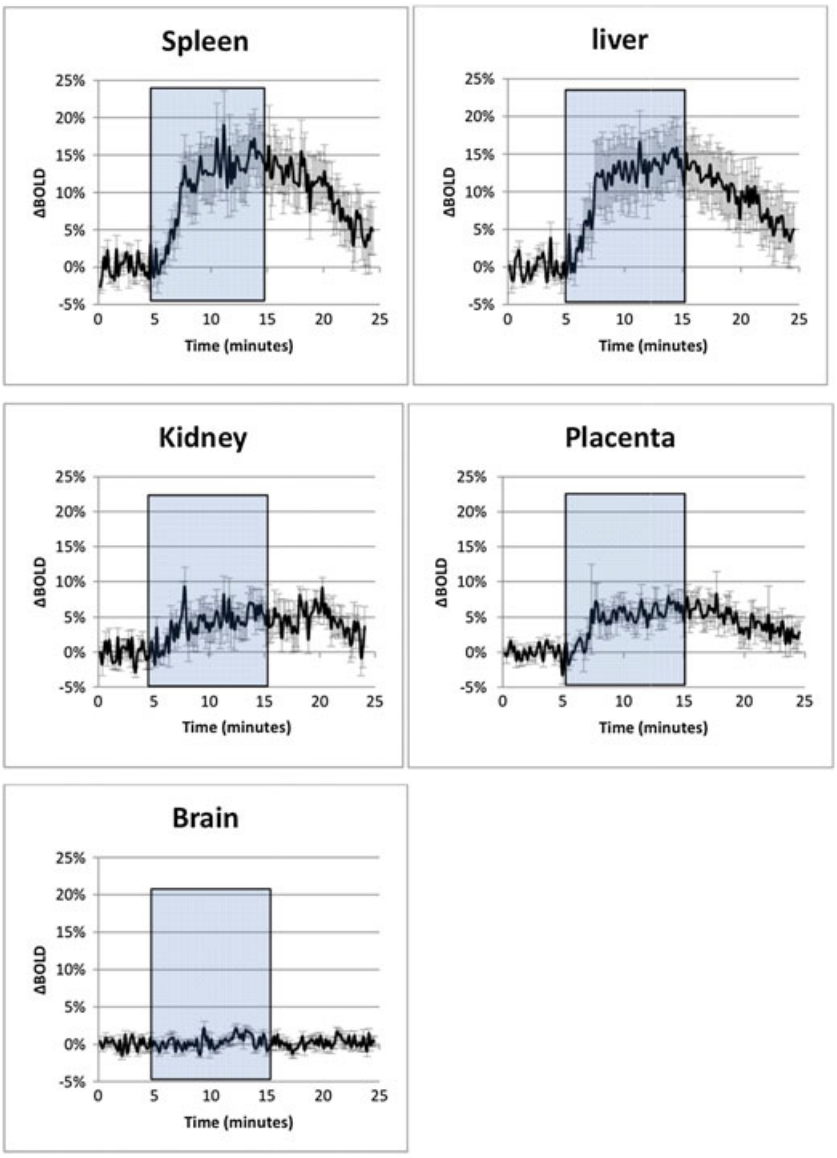

Figure 3 Data are pooled for the eight participants and each graph represents the BOLD signal changes (mean ±SEM) for one fetal organ. The gray box marks the hyperoxic episode

Table 1 The eight participants are presented and the average BOLD for each organ (mean ± SEM) are calculated. The *P*-values are based on a paired *t* test, and $P < 0.05$ is considered significant

Fetus number	Gestational age (weeks + days)	Fetal weight UL estimated (gram)	ΔBOLD fetal liver (%)	ΔBOLD fetal spleen (%)	ΔBOLD fetal kidney (%)	ΔBOLD placenta (%)	ΔBOLD fetal brain (%)
1	28 + 2	1381	14.6	15.3	5.2	5.5	−0.3
2	28 + 0	1350	−0.6	2.2	0.5	0.5	−0.01
3	28 + 6	1555	33.3	33.2	14.4	13.1	0.8
4	27 + 4	1038	13.9	16.0	5.3	4.7	0.7
5	34 + 1	2227	22.9	23.2	12.7	12.9	−0.3
6	33 + 6	2392	4.8	5.6	0.3	2.2	0.1
7	33 + 2	2190	9.1	9.0	3.8	4.6	1.5
8	33 + 6	2273	16.0	17.4	7.3	8.5	0.3
Mean (±SEM)			14.3 (±3.7)	15.2 (±3.5)	6.2 (±1.8)	6.5 (±1.6)	0.3 (±0.2)
P-value			0.006	0.003	0.006	0.005	n.s.

ΔBOLD of the liver and spleen were approximately twice the ΔBOLD of the kidney and the placenta.

DISCUSSION

This present study demonstrated that during maternal hyperoxia, oxygenation changes in a number of human fetal organs could be estimated by using the non-invasive BOLD technique.

The BOLD MRI technique provides information about changes in the fetal oxygenation status, as previously demonstrated in a study using oxygen sensitive optodes as a reference.[11] Furthermore, this technique allows real-time assessment of oxygenation changes in a number of fetal organs simultaneously. It is considered safe when performed in the second and third trimester at a magnetic field strength of 1.5 Tesla.[12]

One limitation of BOLD MRI is that oxygenation is measured in relative hence not in absolute values. The acquired BOLD MRI signal depends not only on the proportion of paramagnetic deoxyhemoglobin but also on physical parameters such as the distance to the radiofrequency coil, the magnetic shimming, sequence parameters (especially the echo-time) and physiological conditions including the blood flow, the volume fraction of blood in the fetal tissue, the hematocrit, and the hemoglobin concentration within fetal erythrocytes and so forth.[13] Therefore, the absolute BOLD MRI signal is expected to vary not only between individuals but also from day to day in the same individual.

Reducing the movement artifacts and keeping the ROI in the exact same position in the fetal organs during the BOLD MRI acquisition are important for acquiring accurate assessment. In this study, the pregnant woman remained inside the magnet bore during the entire BOLD MRI scan. No interruption was made for application of the facial mask. In case of fetal movements, the ROI position was adjusted by hand in each BOLD image.

In this present study, we did not include assessment of maternal arterial pO_2. Previously, however, in unpublished data, we have demonstrated an increased maternal arterial pO_2 to (mean ± SD) 45.0 ± 7.6 kPa (data not shown) when using the exact same facial mask for maternal hyperoxia. The differences in pO_2 were mainly due to inaccurate maternal oxygen supply. The facial mask administered oxygen at a flow rate of 12 L per minute. However, the mask was not completely tight; and therefore, some inhalation of room air was allowed. This variation in maternal pO_2 might to some extent explain the observed differences in ΔBOLD MRI signals among the fetuses.

The graphs in Figures 2 and 3 all showed a rapid increase in BOLD signal during hyperoxia and a decrease at a much slower pace when the oxygen was reduced to normoxia. The oxygen binding capacities of fetal hemoglobin might explain the shape of the graphs. Fetal hemoglobin has high oxygen affinity when compared with maternal hemoglobin, which facilitates fetal tissue oxygenation and hampers fetal hemoglobin unloading of oxygen.

Another interesting observation was that the oxygenation of the fetal brain remained unaffected by maternal hyperoxia. It is well known from Doppler flow measurements that cerebral blood flow is subjected to autoregulation.[14] During hypoxia, a compensatory increase in the cerebral blood flow is seen, known as the brain sparing mechanism.[15] The fetal hemodynamic response during hyperoxia is sparsely described, but a few studies have shown a decrease in the cerebral blood flow[16–18] during maternal hyperoxia, which could be considered as a 'reversed' brain sparing mechanism. The lack of oxygenation changes in the fetal brain observed in our study may therefore support the view that the cerebral blood flow is reduced during hyperoxia.

In addition, we found a fixed relationship between the ΔBOLD signals of the different organs in each individual. In each fetus, the ΔBOLD signal of the fetal spleen and liver were similar, and it was nearly doubled when compared with the ΔBOLD signal of the fetal kidney and placenta. These observations are likely explained by biological variations among organs, for example, different fractions of blood volume. As mentioned earlier, the imaging parameters, especially the echo-time, are important for the magnitude of the BOLD MRI signal, and the echo-time chosen in this study might favor an increased ΔBOLD in the fetal liver and spleen.

Two previous studies using BOLD MRI, a pilot study of nine fetuses[19] and a larger study including 41 growth restricted

fetuses and 39 normal fetuses,[20] have investigated the human fetal liver oxygenation during maternal hyperoxia. The later study demonstrated no changes in BOLD signal in fetal liver during hyperoxia. The discrepancy between these findings and our present results could be due to differences in experimental design, MRI protocol and in handling of the pregnant woman during the BOLD MRI procedure.

A clinical perspective of this method could be BOLD MRI scans of growth restricted fetuses with impaired placental function. Two previous studies have investigated the potential of maternal hyperoxia as a test of placental function and fetal outcome.[1,21] Cordocentesis in growth restricted fetuses during maternal hyperoxia showed that no increase in fetal oxygenation was associated with severe placental dysfunction and adverse fetal outcome.[1] Another study investigated the changes in fetal cerebral resistance by Doppler ultrasound during maternal hypoxia. In a group of growth restricted fetuses with brain sparing normalization of cerebral flow was associated with better fetal outcome, and no change of cerebral blood flow was associated with adverse fetal outcome.[21] These findings suggest that fetuses with seriously impaired placental function do not respond to maternal hyperoxia; and therefore, fetal non-responsiveness could be a predictor of poor fetal outcome. However, this needs to be tested further. To our knowledge, this is the first study to successfully demonstrate oxygenation changes in a number of human fetal organs during maternal hyperoxia. The BOLD MRI technique provides new possibilities in observing normal fetal physiology, and it introduces a new tool to the field of fetal monitoring and fetal testing. Further research should be conducted in healthy as well as growth retarded fetuses suffering from impaired placental function.

ACKNOWLEDGEMENT

We wish to thank statistician Steffen Falgreen Larsen M.Sc. at the Cardiovascular Research Center, Aalborg Hospital for very helpful advice in statistical matters.

WHAT'S ALREADY KNOWN ABOUT THIS TOPIC?

- The BOLD MRI signal depends upon the magnetic properties of hemoglobin.
- In the sheep fetus, changes in the BOLD MRI signal reflect changes in fetal tissue oxygenation.
- Maternal hyperoxia increases the fetal oxygen supply when estimated by cordocentesis.

WHAT DOES THIS STUDY ADD?

- In the human fetus, the BOLD technique is capable of measuring changes in tissue oxygenation in various fetal organs.
- Maternal hyperoxia increases fetal tissue oxygenation in a number of fetal organs.
- The oxygenation of the fetal brain is unaffected by maternal hyperoxia, this could be caused by autoregulation of fetal cerebral bloodflow – reversed brain sparing.

REFERENCES

1. Nicolaides KH, Campbell S, Bradley RJ, *et al.* Maternal oxygen therapy for intrauterine growth retardation. Lancet 1987;1(8539):942-5.
2. Haydon ML, Gorenberg DM, Nageotte MP, *et al.* The effect of maternal oxygen administration on fetal pulse oximetry during labor in fetuses with nonreassuring fetal heart rate patterns. Am J Obstet Gynecol 2006;195(3):735-8.
3. Bartnicki J, Saling E. The influence of maternal oxygen administration on the fetus. Int J Gynaecol Obstet 1994;45(2):87-95.
4. Battaglia FC, Meschia G, Makowski EL, *et al.* The effect of maternal oxygen inhalation upon fetal oxygenation. J Clin Invest 1968;47(3):548-55.
5. Srisupundit K, Wanapirak C, Piyamongkol W, *et al.* Comparisons of outcomes after cordocentesis at mid-pregnancy between singleton and twin pregnancies. Prenat Diagn 2011;31(11):1066-9
6. Logothetis NK. What we can do and what we cannot do with fMRI. Nature 2008;453(7197):869-78.
7. Blatow M, Nennig E, Durst A, *et al.* fMRI reflects functional connectivity of human somatosensory cortex. Neuroimage 2007;37(3):927-36.
8. Thulborn KR, Waterton JC, Matthews PM, *et al.* Oxygenation dependence of the transverse relaxation time of water protons in whole blood at high field. Biochim Biophys Acta 1982;714(2):265-70.
9. Wedegartner U, Tchirikov M, Schafer S, *et al.* Functional MR imaging: comparison of BOLD signal intensity changes in fetal organs with fetal and maternal oxyhemoglobin saturation during hypoxia in sheep. Radiology 2006;238(3):872-80.
10. Wedegartner U, Kooijman H, Andreas T, *et al.* T2 and T2* measurements of fetal brain oxygenation during hypoxia with MRI at 3T: correlation with fetal arterial blood oxygen saturation. Eur Radiol 2010;20(1):121-7
11. Sorensen A, Pedersen M, Tietze A, *et al.* BOLD MRI in sheep fetuses: a non-invasive method for measuring changes in tissue oxygenation. Ultrasound Obstet Gynecol 2009;34(6):687-92.
12. Kanal E, Barkovich AJ, Bell C, *et al.* ACR guidance document for safe MR practices: 2007. AJR Am J Roentgenol 2007;188(6):1447-74.
13. Lu H, Zhao C, Ge Y, *et al.* Baseline blood oxygenation modulates response amplitude: physiologic basis for intersubject variations in functional MRI signals. Magn Reson Med 2008;60(2):364-72.
14. Kiserud T, Acharya G. The fetal circulation. Prenat Diagn 2004;24 (13):1049-59.
15. Baschat AA. Fetal responses to placental insufficiency: an update. BJOG 2004;111(10):1031-41.
16. Almstrom H, Sonesson SE. Doppler echocardiographic assessment of fetal blood flow redistribution during maternal hyperoxygenation. Ultrasound Obstet Gynecol 1996;8(4):256-61.
17. Hsu YY, Kuan WC, Lim KE, *et al.* Breathhold-regulated blood oxygenation level-dependent (BOLD) MRI of human brain at 3 Tesla. J Magn Reson Imaging 2010;31(1):78-84.
18. Simchen MJ, Tesler J, Azami T, *et al.* Effects of maternal hyperoxia with and without normocapnia in uteroplacental and fetal Doppler studies. Ultrasound Obstet Gynecol 2005;26(5):495-9.
19. Semple SI, Wallis F, Haggarty P, *et al.* The measurement of fetal liver T(*)(2) *in utero* before and after maternal oxygen breathing: progress towards a non-invasive measurement of fetal oxygenation and placental function. Magn Reson Imaging 2001;19 (7):921-8.
20. Morris DM, Ross JA, McVicar A, *et al.* Changes in foetal liver T2* measurements by MRI in response to maternal oxygen breathing: application to diagnosing foetal growth restriction. Physiol Meas 2010;31(9):1137-46.
21. Arduini D, Rizzo G, Romanini C, *et al.* Hemodynamic changes in growth retarded fetuses during maternal oxygen administration as predictors of fetal outcome. J Ultrasound Med 1989;8(4):193-6.

Paper 4

Ultrasound Obstet Gynecol 2013; **42**: 310–314
Published online in Wiley Online Library (wileyonlinelibrary.com). **DOI:** 10.1002/uog.12395

Changes in human placental oxygenation during maternal hyperoxia estimated by blood oxygen level-dependent magnetic resonance imaging (BOLD MRI)

A. SØRENSEN*, D. PETERS†, E. FRÜND*, G. LINGMAN‡, O. CHRISTIANSEN* and N. ULDBJERG§

**Department of Obstetrics and Gynecology, Aalborg University Hospital, Aalborg, Denmark; †Department of Clinical Engineering, Aarhus University Hospital, Aarhus, Denmark; ‡Department of Obstetrics, Lund University Hospital, Lund, Sweden; §Department of Obstetrics and Gynecology, Aarhus University Hospital, Aarhus, Denmark*

KEYWORDS: BOLD; hyperoxia; MRI; oxygen; placenta

ABSTRACT

Objectives *To investigate changes in human placental oxygenation during maternal hyperoxia using non-invasive blood oxygen level-dependent (BOLD) magnetic resonance imaging (MRI).*

Methods *Eight healthy pregnant women with uncomplicated singleton pregnancies at gestational weeks 28–36 were examined with BOLD MRI, over two consecutive 5-min periods of different oxygenation: first normoxia (21% O_2) and then hyperoxia (12 L O_2/min), achieved by controlling the maternal oxygen supply with a non-rebreather facial mask. Selecting three slices showing cross-sections of the central part of the placenta, we investigated total placental oxygenation by drawing regions of interest (ROIs) covering the entire placenta, and regional placental oxygenation by drawing smaller ROIs in the darker and brighter areas of the placenta. For each ROI, the difference in BOLD signal between the two episodes was determined and the percentage increase in BOLD signal during hyperoxia (ΔBOLD) was calculated.*

Results *In the BOLD image, the normoxic placenta appeared heterogeneous, with darker areas located to the fetal side and brighter areas to the maternal side. During hyperoxia, the placenta became brighter and the structure more homogeneous, and the BOLD signal of the total placenta increased ($\Delta BOLD_{tot}$, $15.2 \pm 3.2\%$ (mean ± SD), $P < 0.0001$). The increase was seen predominantly in the dark areas in the fetal part of the placenta ($\Delta BOLD_{fet}$, $32.1 \pm 9.3\%$) compared with in the bright areas in the maternal part of the placenta ($\Delta BOLD_{mat}$, $5.4 \pm 3.5\%$).*

Conclusion *During hyperoxia, placental oxygenation was increased predominantly in the darker placental areas, which, given their anatomical location, represent the fetal circulation of the placenta. To our knowledge, this is the first study to successfully visualize changes in placental oxygenation using BOLD MRI.*

INTRODUCTION

An adequate supply of oxygen is crucial in fetal growth and development. The oxygen supply to the fetus is determined by the maternal uterine blood flow and oxygen content, placental diffusion of oxygen and umbilical venous blood flow[1,2]. Oxygen molecules, which are small and lipophilic, diffuse easily across the placental membrane[3,4], driven by the partial pressure gradient of oxygen[5,6]. In the normal placenta the efficiency of oxygen transfer is dependent more on blood flow and oxygen content than on diffusion[1]. Impaired placental function is associated with fetal growth restriction[7,8], hypoxia[9,10] and adverse perinatal outcome[11].

Placental oxygen transport can be estimated by cordocentesis, which provides information about the oxygen content of the umbilical cord vessels. This invasive procedure is not used routinely because of the procedure-related risk of fetal loss of approximately 1%[12]. The major tools in fetal monitoring are ultrasound Doppler flow measurements and cardiotocography, including ST waveform analysis of the fetal electrocardiogram. However, these methods are indirect, based on the fact that specific changes in umbilical blood flow[13], fetal cerebral blood flow[14] and fetal electrocardiogram findings[15] are associated with fetal hypoxia and acidosis[9].

It is now possible, using the non-invasive blood oxygen level-dependent (BOLD) magnetic resonance imaging

Correspondence to: Dr A. Sørensen, Aarhus University Hospital, Department of Gynecology and Obstetrics, Aalborg Hospital North Region, Reberbangade Aalborg 9100, Denmark (e-mail: annenoedgaard@hotmail.com)

Accepted: 30 December 2012

(MRI) technique, to estimate changes in oxygenation directly in specific areas of placental and fetal tissue. The technique is based on the fact that the magnetic properties of hemoglobin and deoxyhemoglobin are different[16]; deoxyhemoglobin induces local field inhomogeneities, which leads to a reduction in the BOLD signal[17]. During hyperoxia, the amount of deoxyhemoglobin is reduced, and therefore the BOLD signal is expected to increase. The BOLD MRI technique is used widely in neuroscience, linking brain anatomy and cognitive function through brain activation studies[18]. A few studies have been published using this technique for estimating changes in oxygenation in the sheep fetus[19–24]. To our knowledge, this is the first BOLD MRI study focusing on human placental oxygenation.

In this study, we aimed to investigate changes in human placental oxygenation during maternal hyperoxia using the non-invasive BOLD MRI technique. Furthermore, we discuss the potential of the BOLD MRI technique as a tool for future placental testing.

METHODS

The study was approved by the regional Committee on Biomedical Research Ethics (Journal number M-20090006). Oral and written informed consent was obtained from all participating women.

We included in the study eight healthy women with uncomplicated singleton pregnancies at gestational weeks 28–36 and with normal estimated fetal weight and normal Doppler flow in the umbilical artery, middle cerebral artery and maternal uterine arteries. During the BOLD MRI procedure, the maternal oxygen supply was controlled by a non-rebreather facial mask (Hudson Respiratory Care, Durham, NC, USA). We investigated two consecutive episodes of different oxygenation, each lasting 5 min: an initial normoxic episode (21% O_2) followed by a hyperoxic episode (12 L O_2/min). The facial mask was applied without interfering with the BOLD MRI examination, while the pregnant woman remained within the bore magnet in the left lateral position.

The BOLD MRI examination was performed with a GE Discovery MR450 1.5-Tesla MRI system (GE Healthcare, Milwaukee, WI, USA). An eight-channel cardiac coil was placed over the maternal abdomen, covering the uterus. Data were acquired with a gradient echo planar imaging sequence with the following parameters: repetition time, 8000 ms; echo-time (effective), 50 ms; flip angle, 90°; number of slices, 22; slice thickness, 6 mm with a slice gap of 6 mm; matrix 128×128 pixels; field-of-view, 36×36 cm, resulting in an in-plane spatial resolution of 3.6×3.6 mm. A total of 75 dynamics was acquired in each 10-min BOLD scan.

The BOLD MRI DICOM (Digital Imaging and Communications in Medicine) data were processed using a program, developed in-house, written in MATLAB (The MathWorks Inc, Natick, MA, USA). From the BOLD MRI images we selected three slices showing cross-sections of the central part of the placenta, with a minimum distance between slices of 30 mm, and further calculations were based on the mean of the three slices. To investigate total placental oxygenation, a region of interest (ROI) was drawn covering the entire placenta in each slice (see Figure 2). To investigate regional placental oxygenation, smaller ROIs were drawn in two different areas of the placenta in each slice; one ROI was placed in the darker area located on the fetal side and the other ROI was placed in the brighter area on the maternal side of the placenta (see Figure 3). The location of the ROI was adjusted in each dynamic image, correcting for maternal breathing movements. All ROIs were drawn by a single examiner (A.S.).

The BOLD signal of each ROI was recorded at 75 time points during the entire 10-min BOLD scan and for each ROI the BOLD signal at each time point was normalized using the mean BOLD signal of the initial 3 min of normoxia ($BOLD_{Normoxia}$) as a reference. Furthermore, ΔBOLD was calculated using the following equation: $\Delta BOLD = (BOLD_{Hyperoxia} - BOLD_{Normoxia}) \times 100\%$, where $BOLD_{Hyperoxia}$ was the mean BOLD signal of the last 2 min of the BOLD scan. ΔBOLD was calculated for the total placenta ($\Delta BOLD_{tot}$) and for the dark ($\Delta BOLD_{fet}$) and the bright ($\Delta BOLD_{mat}$) placental areas. In every patient ΔBOLD was calculated as a mean value of the three slices.

The hyperoxic BOLD signal was tested against the initial normoxic BOLD signal using a paired Student's *t*-test. $P < 0.05$ was considered statistically significant. Statistical analysis was performed with the Stata®11 (StataCorp LP, College Station, TX, USA) statistical package.

RESULTS

In the normoxic BOLD image the placenta appeared heterogeneous. Dark areas were scattered along the fetal surface of the placenta, stretching towards the maternal surface as thin finger-like structures (Figure 1a). The surrounding placental tissue looked brighter, increasing in brightness towards the maternal side. During hyperoxia, a clear visual change occurred in the BOLD image; the placental structure now appeared brighter and homogeneous and the dark areas were no longer visible (Figure 1b).

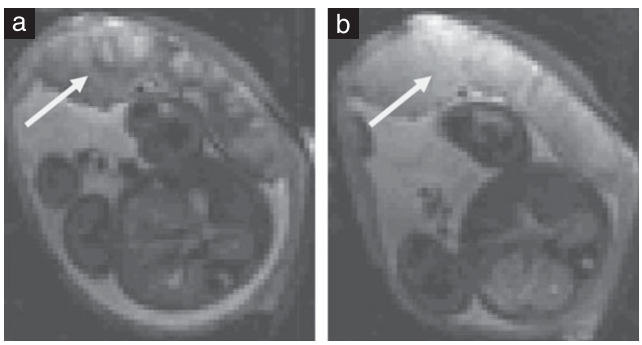

Figure 1 Blood oxygen level-dependent (BOLD) images: cross-section through uterus showing an axial plane through fetal abdomen and central part of placenta (arrow) during maternal normoxia (a) and hyperoxia (b).

The total placental oxygenation was investigated using ROIs covering the entire placenta (Figure 2) in three different slices from each patient. In each ROI the BOLD signal was obtained at 75 consecutive time-points during the 10-min scan, and the normalized BOLD signal *vs* time curves for one participant (Case 3) are presented in Figure 2. The three curves in Figure 2 are very similar, indicating that $\Delta BOLD_{tot}$ is highly reproducible in different slices within the same placenta. For all eight participants in our study, the BOLD signal for the total placenta was significantly increased during maternal hyperoxia: $\Delta BOLD_{tot} = 15.2 \pm 3.2\%$ (mean ± SD). Individual findings are shown in Table 1.

Regional placental oxygenation was investigated by drawing smaller ROIs in both the darker and the brighter areas of the placenta. The normalized BOLD signal *vs* time curves for the two regions in one participant (Case 3) are presented in Figure 3. These two curves are very different; the one representing the dark fetal part of the placenta increases to a higher level during maternal hyperoxia when compared with that representing the bright maternal part of the placenta. For all eight participants the hyperoxic increase in BOLD signal was seen predominantly in the dark fetal parts of the placenta ($\Delta BOLD_{fet}$, $32.1 \pm 9.3\%$ (mean ± SD)) when compared with the brighter maternal parts of the placenta ($\Delta BOLD_{mat}$, $5.4 \pm 3.5\%$ (mean ± SD)). Individual findings are presented in Table 1.

DISCUSSION

This study based on BOLD MRI of the normal human placenta demonstrated a significant increase in total placental oxygenation ($\Delta BOLD_{tot}$, $15.2 \pm 3.2\%$) during maternal hyperoxia. The increase was seen predominantly in the darker areas located close to the fetal side of the placenta ($\Delta BOLD_{fet}$: $32.1 \pm 9.3\%$). In the BOLD MR image the changes in oxygenation were visualized clearly

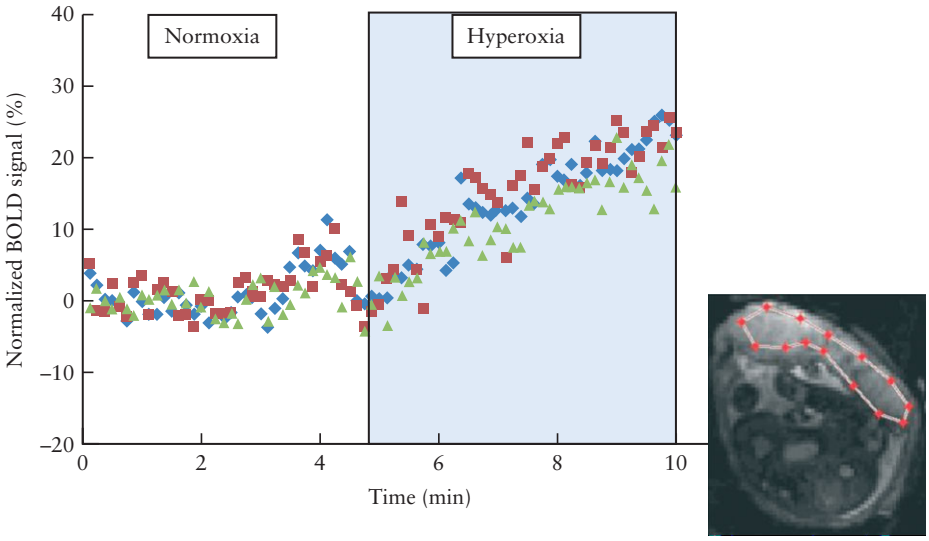

Figure 2 Normalized blood oxygen level-dependent (BOLD) signal *vs* time curves of total placenta during 10-min BOLD scan: three curves represent three slices within the same placenta (Case 3). Region of interest is shown in inset BOLD image. ◆ Slice 1, ■ Slice 2, ▲ Slice 3.

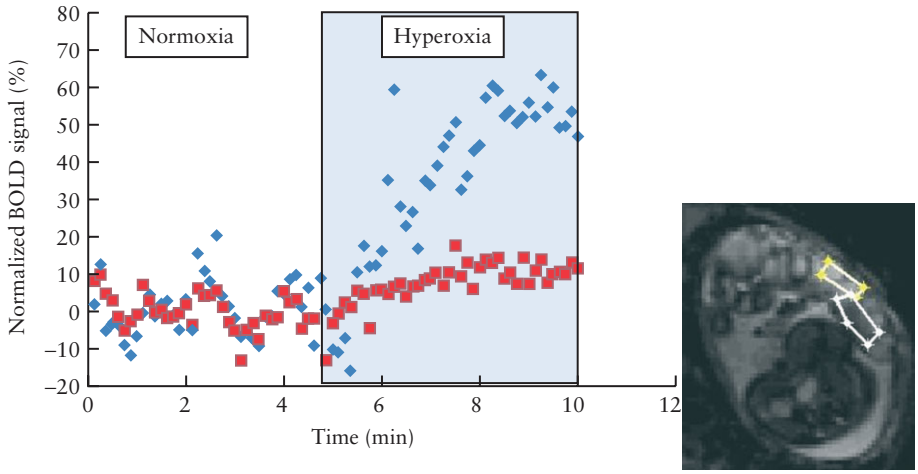

Figure 3 Normalized blood oxygen level-dependent (BOLD) signal *vs* time curves of two different placental regions: dark placental area on fetal side of placenta (◆) and bright placental area on maternal side of placenta (■). Regions of interest are shown in inset BOLD image (Case 3).

Table 1 Increase in blood oxygen level-dependent (BOLD) signal of total placenta ($\Delta BOLD_{tot}$) and different regions of placenta ($\Delta BOLD_{fet}$ and $\Delta BOLD_{mat}$) during maternal hyperoxia in eight healthy women with uncomplicated singleton pregnancies

Case	*GA (weeks)*	*Total placenta* $\Delta BOLD_{tot}$ *(%)*	*Dark placental area: fetal side* $\Delta BOLD_{fet}$ *(%)*	*Bright placental area: maternal side* $\Delta BOLD_{mat}$ *(%)*
1	30 + 5	19.4 ± 5.4	48.3 ± 19.2	10.9 ± 0.8
2	28 + 2	12.6 ± 2.2	30.6 ± 15.6	4.4 ± 1.4
3	32 + 1	19.1 ± 2.5	43.1 ± 16.4	6.8 ± 8.4
4	35 + 1	12.9 ± 3.4	27.5 ± 8.5	3.2 ± 6.4
5	35 + 5	12.3 ± 4.4	27.9 ± 11.1	1.8 ± 3.3
6	33 + 0	12.1 ± 1.3	34.4 ± 20.9	2.1 ± 5.5
7	36 + 3	17.9 ± 3.6	23.2 ± 12.5	4.3 ± 8.6
8	35 + 2	15.4 ± 1.0	22.2 ± 7.8	10.0 ± 6.5
1–8 (overall)		15.2 ± 3.2	32.1 ± 9.3	5.4 ± 3.5
P		< 0.0001	< 0.0001	0.003

Data are mean ± SD of three slices in each case and of the eight cases overall. *P*-values are based on paired *t*-test. GA, gestational age.

as the placenta became brighter and more homogeneous during hyperoxia.

A strength of the BOLD MRI technique is that it has been evaluated in sheep fetuses with oxygen-sensitive optodes inserted into the fetal liver[23]. That study demonstrated a very close correlation between changes in organ tissue oxygenation and changes in the BOLD signal. However, the absolute BOLD signal depends not only on the proportion of paramagnetic deoxyhemoglobin but also on other variables, including the hemoglobin concentration, hematocrit, blood flow and blood volume within the tissue[25,26]. Nevertheless, we found the reproducibility of $\Delta BOLD_{tot}$ in different slices within the same placenta to be very high (Figure 2). The lower reproducibility of $\Delta BOLD_{mat}$ and $\Delta BOLD_{fet}$ within the same placenta might depend on difficulties in the complete separation of maternal and fetal parts when drawing the ROIs. The small inter-individual differences in $\Delta BOLD_{tot}$ could be due to physiological differences between individuals; however, we cannot exclude minor differences in the maternal oxygen supply as another possible explanation for these differences.

Maternal hyperoxia is known to increase fetal oxygen supply provided there is normal placental function[27]. This has been demonstrated in the human fetus by cordocentesis[28], pulse oximetry[29] and postpartum umbilical cord blood sampling[30]. Furthermore, using the BOLD MRI technique in the sheep fetus we have demonstrated that maternal hyperoxia increases fetal tissue oxygenation in a number of fetal organs[23]. This effect is probably mediated by increased partial pressure of oxygen in the maternal blood of the intervillous space, which improves the diffusion of oxygen across the placental membrane from the mother to the fetus[5]. During normoxia the maternal blood is already fully saturated; this is in contrast to fetal blood, which is only 70% saturated[31]. This means that the fetus is situated at a lower and steeper part of the hemoglobin dissociation curve when compared to the mother. Therefore, the same increase in oxygen partial pressure generates a larger increase in saturation in the fetus. As the changes in the BOLD MRI signal are dependent on changes in hemoglobin saturation, the BOLD MRI response to hyperoxia is expected to be more pronounced in fetal blood. A precise conclusion concerning the heterogeneous pattern of the placenta observed in the normoxic BOLD MR image cannot be drawn from the present study. However, according to the anatomical location of the dark areas, their size and their response to maternal hyperoxygenation, it seems reasonable to hypothesize that the darker areas represent the villous trees dominated by fetal blood. A histopathological examination of these normal placentae would not have determined the origin of the dark and bright areas of the placenta on the BOLD image. However, in future studies based on pregnancies complicated by placental insufficiency, histopathological examination of the placenta will be of great interest as an altered oxygen response might have a histopathological explanation.

To our knowledge, this is the first BOLD MRI study of the human placenta. Previous BOLD MRI studies published in sheep models[19–24] did not focus on placental oxygenation. This is because the sheep placenta is very different from the human placenta in both shape and structure. The sheep placenta consists of separate cotyledons scattered on the amniotic sac; in contrast, the human placenta is discoid in shape and therefore more suitable for imaging and drawing of ROIs. Furthermore, the sheep placenta is considered a concurrent system, which is less efficient than the multivillous system in the human placenta[3,32]. However, in individual cotyledons of the sheep placenta, the BOLD signal was reduced during maternal hypoxia[20]. Comparable findings were reported in rat experiments, in which the BOLD signal of the total placenta was reduced during hypoxia induced by prostaglandin[33].

The clinical perspective of these results might be that the BOLD MRI technique provides a new tool in the difficult field of testing placental function. In particular, $\Delta BOLD_{tot}$ seems like a robust measurement. Testing of pathological pregnancy with impaired placental function, as seen in the growth-restricted fetus, would be an obvious target for this method. Because of the high cost and limited availability of BOLD MRI, the method is only suitable for selected cases.

Cordocentesis in severely growth-restricted fetuses has demonstrated three different types of fetal response to maternal hyperoxia: 1) increase in fetal oxygen partial pressure (pO_2) above normal, indicating unimpaired placental function; 2) increase in fetal pO_2 below normal, indicating some degree of impaired placental function; and 3) no response, indicating severely impaired placental function. Non-responding fetuses have poor neonatal prognosis and they require immediate delivery[28]. This is known as the non-responder hypothesis. According to this hypothesis reduced or no increase in placental BOLD signal during maternal hyperoxia might be associated with impaired placental function and poor neonatal outcome. Further research should be performed in healthy as well as pathological pregnancies.

REFERENCES

1. Goplerud JM, Delivoria-Papadopoulos M. Physiology of the placenta--gas exchange. *Ann Clin Lab Sci* 1985; **15**: 270–278.
2. Carter AM. Factors affecting gas transfer across the placenta and the oxygen supply to the fetus. *J Dev Physiol* 1989; **12**: 305–322.
3. Schroder HJ. Comparative aspects of placental exchange functions. *Eur J Obstet Gynecol Reprod Biol* 1995; **63**: 81–90.
4. Desforges M, Sibley CP. Placental nutrient supply and fetal growth. *Int J Dev Biol* 2010; **54**: 377–390.
5. Carter AM. Placental oxygen transfer and the oxygen supply to the fetus. *Fetal Matern Med Rev* 1999; **11**: 151–161.
6. Gill JS, Salafia CM, Grebenkov D, Vvedensky DD. Modeling oxygen transport in human placental terminal villi. *J Theor Biol* 2011; **291**: 33–41.
7. Cetin I, Alvino G. Intrauterine growth restriction: implications for placental metabolism and transport. A review. *Placenta* 2009; **30** (Suppl A): S77–S82.
8. Pardi G, Marconi AM, Cetin I. Placental-fetal interrelationship in IUGR fetuses--a review. *Placenta* 2002; **23** (Suppl A): S136–141.
9. Pardi G, Cetin I, Marconi AM, Lanfranchi A, Bozzetti P, Ferrazzi E, Buscaglia M, Battaglia FC. Diagnostic value of blood sampling in fetuses with growth retardation. *N Engl J Med* 1993; **328**: 692–696.
10. Nicolaides KH, Economides DL, Soothill PW. Blood gases, pH, and lactate in appropriate- and small-for-gestational-age fetuses. *Am J Obstet Gynecol* 1989; **161**: 996–1001.
11. Baschat AA. Neurodevelopment following fetal growth restriction and its relationship with antepartum parameters of placental dysfunction. *Ultrasound Obstet Gynecol* 2011; **37**: 501–514.
12. Liao C, Wei J, Li Q, Li L, Li J, Li D. Efficacy and safety of cordocentesis for prenatal diagnosis. *Int J Gynaecol Obstet* 2006; **93**: 13–17.
13. Madazli R, Somunkiran A, Calay Z, Ilvan S, Aksu MF. Histomorphology of the placenta and the placental bed of growth restricted foetuses and correlation with the Doppler velocimetries of the uterine and umbilical arteries. *Placenta* 2003; **24**: 510–516.
14. Baschat AA. Pathophysiology of fetal growth restriction: implications for diagnosis and surveillance. *Obstet Gynecol Surv* 2004; **59**: 617–627.
15. Rosen KG, Amer-Wahlin I, Luzietti R, Noren H. Fetal ECG waveform analysis. *Best Pract Res Clin Obstet Gynaecol* 2004; **18**: 485–514.
16. Pauling L, Coryell CD. The magnetic properties and structure of hemoglobin, oxyhemoglobin and carbonmonoxyhemoglobin. *Proc Natl Acad Sci U S A* 1936; **22**: 210–216.
17. Ogawa S, Lee TM. Magnetic resonance imaging of blood vessels at high fields: in vivo and in vitro measurements and image simulation. *Magn Reson Med* 1990; **16**: 9–18.
18. Logothetis NK. The neural basis of the blood-oxygen-level-dependent functional magnetic resonance imaging signal. *Philos Trans R Soc Lond B Biol Sci* 2002; **357**: 1003–1037.
19. Wedegartner U, Tchirikov M, Koch M, Adam G, Schroder H. Functional magnetic resonance imaging (fMRI) for fetal oxygenation during maternal hypoxia: initial results. *Rofo* 2002; **174**: 700–703.
20. Wedegartner U, Tchirikov M, Schafer S, Priest AN, Kooijman H, Adam G, Schroder HJ. Functional MR imaging: comparison of BOLD signal intensity changes in fetal organs with fetal and maternal oxyhemoglobin saturation during hypoxia in sheep. *Radiology* 2006; **238**: 872–880.
21. Wedegartner U, Tchirikov M, Schafer S, Priest AN, Walther M, Adam G, Schroder HJ. Fetal sheep brains: findings at functional blood oxygen level-dependent 3-T MR imaging--relationship to maternal oxygen saturation during hypoxia. *Radiology* 2005; **237**: 919–926.
22. Wedegartner U, Kooijman H, Andreas T, Beindorff N, Hecher K, Adam G. T2 and T2* measurements of fetal brain oxygenation during hypoxia with MRI at 3T: correlation with fetal arterial blood oxygen saturation. *Eur Radiol* 2010; **20**: 121–127.
23. Sorensen A, Pedersen M, Tietze A, Ottosen L, Duus L, Uldbjerg N. BOLD MRI in sheep fetuses: a non-invasive method for measuring changes in tissue oxygenation. *Ultrasound Obstet Gynecol* 2009; **34**: 687–692.
24. Sorensen A, Holm D, Pedersen M, Tietze A, Stausbol-Gron B, Duus L, Uldbjerg N. Left–right difference in fetal liver oxygenation during hypoxia estimated by BOLD MRI in a fetal sheep model. *Ultrasound Obstet Gynecol* 2011; **38**: 665–672.
25. Kennan RP, Scanley BE, Gore JC. Physiologic basis for BOLD MR signal changes due to hypoxia/hyperoxia: separation of blood volume and magnetic susceptibility effects. *Magn Reson Med* 1997; **37**: 953–956.
26. Lu H, Zhao C, Ge Y, Lewis-Amezcua K. Baseline blood oxygenation modulates response amplitude: Physiologic basis for intersubject variations in functional MRI signals. *Magn Reson Med* 2008; **60**: 364–372.
27. Battaglia FC, Meschia G, Makowski EL, Bowes W. The effect of maternal oxygen inhalation upon fetal oxygenation. *J Clin Invest* 1968; **47**: 548–555.
28. Nicolaides KH, Campbell S, Bradley RJ, Bilardo CM, Soothill PW, Gibb D. Maternal oxygen therapy for intrauterine growth retardation. *Lancet* 1987; **1**: 942–945.
29. Haydon ML, Gorenberg DM, Nageotte MP, Ghamsary M, Rumney PJ, Patillo C, Garite TJ. The effect of maternal oxygen administration on fetal pulse oximetry during labor in fetuses with nonreassuring fetal heart rate patterns. *Am J Obstet Gynecol* 2006; **195**: 735–738.
30. Ngan Kee WD, Khaw KS, Ma KC, Wong AS, Lee BB. Randomized, double-blind comparison of different inspired oxygen fractions during general anaesthesia for Caesarean section. *Br J Anaesth* 2002; **89**: 556–561.
31. Meschia G. Fetal oxygenation and maternal ventilation. *Clin Chest Med* 2011; **32**: 15–19, vii.
32. Wilkening RB, Meschia G. Current topic: comparative physiology of placental oxygen transport. *Placenta* 1992; **13**: 1–15.
33. Girsh E, Plaks V, Gilad AA, Nevo N, Schechtman E, Neeman M, Dekel N. Cloprostenol, a prostaglandin F(2alpha) analog, induces hypoxia in rat placenta: BOLD contrast MRI. *NMR Biomed* 2007; **20**: 28–39.

Paper 5

The reproducibility of human placental T2* measurements and hyperoxic response

David Alberg Peters[1], Anne Nødgaard Sørensen[2], Marianne Munk Sinding[2], Carsten Simonsen[3], Niels Uldbjerg[4]

1 Department of Clinical Engineering, Aarhus University Hospital, Aarhus, Denmark

2 Department of Obstetrics and Gynecology, Aalborg Hospital, Aarhus University Aalborg, Denmark

3 Department of Radiology, Aalborg Hospital, Aalborg, Denmark

4 Department of Obstetrics and Gynecology, Aarhus University Hospital, Aarhus, Denmark

Abstract

Purpose

The aim of this study was to investigate placental T2* from normal pregnancies with regards to the reproducibility, dependence on gestational age, and the response to maternal oxygen breathing.

Materials and Methods

Twenty-four pregnant women with confirmed normal pregnancies between gestational week 24 and 40 underwent MRI examination. T2* measurement were performed using a gradient recalled echo sequence with multiple readouts at 16 different echo times. T2* value was calculated using a non-linear least squares fitting algorithm.

T2* measurement were repeated during 10 minutes of maternal oxygen breathing through a Hudson mask (12 litre O_2/min).

Results

The mean placental T2* was 81.3±28.1 ms and a negative linear correlation between placental T2* and gestation age was found with a decline of 4.8 ms per week.

The reproducibility of placental T2* was tested

1. Slice-to-slice (N=24) comparing two separate slices of each placenta (95%-limits of agreement -1.8±13.1 ms)
2. Scan-to-scan (N=16) comparing repeat scans within two minutes (95%-limits of agreement -0.1±17.8 ms).
3. Session-to-session (N=8) comparing repeat scan sessions within 45 minutes (95%-limits of agreement -0.3±15.7 ms)

During hyperoxia a statistically significant increase of 14.4±12.8 ms in placental T2* was demonstrated.

Conclusion

We have estimated the reproducibility of placental T2* measurements, and demonstrated that placental T2* decreases with gestational age. Thereby, we have established a normal material that may be useful for future investigation of placental pathology. We have further demonstrated that T2* of the placenta increases during maternal hyperoxia.

Introduction

In the developing fetus the oxygen supply from the placenta is essential to maintain normal growth. Therefore a non-invasive method to detect the oxygen concentration in the placenta would be of huge benefit, as it could be used as a tool in the diagnosis and surveillance of growth-retarded fetuses.

As deoxyhemoglobin is paramagnetic it decreases the transversal relaxation time in MRI (T2*), while oxyhemoglobin is diamagnetic and has no affect on T2*, therefore the amount of oxygen bound to hemoglobin affects the MR signal(1). This effect can be monitored using heavily T2* weighted imaging (Blood oxygen level dependent – BOLD) or by measuring T2* directly(2,3). As opposed to conventional structural MR imaging, this method assess tissue function, and therefore it is termed functional MR imaging.

The very first functional MRI studies of pregnancies were performed using the BOLD method and focused on detecting changes in fetal brain activity during visual and acoustic fetal stimulation in utero (4-7). These studies were followed by studies in sheep fetuses estimating the fetal response on altering maternal oxygen supply in the ventilating gas(8-11). Good correlation between changes in fetal oxygenation and changes in BOLD signal were shown (9,10). As the MR signal is not quantitative, BOLD weighted imaging is only able to detect changes in oxygenation and cannot be used to evaluate the absolute oxygenation status of the fetus. The first step towards absolute quantification of oxygenation is therefore to switch to quantitative imaging. Previously, only one study has reported human placental T2* (12), however the precision and reproducibility of the method has not been investigated. In this study we aim to assess the reproducibility of human placental T2* measurements.

A further aim of the study is to establish a normal material against which pathological pregnancies could be compared.

Lastly the effect of maternal oxygen breathing on the placental T2* values is investigated.

Materials and Methods

The study was approved by the regional Committee on Biomedical Research Ethics (Journal number M-20090006). Oral and written informed consent was obtained from all participating women.

Subjects

Twenty-four pregnant women carrying uncomplicated singleton pregnancies in gestational week 24 - 40 with normal fetal weight estimated by ultrasound and normal Doppler flow in the umbilical artery; the middle cerebral artery and the maternal uterine arteries were included in the study.

MRI

All measurements were performed in a GE Discovery MR450 1.5 Tesla MRI System (GE Healthcare, Milwaukee, USA). An eight channel cardiac coil was placed over the abdomen covering the uterus.

T2* was measured using a gradient recalled echo sequence with multiple readouts with the following parameters: TR=70.9 ms, TE=3.0 to 67.5 ms in steps of 4.3 ms (16 echoes), FOV 350x350 mm, Matrix 256x128 resulting in an inplane resolution of 1.37x2.73mm, Two eight mm thick slices with a distance of at least three cm were acquired within a single breath hold.

Study design

The study design is shown in figure 1. Following initial localizer and T2 weighted reference scans one (N=8) or two (N=16) normoxic placental T2* measurements were performed. A 10-minute BOLD weighted EPI sequence was then performed (results from the first eight subjects are reported in (13)). Halfway through the BOLD sequence the scanning was paused and the maternal facial Hudson oxygen mask (Hudson Respiratory Care, Durham, NC) receiving 12 liters of oxygen per minute was applied. The pregnant women stayed in the bore in the left lateral position while the mask was fitted and care was taken that to avoid maternal movements

After the 10 minute BOLD scan hyperoxic placental T2* measurements were performed, while the mother was still breathing oxygen. In a subset of women (N=8) the protocol was repeated in separate scanning session after a 45-minute break.

MRI analysis

The BOLD MRI DICOM images were processed using an in-house developed program written in MATLAB (The MathWorks Inc, Natick, MA, USA).
Regions of interest (ROIs) were drawn for each echo time in each scan covering the entire placenta by a single examiner (A.S). In case of severe placental movement due to maternal breathing the ROI was either moved according to the new position of the placenta or in cases of severe movement artifacts the given echo time was discarded. Placental T2* values were obtained by fitting the average signal from each ROI as a function of echo time with a mono-exponentially decaying function having M0 and T2* as free parameters (Figure 2). Fitting was performed with a non linear least squares method (14).
Reproducibility was assessed in three different ways.
(1) The slice-to-slice reproducibility: comparing the measured placental T2* value in two different slices which were at least 3 cm apart. (N=24).
(2) The scan-to-scan reproducibility: comparing two normoxic placental T2* measurements performed within a few minutes (N=16). Each measurement was performed in two slices and the average value for the two was used.
(3) The session-to-session reproducibility: comparing the normoxic T2* measurement performed within a 45 minute break (N=8). Each measurement was performed in two slices and the average value for the two was used.

Statistics

Bland-Altman plotting (15) was used to investigate the reproducibility of the studies and to estimate 95% limits of agreement between repeat measurements.
The relation between the normoxic placental T2* and gestational age was estimated using an ordinary linear regression in Stata®11 (StataCorp LP, College Station, TX, USA). 95% confidence and prediction intervals were calculated.
A students T-test was used to test the hyperoxic increase in placental T2*. A p-value < 0.05 was considered statistically significant.

Results

Reproducibility

Reproducibility is demonstrated by Bland-Altman plots which show the difference between two placental T2* measurements on the y-axis as a function of the mean of the two placental T2* values on the x-axis. The mean difference

between measurements and the 95% limits of agreement are indicated as horizontal lines.

Slice to slice reproducibility (figure 3 top). The difference between placental T2* of slice 1 and slice 2 did not change systematically as a function of the mean placental T2* value. The 95% limits of agreement were -1.8±13.1 ms.

Scan to scan reproducibility (figure 3 middle). The difference between the placental T2* measurements of scan 1 and scan 2 did not change systematically as a function of the mean placental T2* value. The 95% limits of agreement were -0.1±17.8 ms.

Session to session reproducibility: figure 3 bottom). Again the difference between the placental T2* measurement of session 1 and session 2 did not change systematically as a function of the mean placental T2* value. The 95% limits of agreement were -0.3±15.7 ms.

T2* as a function of gestational age

Figure 4 demonstrates the relation between the normoxic placental T2* and gestational age. Possible correlation was tested using ordinary least squares regression and a significant correlation was found. (R^2 =0.68, p<0.001). Placental T2* decreased with 4.8 ms per gestational week.

T2* in response to oxygen

The mean normoxic placental T2* was measured to 81.3±28.1 ms, while hyperoxic T2* was measured to 95.7±26.3 ms.

The hyperoxic increase in placental T2* after oxygen inhalation is shown in figure 5. The change in placental T2* range from a 19.0 ms decrease to a 35.3 ms increase. On average the hyperoxic increase in placental T2* was 14.4±12.8 ms and this increase was statistically significant with a p-value less than 0.00002. No correlation could be demonstrated between the gestational age and the change in placental T2* (Spearmans rho=0.21, p=0.34).

Discussion

Reproducibility

In this study we have investigated several aspects of placental T2* reproducibility

The technical reproducibility of the method was tested by comparing two different slices of each placenta acquired in the same scan (slice-to-slice variability) as well as comparing two baseline scans performed within a couple of minutes (scan-to-scan variability). In eight women the experiment was repeated after a break of 45 minutes (session-to-session variability). The variation between sessions would be expected to come from technical as well as biological variations. The 95 % limits of agreement for scan-to-scan and session-to-session variability were very similar (-0.1±17.8 ms and -0.3±15.7 ms respectively) while the slice-to-slice limits were more narrow (-1.8±13.1 ms). This finding suggests that the variation seen in this study mainly relies on technical variations (such as fitting inaccuracy, movement artefacts and differences in scanner calibration) and not biological variation.
The scan-to-scan variability was higher than the slice-to-slice variability. The additional preparation steps, which are performed when starting a new scan, for instance adjustment of gain and frequency and the acquisition of parallel imaging sensitivity maps, might explain this finding.
The reproducibility of this method needs to be evaluated in a clinical perspective. This is difficult as the difference in placental T2* measurement between normal and pathological placentas are not known. The studies of placental T2 measurement indicate, that placental T2* should be reduced in the IUGR placenta (16-18). However placental T2* needs to be investigated in the human IUGR placenta.

Normoxic T2* as a function of gestational age

We found a mean normoxic T2* in the placenta of 81.3±28.1 ms which is higher than the 54.6±15.9 ms reported by A possible explanation could be that Huen et al. (12) used 10 echo-times (TE=5-50 ms), while this study used 16 echo-times (TE=3-67.5 ms) to estimate T2*. Increasing the number of echo times should increase the precision of measuring especially long T2* values.

A negative linear correlation between placental T2* and gestational age was demonstrated with a decrease in placental T2* value of 4.8 ms per gestational week. This finding is in conflict with data previously published by Huen et al, as they failed to demonstrate any relation between placental T2* and gestational

age (12). However, previously a negative linear correlation between placental T2 and gestational age has been demonstrated with a decrease in placenta T2 value of 4.0 ms/week in a 0.5T MRI system(16) and 2.4 ms/week in a 1.5T system(19) respectively. Furthermore it was demonstrated that placental T2 was correlated to the amount of fibrin deposition thereby suggesting an morphological explanation for this relation(19). It is well known, that specific tissue characteristics are important determinants of tissue relaxation times. In general T2 relaxation time is increased with increasing tissue water content(20), increasing surface area and increasing amount of macromolecular deposition(19). The T2* relaxation time depend on the T2 relaxation time, but it is also influenced by the local magnetic field inhomogeneities as created by the presence of deoxyhemoglobin (21).

It is well know, that the oxygenation of the intervillous placental blood is decreased with increasing gestational age, probably as a consequence of the increasing metabolic demand of the placenta and the fetus(22).

We therefore suggest, that the decrease in placental T2* value demonstrated in our study could be explained partly by morphological changes in the maturation of the normal placenta, and partly by the well known decrease in placental oxygenation with increasing gestational age(22).

T2* in response to oxygen

We demonstrated a significant hyperoxic increase in placental T2* of 14.4±12.8 ms, which is in agreement with the 18.4±30.2 ms previously reported by Huyen (12).

The hyperoxic placental T2* response varied between subjects and in three cases placental T2* even decreased. Apart from the placental T2* measurements a dynamic T2* weighted (BOLD) scan was acquired in each subject. In the majority of subjects with poor T2* response demonstrated a corresponding drop in the placental BOLD signal.. Uterine contractions could be responsible for the observed drops in BOLD signal. However, this particular finding needs to be investigated in another study including cardiotocographs for monitoring uterine contractions. However, this finding highlights the importance of following the placenta dynamically when studying the effects of oxygen inhalation.

Another possible explanation of the variation in the hyperoxic placental T2* response would be the rather limited reproducibility of the method. As previously demonstrated the session to session 95% limits of agreement are -16.0 – 15.5 ms. Therefore this method is not perfectly suitable for detecting increases in T2* value of only 14.4 ms. Furthermore, differences in maternal oxygen delivery could explain some of the variation. The facial mask was not perfectly tight, and therefore some variation could rely on differences in maternal oxygen supply.
Previous publications by our group have demonstrated a significant increase in placental BOLD signal of 15.2 ± 3.2% (mean±SD) during maternal hyperoxia(13). During hyperoxia, the placenta BOLD response seems more robust than the placental T2* response, and this might rely on technical inaccuracy in the calculation of T2*. Furthermore, in contrast to the single measurements of placental T2* value, the dynamic BOLD scan measure the placental BOLD signal at multiple time points.

Placental T2 has been investigated in pregnancies complicated by fetal growth restriction, and a lower placental T2 value was found in the group of complicated pregnancies when compared to healthy pregnancies(16-18). Morphological changes of the pathological placenta, as for instance; increased necrosis and infarction, might explain the lower placental T2 value. One study investigated the value of placental T2 performed in gestational week 26 in order to predict fetal growth restriction (18). It was demonstrated that low placental T2 value already in the second trimester was a strong predictor of fetal growth restriction later in pregnancy, even when fetal growth was normal at the time of MRI scan. As T2* is more sensitive to changes in oxygenation than T2(21) it is likely that T2* will be able to further separate the groups. These findings are very interesting as they suggest placental relaxation time (T2 and T2*) measurements as a future non-invasive test of placental function. Placental relaxation time may not only be capable of detecting differences between healthy and pathological pregnancies; it may also predict pregnancies complicated by fetal growth restriction. Thereby suggesting, that alterations in placental relaxation time

might precede the clinical signs of disease, which is very important for the clinical perspective of this method.

Figure 1 – Study design

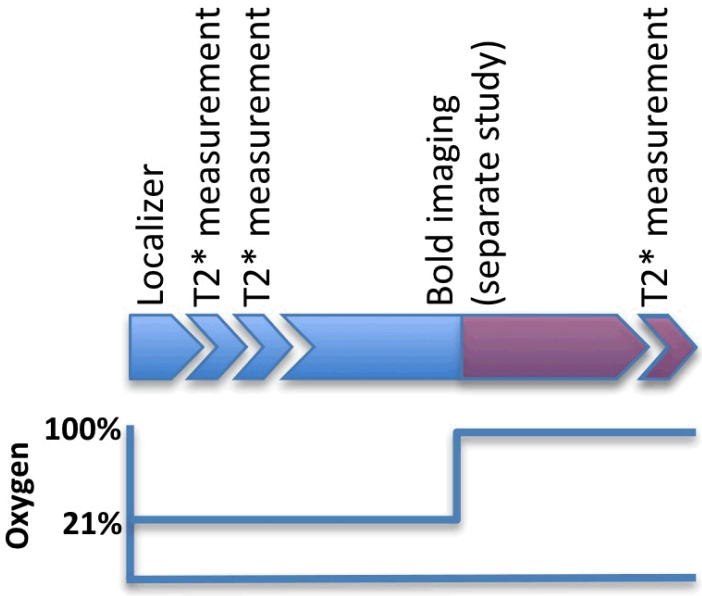

Timeline of a placental MRI examination. BOLD imaging was performed for 10 minutes (5 min normoxia, 5 min hyperoxia)
Initially a localizer was performed followed by a number of placental T2* measurements during normoxia (blue) and hyperoxia (red). In each patient a 10 minute T2*-weighted BOLD scan was performed (another study)

Figure 2 – Placental T2* measurement

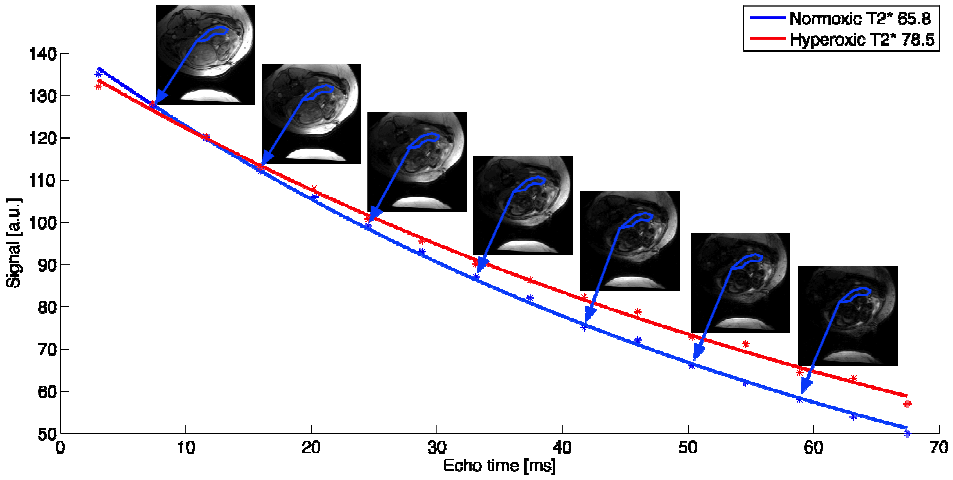

Normoxic (blue) and hyperoxic (red) placental T2* decay curves. The mean MRI signal (arbitrary units) of the placental ROI plotted at each echo-time. A number of MRI images obtained at different echo times are included in the figure.

Figure 3 – Reproducibility

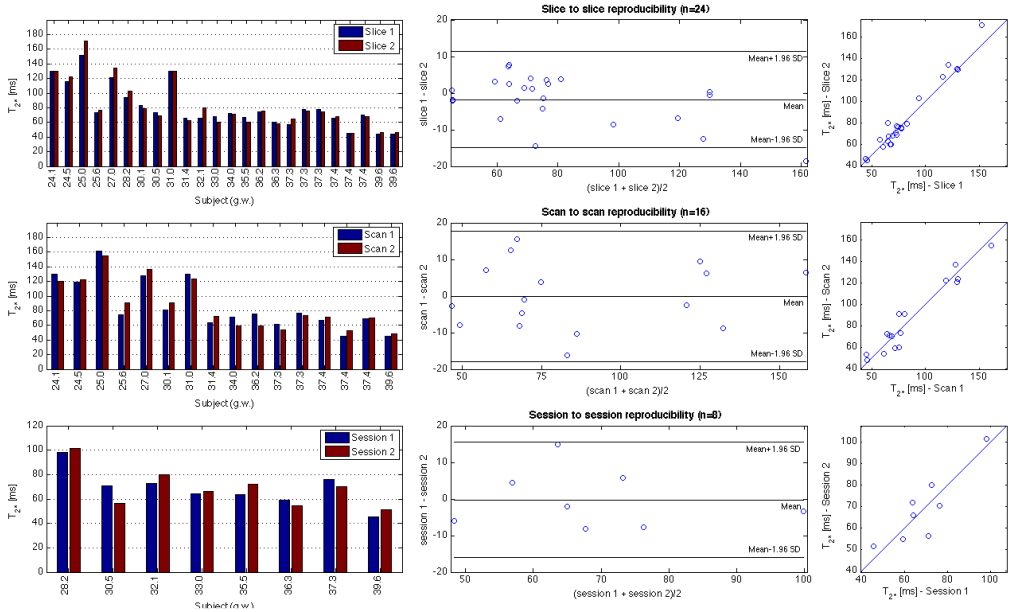

Reproducibility plots demonstrating (a) slice-to-slice variation, (b) scan-to-scan variation and (c) session-to-session variation.
Each section contains barplots of the compaired values, Bland-Altman plots including 95% limits of agreement and identity plot of the compared values.

Figure 4

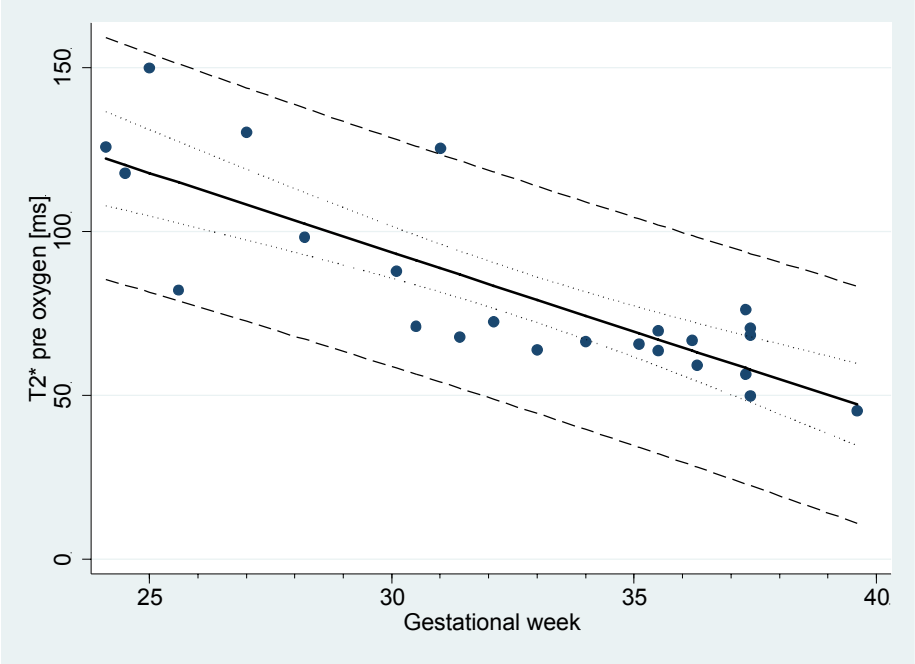

The linear relation between placental T2* and gestational week . Thick line is ordinary least squares fit ($P<0.001$. $R^2=0.68$). Dotted lines indicate 95% confidence interval while dashed lines indicate 95% prediction interval.

Figure 5

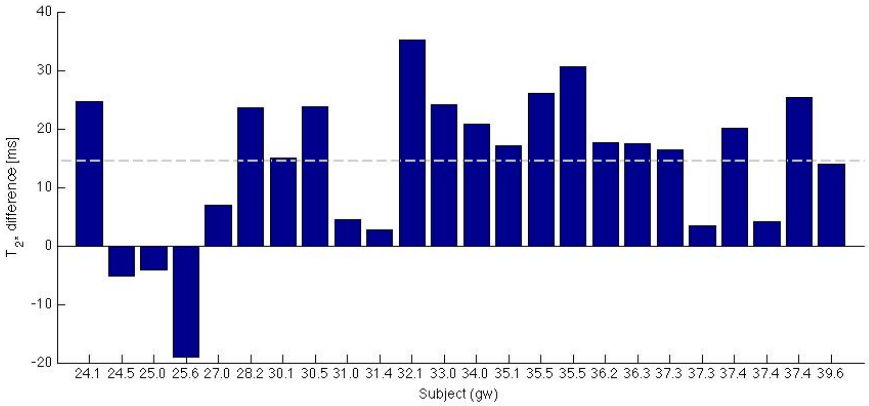

The hyperoxic placental T2* response. The subjects are sorted by gestational age. The dashed line indicates the average increase in placental T2* of 14.4±12.8 ms during hyperoxia.

Referencelist

1. Ogawa S, Lee TM. Magnetic resonance imaging of blood vessels at high fields: in vivo and in vitro measurements and image simulation. Magnetic Resonance in Medicine: Official Journal of the Society of Magnetic Resonance in Medicine / Society of Magnetic Resonance in Medicine. 1990;16(1):9–18.

2. Ogawa S, Lee TM, Kay AR, Tank DW. Brain magnetic resonance imaging with contrast dependent on blood oxygenation. Proceedings of the National Academy of Sciences of the United States of America. 1990;87(24):9868–72.

3. Logothetis NK, Pfeuffer J. On the nature of the BOLD fMRI contrast mechanism. Magn Reson Imaging. 2004Dec.;22(10):1517–31.

4. Hykin J, Moore R, Duncan K, Clare S, Baker P, Johnson I, et al. Fetal brain activity demonstrated by functional magnetic resonance imaging. Lancet. 1999Aug.21;354(9179):645–6.

5. Moore RJ, Vadeyar S, Fulford J, Tyler DJ, Gribben C, Baker PN, et al. Antenatal determination of fetal brain activity in response to an acoustic stimulus using functional magnetic resonance imaging. Hum Brain Mapp. 2001Feb.;12(2):94–9.

6. Fulford J, Vadeyar SH, Dodampahala SH, Ong S, Moore RJ, Baker PN, et al. Fetal brain activity and hemodynamic response to a vibroacoustic stimulus. Hum Brain Mapp. 2004Jun.;22(2):116–21.

7. Fulford J, Vadeyar SH, Dodampahala SH, Moore RJ, Young P, Baker PN, et al. Fetal brain activity in response to a visual stimulus. Hum Brain Mapp. 2003Dec.;20(4):239–45.

8. Wedegärtner U, Tchirikov M, Schäfer S, Priest AN, Walther M, Adam G, et al. Fetal Sheep Brains: Findings at Functional Blood Oxygen Level–Dependent 3-T MR Imaging—Relationship to Maternal Oxygen Saturation during Hypoxia1. Radiology. 2005;237(3):919–26.

9. Wedegärtner U, Tchirikov M, Schäfer S, Priest AN, Kooijman H, Adam G, et al. Functional MR Imaging: Comparison of BOLD Signal Intensity Changes in Fetal Organs with Fetal and Maternal Oxyhemoglobin Saturation during Hypoxia in Sheep1. Radiology. 2006;238(3):872–80.

10. Sørensen A, Pedersen M, Tietze A, Ottosen L, Duus L, Uldbjerg N. BOLD MRI in sheep fetuses: a non-invasive method for measuring changes in tissue oxygenation. Ultrasound Obstet Gynecol. 2009;34(6):687–92.

11. Sørensen A, Holm D, Pedersen M, Tietze A, Stausbøl-Grøn B, Duus L, et al. The left-right difference in fetal liver oxygenation during hypoxia, as

estimated by BOLD MRI in a fetal sheep model. Ultrasound Obstet Gynecol. 2011;38(6):665–72.

12. Huen I, Morris DM, Wright C, Parker GJ, Sibley CP, Johnstone ED, et al. R1 and R2* changes in the human placenta in response to maternal oxygen challenge. Magn Reson Med. Wiley Online Library; 2012.

13. Sørensen A, Peters D, Fründ E, Lingman G, Christiansen O, Uldbjerg N. Changes in human placental oxygenation during maternal hyperoxia as estimated by BOLD MRI. Ultrasound Obstet Gynecol. 2013Jan.10.

14. Marquardt DW. An algorithm for least-squares estimation of nonlinear parameters. 1963;11:431–41.

15. Bland JM, Altman DG. Measuring agreement in method comparison studies. Statistical methods in medical research. SAGE Publications; 1999;8(2):135–60.

16. Gowland PA, Freeman A, Issa B, Boulby P, Duncan KR, Moore RJ, et al. In vivo relaxation time measurements in the human placenta using echo planar imaging at 0.5 T. Magn Reson Imaging. 1998Apr.;16(3):241–7.

17. Duncan KR, Gowland P, Francis S, Moore R, Baker PN, Johnson IR. The investigation of placental relaxation and estimation of placental perfusion using echo-planar magnetic resonance imaging. Placenta. 1998Sep.;19(7):539–43.

18. Derwig I, Barker GJ, Poon L, Zelaya F, Gowland P, Lythgoe DJ, et al. Association of placental T2 relaxation times and uterine artery Doppler ultrasound measures of placental blood flow. Placenta. Elsevier Ltd; 2013Jun.1;34(6):474–9.

19. Wright C, Morris DM, Baker PN, Crocker IP, Gowland PA, Parker GJ, et al. Magnetic resonance imaging relaxation time measurements of the placenta at 1.5T. Placenta. Elsevier Ltd; 2011Dec.1;32(12):1010–5.

20. Cameron IL, Ord VA, Fullerton GD. Characterization of proton NMR relaxation times in normal and pathological tissues by correlation with other tissue parameters. Magn Reson Imaging. 1984;2(2):97–106.

21. Bandettini PA, Wong EC, Jesmanowicz A, Hinks RS, Hyde JS. Spin-echo and gradient-echo EPI of human brain activation using BOLD contrast: a comparative study at 1.5 T. NMR Biomed. 1994Mar.;7(1-2):12–20.

22. Soothill PW, Nicolaides KH, Rodeck CH, Campbell S. Effect of gestational age on fetal and intervillous blood gas and acid-base values in human pregnancy. Fetal Ther. 1986;1(4):168–75.